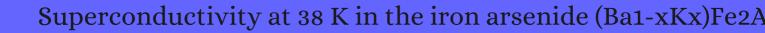
# CITATION REPORT List of articles citing



DOI: 10.1103/physrevlett.101.107006 Physical Review Letters, 2008, 101, 107006.

Source: https://exaly.com/paper-pdf/43873206/citation-report.pdf

Version: 2024-04-19

This report has been generated based on the citations recorded by exaly.com for the above article. For the latest version of this publication list, visit the link given above.

The third column is the impact factor (IF) of the journal, and the fourth column is the number of citations of the article.

#	Paper	IF	Citations
2317	The superconductivity at 18 K in LiFeAs system. <b>2008</b> , 148, 538-540		818
2316	High-temperature superconductivity in iron-based layered iron compounds. <b>2008</b> , 51, 1201-1227		190
2315	Upper critical field, anisotropy, and superconducting properties of Ba1â⊠KxFe2As2 single crystals. <b>2008</b> , 78,		128
2314	Density functional study of FeS, FeSe, and FeTe: Electronic structure, magnetism, phonons, and superconductivity. <b>2008</b> , 78,		644
2313	Unconventional superconductivity in Ba(0.6)K(0.4)Fe2As2 from inelastic neutron scattering. <b>2008</b> , 456, 930-2		499
2312	Electronic structure of new AFFeAs prototype of iron arsenide superconductors. 2008, 88, 679-682		16
2311	Band structure of SrFeAsF and CaFeAsFâEhe base phases of a new group of oxygen-free FeAs superconductors. <b>2008</b> , 88, 683-687		14
2310	Structural and magnetic phase diagram of CeFeAsO(1- $x$ )F( $x$ ) and its relation to high-temperature superconductivity. <b>2008</b> , 7, 953-9		657
2309	Correlated pressure effects on the structure and superconductivity of LaFeAsO0.9F0.1. <b>2008</b> , 78,		54
2308	Neutron-diffraction measurements of magnetic order and a structural transition in the parent BaFe2As2 compound of FeAs-based high-temperature superconductors. <i>Physical Review Letters</i> , <b>2008</b> , 101, 257003	7.4	691
2307	Commensurate Itinerant Antiferromagnetism in BaFe2As2: 75As-NMR Studies on a Self-Flux Grown Single Crystal. <b>2008</b> , 77, 114709		202
2306	Effects of Co substitution on thermodynamic and transport properties and anisotropic Hc2 in Ba(Fe1â\( \text{LCox}\))2As2 single crystals. <b>2008</b> , 78,		483
2305	Iron-specific phonon density of states in the superconductors LaFeAsO1âNFx and La1âNCaxFePO. <b>2008</b> , 78,		27
2304	The optical phonon spectrum of SmFeAsO. <b>2008</b> , 84, 67013		25
2303	Momentum dependence of the superconducting gap in NdFeAsO0.9F0.1 single crystals measured by angle resolved photoemission spectroscopy. <i>Physical Review Letters</i> , <b>2008</b> , 101, 147003	7.4	230
2302	High-temperature superconductivity in layered iron compounds. 2008, 178, 1243		53
2301	Superconductivity induced by co-doping in quaternary fluoroarsenide CaFeAsF. <b>2008</b> , 130, 14428-9		181

2300	Crystallographic phase transition and high-Tcsuperconductivity in LaFeAsO:F. <b>2008</b> , 21, 125028	212
2299	Magnetism, superconductivity, and pairing symmetry in iron-based superconductors. 2008, 78,	599
2298	Structure and superconductivity of LiFeAs. <b>2008</b> , 5918-20	256
2297	Phonon dynamics in Sr0.6K0.4Fe2As2 and Ca0.6Na0.4Fe2As2 from neutron scattering and lattice-dynamical calculations. <b>2008</b> , 78,	22
2296	K-doping dependence of the Fermi surface of the iron-arsenic Ba1-xKxFe2As2 superconductor using angle-resolved photoemission spectroscopy. <i>Physical Review Letters</i> , <b>2008</b> , 101, 177005	203
2295	Spin and lattice structures of single-crystalline SrFe2As2. <b>2008</b> , 78,	178
2294	Pressure effects on the electron-doped highTcsuperconductor BaFe2â⊠CoxAs2. <b>2008</b> , 20, 472201	44
2293	Thermodynamic properties of Ba1â⊠KxFe2As2and Ca1â⊠NaxFe2As2. <b>2008</b> , 10, 123031	36
2292	Growth and characterization of A1â⊠KxFe2As2(A = Ba, Sr) single crystals withx= 0âŪ.4. <b>2008</b> , 21, 125014	95
2291	Evidence of nodeless superconductivity in FeSe0.85 from a muon-spin-rotation study of the in-plane magnetic penetration depth. <b>2008</b> , 78,	92
2290	Lattice and magnetic structures of PrFeAsO, PrFeAsO0.85F0.15, and PrFeAsO0.85. 2008, 78,	125
2289	Evidence for Unconventional Superconductivity in Arsenic-Free Iron-Based Superconductor FeSe: A 77Se-NMR Study. <b>2008</b> , 77, 113703	82
2288	Determination of anisotropic Hc2 up to 60 T in Ba0.55K0.45Fe2As2 single crystals. <b>2008</b> , 78,	148
2287	Low energy spin waves and magnetic interactions in SrFe2As2. <i>Physical Review Letters</i> , <b>2008</b> , 101, 16720 <del>3</del> .4	152
2286	High-energy spin excitations in BaFe2As2 observed by inelastic neutron scattering. 2008, 78,	113
2285	High-temperature superconductivity in Eu0.5K0.5Fe2As2. <b>2008</b> , 78,	179
2284	Superconductivity in SrNi2As2 single crystals. <b>2008</b> , 78,	92
2283	Suppression of Magnetic Order by Pressure in BaFe2As2. <b>2008</b> , 77, 105004	71

2282	Structural and magnetic phase transitions in the ternary iron arsenides SrFe2As2and EuFe2As2. <b>2008</b> , 20, 452201		175
2281	Transport properties and superconductivity in Ba 1-x M x Fe 2 As 2 (M=La and K) with double FeAs layers. <b>2008</b> , 84, 27010		73
2280	Pressure-induced volume-collapsed tetragonal phase of CaFe2As2 as seen via neutron scattering. <b>2008</b> , 78,		301
2279	Superconducting Fe-based compounds (A1-xSrx)Fe2As2 with A=K and Cs with transition temperatures up to 37 K. <i>Physical Review Letters</i> , <b>2008</b> , 101, 107007	7.4	635
2278	Electronic structure and doping in BaFe2As2 and LiFeAs: Density functional calculations. 2008, 78,		384
2277	Fishtail effect and the vortex phase diagram of single crystal Ba0.6K0.4Fe2As2. <b>2008</b> , 93, 142506		141
2276	Trapped Phonons Improve Photon Detection. <b>2008</b> , 1,		151
2275	FeAs systems: a new class of high-temperature superconductors. <b>2008</b> , 51, 1261-1286		60
2274	High-Pressure Studies on Superconducting Iron-Based LaFeAsO1-xFx, LaFePO and SrFe2As2. <b>2008</b> , 77, 78-83		38
2273	Magnetic Property of BaFe2As2Probed by75As NMR. <b>2008</b> , 77, 138-139		3
2272	Superconductivity in Epitaxial Thin Films of Co-Doped SrFe2As2with Bilayered FeAs Structures and their Magnetic Anisotropy. <b>2008</b> , 1, 101702		101
2271	New high-temperature superconductors based on rare-earth and transition metal oxyarsenides and related phases: synthesis, properties and simulations. <b>2008</b> , 51, 1229-1260		122
2270	Electronic Structure, Magnetism and Spin-Fluctuations in Fe-As Based Superconductors. <b>2008</b> , 1148, 1		
2269	Synthesis, crystal structure and spin-density-wave anomaly of the iron arsenide-fluoride SrFeAsF. <b>2008</b> , 84, 67007		83
2268	Pseudogap and Superconductivity in Iron-Based Layered Superconductor Studied by Fluctuationâ <b>E</b> xchange Approximation. <b>2008</b> , 77, 123707		118
2267	Chemistry of layered -metal pnictide oxides and their potential as candidates for new superconductors. <b>2008</b> , 9, 033003		104
2266	Doping Dependence of Superconductivity and Lattice Constants in Hole Doped La1-xSrxFeAsO. <b>2008</b> , 77, 15-18		19
2265	Layered Iron Pnictide Superconductors: Discovery and Current Status. <b>2008</b> , 77, 1-8		43

#### (2008-2008)

2264	His-wave scenario. <b>2008</b> , 10, 103026		75
2263	SrFeAsF as a parent compound for iron pnictide superconductors. <b>2008</b> , 78,		79
2262	Characteristic muon precession and relaxation signals in FeAs and FeAs2: Possible impurity phases in pnictide superconductors. <b>2008</b> , 78,		10
2261	Microscopic A75s NMR study of the effect of impurities on the first-order spin-density-wave transition in BaFe2As2. <b>2008</b> , 78,		32
2260	Fermi surface and band renormalization of Sr1â\(\mathbb{R}\)KxFe2As2 from angle-resolved photoemission spectroscopy. <b>2008</b> , 78,		46
2259	Superconducting state in SrFe2-xCoxAs2 by internal doping of the iron arsenide layers. <i>Physical Review Letters</i> , <b>2008</b> , 101, 207004	7.4	215
2258	Thermal properties of SmFeAsO1âNFx as a probe of the interplay between electrons and phonons. <b>2008</b> , 78,		44
2257	Effect of pressure on the structural phase transition and superconductivity in (Ba1â\(\text{M}\times\))Fe2As2 (x=0 and 0.45) and SrFe2As2 single crystals. <b>2008</b> , 78,		74
2256	Flux-lattice melting in LaFeAsO1â¼Fx: First-principles prediction. <b>2008</b> , 78,		6
2255	Transport and anisotropy in single-crystalline SrFe2As2 and A0.6K0.4Fe2As2 (A=Sr, Ba) superconductors. <b>2008</b> , 78,		143
2254	Heteroepitaxial growth and optoelectronic properties of layered iron oxyarsenide, LaFeAsO. <b>2008</b> , 93, 162504		88
2253	Hall effect and magnetoresistance in single crystals of NdFeAsO1â⊠Fx (x=0 and 0.18). <b>2008</b> , 78,		68
2252	Experimental observables near a nematic quantum critical point in the pnictide and cuprate superconductors. <b>2008</b> , 78,		36
2251	Enhanced spin-density wave in LaFeSbO from first principles. <b>2008</b> , 78,		10
2250	Origin of the spin density wave instability in AFe2As2 (A=Ba,Sr) as revealed by optical spectroscopy. <i>Physical Review Letters</i> , <b>2008</b> , 101, 257005	7.4	238
2249	Pressure-induced shift of Tc in KxSr1â⊠Fe2As2 (x=0.2,0.4,0.7): Analogy to the high-Tc cuprate superconductors. <b>2008</b> , 78,		42
2248	Possible superconductivity in Fe-Sb based materials: Density functional study of LiFeSb. <b>2008</b> , 78,		17
2247	Evidence for two energy gaps in superconducting Ba0.6K0.4Fe2As2 single crystals and the breakdown of the Uemura plot. <i>Physical Review Letters</i> , <b>2008</b> , 101, 257006	7.4	94

2246	Strong coupling between magnetic and structural order parameters in SrFe2As2. 2008, 78,		119
2245	Experimental consequences of the s-wave cos(kx)cos(ky) superconductivity in the iron pnictides. <b>2008</b> , 78,		94
2244	Muon-spin-relaxation studies of magnetic order and superfluid density in antiferromagnetic NdFeAsO, BaFe2As2, and superconducting Ba1â\(\text{M}\)KxFe2As2. <b>2008</b> , 78,		84
2243	Inelastic neutron scattering and lattice-dynamical calculations of BaFe2As2. 2008, 78,		54
2242	Synthesis and characterization of the hole-doped nickel-based superconductor La1â⊠SrxNiAsO. <b>2008</b> , 78,		21
2241	Competing orders in FeAs layers. <i>Physical Review Letters</i> , <b>2008</b> , 101, 186402	7.4	76
2240	Spin fluctuation dynamics and multiband superconductivity in iron pnictides. <b>2008</b> , 78,		69
2239	Lattice and magnetic instabilities in CaFe2As2: A single-crystal neutron diffraction study. <b>2008</b> , 78,		283
2238	Superconductivity induced by oxygen deficiency in La0.85Sr0.15FeAsO1â□ <b>2008</b> , 78,		24
2237	Density functional study of BaNi2As2: Electronic structure, phonons, and electron-phonon superconductivity. <b>2008</b> , 78,		67
2236	Single-crystal growth and physical properties of the layered arsenide BaRh2As2. 2008, 78,		26
2235	Cobalt-Substitution-Induced Superconductivity in a New Compound with ZrCuSiAs-Type Structure, SrFeAsF. <b>2008</b> , 77, 113709		63
2234	Tetragonalâ©rthorhombic Phase Transition and F-Doping Effects on the Crystal Structure in the Iron-Based High-TcSuperconductor LaFeAsO. <b>2008</b> , 77, 32-35		7
2233	NMR Measurements of Intrinsic Spin Susceptibility in LaFeAsO0.9F0.1. <b>2008</b> , 77, 47-53		16
2232	Large Thermoelectric Power Factor in Iron-Pnictide Derivatives. 2008, 77, 58-60		2
2231	A Resistive Transition between the Normal and Superconducting State of BaNi2P2Single Crystals. <b>2008</b> , 77, 136-137		5
2230	Superconductivity in R(O,F)FeAs, AFe2As2, (A,A')Fe2As2, AFeAs and LaNFeAs, where R = Rare Earth, $A = Alkaline$ , and $A = Alkaline$ Earth. <b>2008</b> , 77, 72-77		9
2229	Properties of LaFeAsO/MgO(001) Interfaces fromab initioCalculations. <b>2008</b> , 77, 113-116		

2228	75As-NMR Studies on LaFeAsO1-xFx (x=0.14) under a Pressure of 3 GPa. <b>2009</b> , 78, 023709	23
2227	Epitaxial Growth of NdFeAsO Thin Films by Molecular Beam Epitaxy. <b>2009</b> , 2, 093002	50
2226	Pressure Effect on Electrical Resistivity and Magnetic Susceptibility of Newly Discovered Iron-based High Tc Superconductors. <b>2009</b> , 19, 123-128	
2225	Distinct Transport Behaviors of LaFe1-yCoyAsO1-xFx (x=0.11) between the Superconducting and Nonsuperconducting Metallic y Regions Divided by y $\sim$ 0.05. <b>2009</b> , 78, 043703	38
2224	Band structure and Fermi surface of (Sr2VO3)2Fe2As2 and (Sr2ScO3)2Fe2As2. 2009, 80,	21
2223	Structural phase transition in Ba(Fe0.973Cr0.027)2As2 single crystals. <b>2009</b> , 80,	15
2222	Antiferromagnetic ordering and structural phase transition in Ba2Fe2As2 with Sn incorporated from the growth flux. <b>2009</b> , 79,	98
2221	Multigap nodeless superconductivity in FeSex: Evidence from quasiparticle heat transport. <b>2009</b> , 80,	69
2220	Spin gap and magnetic resonance in superconducting BaFe1.9Ni0.1As2. <b>2009</b> , 79,	59
2219	Phonons in doped and undoped BaFe2As2 investigated by inelastic x-ray scattering. <b>2009</b> , 80,	54
2218	Magnetic order in the CaFe1â⊠CoxAsF (x=0.00,0.06,0.12) superconducting compounds. <b>2009</b> , 79,	55
2217	Density functional study of the overdoped iron chalcogenide TlFe2Se2 with ThCr2Si2 structure. <b>2009</b> , 79,	35
2216	Superconductivity and phase diagrams of the 4d- and 5d-metal-doped iron arsenides SrFe2âMxAs2 (M=Rh,Ir,Pd). <b>2009</b> , 80,	102
2215	Density-functional calculations of the electronic structures and magnetism of the pnictide superconductors BaFeAs2 and BaFeSb2. <b>2009</b> , 79,	24
2214	Theory of the excitonic spin-density-wave state in iron pnictides. <b>2009</b> , 79,	40
2213	Anisotropic itinerant magnetism and spin fluctuations in BaFe2As2: A neutron scattering study. <b>2009</b> , 79,	142
2212	Roles of multiband effects and electron-hole asymmetry in the superconductivity and normal-state properties of Ba(Fe1â\( Cox) 2As2. <b>2009</b> , 80,	170
2211	Superconductivity without Fe or Ni in the phosphides Balr2P2 and BaRh2P2. <b>2009</b> , 79,	36

2210	Anisotropy of the iron pnictide superconductor Ba(Fe1â⊠Cox)2As2 (x=0.074, Tc=23 K). <b>2009</b> , 79,	152
2209	Intrinsic pinning on structural domains in underdoped single crystals of Ba(Fe1â⊠Cox)2As2. <b>2009</b> , 80,	94
2208	Dominant role of local-moment interactions in the magnetic ordering of iron pnictide superconductors: A comparative study of arsenides and antimonides from first principles. <b>2009</b> , 80,	11
2207	Band renormalization and Fermi surface reconstruction in iron-based superconductors. <b>2009</b> , 79,	42
2206	Properties of KCo2As2 and alloys with Fe and Ru: Density functional calculations. 2009, 79,	17
2205	Two-dimensional magnetism in the pnictide superconductor parent material SrFeAsF probed by muon-spin relaxation. <b>2009</b> , 79,	17
2204	Water-induced superconductivity in SrFe2As2. <b>2009</b> , 80,	64
2203	Local density of states and superconducting gap in the iron chalcogenide superconductor Fe1+Be1âITex observed by scanning tunneling spectroscopy. <b>2009</b> , 80,	74
2202	Spin excitations in BaFe1.84Co0.16As2 superconductor observed by inelastic neutron scattering. <b>2009</b> , 80,	12
2201	First-principles study of the iron pnictide superconductor BaFe2As2. <b>2009</b> , 79,	38
	First-principles study of the iron pnictide superconductor BaFe2As2. <b>2009</b> , 79,  Tight-binding models for the iron-based superconductors. <b>2009</b> , 80,	38
2200		
2200 2199	Tight-binding models for the iron-based superconductors. <b>2009</b> , 80,	140
2200 2199 2198	Tight-binding models for the iron-based superconductors. <b>2009</b> , 80,  Electronic structure studies of BaFe2As2 by angle-resolved photoemission spectroscopy. <b>2009</b> , 79,	140 72
2200 2199 2198 2197	Tight-binding models for the iron-based superconductors. <b>2009</b> , 80,  Electronic structure studies of BaFe2As2 by angle-resolved photoemission spectroscopy. <b>2009</b> , 79,  Superconductivity and the effects of pressure and structure in single-crystalline SrNi2P2. <b>2009</b> , 79,	140 72 65
2200 2199 2198 2197	Tight-binding models for the iron-based superconductors. 2009, 80,  Electronic structure studies of BaFe2As2 by angle-resolved photoemission spectroscopy. 2009, 79,  Superconductivity and the effects of pressure and structure in single-crystalline SrNi2P2. 2009, 79,  Spin excitations in the excitonic spin-density-wave state of the iron pnictides. 2009, 80,	<ul><li>140</li><li>72</li><li>65</li><li>57</li></ul>
2200 2199 2198 2197 2196	Tight-binding models for the iron-based superconductors. <b>2009</b> , 80,  Electronic structure studies of BaFe2As2 by angle-resolved photoemission spectroscopy. <b>2009</b> , 79,  Superconductivity and the effects of pressure and structure in single-crystalline SrNi2P2. <b>2009</b> , 79,  Spin excitations in the excitonic spin-density-wave state of the iron pnictides. <b>2009</b> , 80,  Effects of cobalt doping and three-dimensionality in BaFe2As2. <b>2009</b> , 80,	<ul> <li>140</li> <li>72</li> <li>65</li> <li>57</li> <li>52</li> </ul>

2192	Synthesis, structural, and transport properties of the hole-doped superconductor Pr1â\subsection SrxFeAsO. <b>2009</b> , 79,		31
2191	Low-temperature thermal conductivity of BaFe2As2: A parent compound of iron arsenide superconductors. <b>2009</b> , 79,		9
2190	Unconventional electronic reconstruction in undoped (Ba,Sr)Fe2As2 across the spin density wave transition. <b>2009</b> , 80,		124
2189	Surface density of states of s∃-wave Cooper pairs in a two-band superconductor model. <b>2009</b> , 79,		32
2188	Superconductivity in Ir-doped LaFe1â⊠IrxAsO. <b>2009</b> , 80,		24
2187	Band- and momentum-dependent electron dynamics in superconducting Ba(Fe1â\( Cox)2As2 as seen via electronic Raman scattering. <b>2009</b> , 80,		76
2186	Electronic structure of the BaFe2As2 family of iron-pnictide superconductors. <b>2009</b> , 80,		110
2185	Superconducting state coexisting with a phase-separated static magnetic order in (Ba,K)Fe2As2, (Sr,Na)Fe2As2, and CaFe2As2. <b>2009</b> , 80,		115
2184	C59o and A75s NMR investigation of lightly doped Ba(Fe1â⊠Cox)2As2 (x=0.02,0.04). <b>2009</b> , 79,		36
2183	Electronic and structural properties of low-temperature superconductors and ternary pnictides ANi2Pn2 (A=Sr,Ba and Pn=P,As). <b>2009</b> , 79,		60
2182	Superconducting properties of the oxygen-deficient iron oxyarsenide TbFeAsO1âlfrom underdoped to overdoped compositions. <b>2009</b> , 80,		11
2181	Muon spin rotation measurement of the magnetic field penetration depth in Ba(Fe0.926Co0.074)2As2: Evidence for multiple superconducting gaps. <b>2009</b> , 80,		62
2180	Two-dimensional resonant magnetic excitation in BaFe1.84Co0.16As2. <i>Physical Review Letters</i> , <b>2009</b> , 102, 107005	7.4	228
2179	Unconventional London penetration depth in single-crystal Ba(Fe0.93Co0.07)2As2 superconductors. <i>Physical Review Letters</i> , <b>2009</b> , 102, 127004	7.4	144
2178	Pseudoisotropic upper critical field in cobalt-doped SrFe2As2 epitaxial films. <i>Physical Review Letters</i> , <b>2009</b> , 102, 117004	7.4	99
2177	In situ fabrication of cobalt-doped SrFe2As2 thin films by using pulsed laser deposition with excimer laser. <b>2009</b> , 95, 062507		38
2176	Insular superconductivity in a Co-doped iron pnictide CaFe1-xCoxAsF. <i>Physical Review Letters</i> , <b>2009</b> , 103, 027002	7.4	39
2175	Optical spectroscopy of superconducting Ba0.55K0.45Fe2As2: evidence for strong coupling to low-energy bosons. <i>Physical Review Letters</i> , <b>2009</b> , 102, 187003	7.4	62

2174	Doping driven (pi, 0) nesting and magnetic properties of Fe_{1+x}Te superconductors. <i>Physical Review Letters</i> , <b>2009</b> , 103, 067001	7.4	90
2173	Superconductivity in the iron-pnictide parent compound SrFe2As2. <b>2009</b> ,		
2172	Effects of magnetic doping and temperature dependence of phonon dynamics in CaFe1â\(\mathbb{U}\)CoxAsF compounds (x=0, 0.06, and 0.12). <b>2009</b> , 79,		20
2171	Enhanced superfluid stiffness, lowered superconducting transition temperature, and field-induced magnetic state of the pnictide superconductor LiFeAs. <b>2009</b> , 79,		41
2170	Vortex core states in a minimal two-band model for iron-based superconductors. 2009, 80,		19
2169	Cleavage surfaces of the BaFe2â\(\mathbb{U}\)CoxAs2 and FeySe1â\(\mathbb{U}\)Tex superconductors: A combined STM plus LEED study. <b>2009</b> , 80,		79
2168	Magnetic and lattice coupling in single-crystal SrFe2As2: A neutron scattering study. 2009, 80,		22
2167	Origin of the structural phase transition in BaNi2As2 at 130 K: A combined study of optical spectroscopy and band structure calculations. <b>2009</b> , 80,		31
2166	Evolution of bulk superconductivity in SrFe2As2 with Ni substitution. <b>2009</b> , 79,		59
2165	Strongly dissimilar vortex-liquid regimes in single-crystalline NdFeAs(O,F) and (Ba,K)Fe2As2: A comparative study. <b>2009</b> , 80,		25
2164	Evidence for two-gap superconductivity in Ba0.55K0.45Fe2As2 from directional point-contact Andreev-reflection spectroscopy. <b>2009</b> , 79,		91
2163	Magnetic structure of EuFe2As2 determined by single-crystal neutron diffraction. <b>2009</b> , 80,		139
2162	Evidence for local moments by electron spin resonance study of polycrystalline LaFeAsO1â\(\text{NF}\xeta\) (x=0 and 0.13). <b>2009</b> , 79,		14
2161	Complete pressure-dependent phase diagrams for SrFe2As2 and BaFe2As2. <b>2009</b> , 79,		158
2160	Lattice collapse and the magnetic phase diagram of Sr1â⊠CaxCo2P2. <b>2009</b> , 80,		43
2159	Thermal expansion of LaFeAsO1â⊠Fx: Evidence for high-temperature fluctuations. <b>2009</b> , 80,		26
2158	Antiphase magnetic boundaries in iron-based superconductors: A first-principles density-functional theory study. <b>2009</b> , 80,		9
2157	Magnetic ordering in EuRh2As2 studied by x-ray resonant magnetic scattering. <b>2009</b> , 79,		17

2156	measurements. <b>2009</b> , 79,	75
2155	Optical study of the spin-density-wave properties of single-crystalline Na1âEeAs. <b>2009</b> , 80,	18
2154	First-principles investigation of the effect of pressure on BaFe2As2. <b>2009</b> , 79,	19
2153	Vortex-glass phase transition and superconductivity in an underdoped (Ba,K)Fe2As2 single crystal. <b>2009</b> , 79,	51
2152	Suppression of spin-density-wave transition and emergence of ferromagnetic ordering of Eu2+moments in EuFe2âNixAs2. <b>2009</b> , 79,	43
2151	Electronic structure and magnetism in BaMn2As2 and BaMn2Sb2. <b>2009</b> , 79,	98
2150	Infrared phonon anomaly in BaFe2As2. <b>2009</b> , 80,	72
2149	Phonon anomalies in pure and underdoped R1â¼KxFe2As2 (R=Ba, Sr) investigated by Raman light scattering. <b>2009</b> , 80,	65
2148	Thermoelectric power and Hall coefficient measurements on Ba(Fe1â⊠Tx)2As2 (T=Co and Cu). <b>2009</b> , 80,	79
2147	Probing microscopic variations of superconductivity on the surface of Ba(Fe1â\( Cox)\) 2As2 single crystals. <b>2009</b> , 80,	5
2146	Fermi-liquid state and enhanced electron correlations in the iron pnictide CaFe4As3. 2009, 80,	16
2145	Unusual doping dependence of superconductivity in NayFeAs. <b>2009</b> , 79,	19
2144	Phonon spectra in CaFe2As2 and Ca0.6Na0.4Fe2As2: Measurement of the pressure and temperature dependence and comparison with ab initio and shell model calculations. <b>2009</b> , 79,	17
2143	Anisotropic phase diagram and strong coupling effects in Ba1â\(\mathbb{R}\)KxFe2As2 from specific-heat measurements. <b>2009</b> , 79,	56
2142	Multiple phase transitions in single-crystalline Na_{1-delta}FeAs. <i>Physical Review Letters</i> , <b>2009</b> , 102, 2270,04	95
2141	Low-temperature magnetothermal transport investigation of a Ni-based superconductor BaNi2As2: evidence for fully gapped superconductivity. <i>Physical Review Letters</i> , <b>2009</b> , 102, 147004	43
2140	Microwave surface-impedance measurements of the magnetic penetration depth in single crystal Ba1-xKxFe2As2 superconductors: evidence for a disorder-dependent superfluid density. <i>Physical Review Letters</i> , <b>2009</b> , 102, 207001	138
2139	Static and dynamic magnetism in underdoped superconductor BaFe1.92Co0.08As2. <i>Physical Review Letters</i> , <b>2009</b> , 103, 087002	145

2138	Transition from three-dimensional anisotropic spin excitations to two-dimensional spin excitations by electron doping the FeAs-based BaFe1.96Ni0.04As2 superconductor. <i>Physical Review Letters</i> , <b>2009</b> , 103, 087005	7.4	34
2137	Raman phonons of ∃-FeTe and Fe1.03Se0.3Te0.7 single crystals. <b>2009</b> , 79,		52
2136	Electronic structure of BaCu2As2 and SrCu2As2: sp-band metals. <b>2009</b> , 79,		38
2135	Observation of the Josephson effect in Pb/Ba1-xKxFe2As2 single crystal junctions. <i>Physical Review Letters</i> , <b>2009</b> , 102, 147002	7.4	83
2134	Renormalized behavior and proximity of BaCo2As2 to a magnetic quantum critical point. <b>2009</b> , 79,		93
2133	Magnetic structure of EuFe2As2 as determined by resonant x-ray scattering. <b>2009</b> , 80,		51
2132	Magnetic order in BaMn2As2 from neutron diffraction measurements. <b>2009</b> , 80,		126
2131	Structural and electronic properties of the 17 K superconductor Sr2ScFePO3 in comparison to Sr2ScFeAsO3 from first principles calculations. <b>2009</b> , 79,		32
2130	Effects of magnetic ordering on dynamical conductivity: Optical investigations of EuFe2As2 single crystals. <b>2009</b> , 79,		84
2129	Microstructure and tetragonal-to-orthorhombic phase transition of AFe2As2 (A=Sr,Ca) as seen via transmission electron microscopy. <b>2009</b> , 79,		26
2128	Dirac nodal pockets in the antiferromagnetic parent phase of FeAs superconductors. 2009, 80,		48
2127	Band-structure reorganization across the magnetic transition in BaFe2As2 seen via high-resolution angle-resolved photoemission. <b>2009</b> , 80,		45
2126	Superconductivity at 2.2 K in the layered oxypnictide La3Ni4P4O2. <b>2009</b> , 79,		22
2125	Magnetic, transport, and thermal properties of single crystals of the layered arsenide BaMn2As2. <b>2009</b> , 79,		93
2124	First-principles calculations of the effect of pressure on the iron-based superconductor LaFeAsO. <b>2009</b> , 80,		6
2123	Electronic phase diagram of the iron-based high-Tc superconductor Ba(Fe1âୟCox)2As2 under hydrostatic pressure (0âୟâŪ.099). <b>2009</b> , 79,		38
2122	Physical properties of the layered pnictide oxides Na2Ti2P2O (P=As,Sb). <b>2009</b> , 80,		51
2121	Inelastic neutron-scattering measurements of a three-dimensional spin resonance in the FeAs-based BaFe1.9Ni0.1As2 superconductor. <i>Physical Review Letters</i> , <b>2009</b> , 102, 107006	7.4	161

2120	resonance. <b>2009</b> , 79,	52
2119	Small anisotropy, weak thermal fluctuations, and high field superconductivity in Co-doped iron pnictide Ba(Fe1â⊠Cox)2As2. <b>2009</b> , 94, 062511	300
2118	Superconductivity in undoped single crystals of BaFe(2)As(2): field and current dependence. <b>2009</b> , 21, 342201	14
2117	Spin gap and resonance at the nesting wave vector in superconducting FeSe_{0.4}Te_{0.6}. <i>Physical Review Letters</i> , <b>2009</b> , 103, 067008	201
2116	Pressure-induced magnetic transition and volume collapse in FeAs superconductors: an orbital-selective Mott scenario. <b>2009</b> , 11, 055064	33
2115	Fabrication of the Iron-Based Superconducting Wire Using Fe(Se,Te). <b>2009</b> , 2, 083004	103
2114	Magnetoresistance in Parent Pnictide AFe 2 As 2 (A = Sr, Ba). <b>2009</b> , 26, 107401	2
2113	Conventional superconductivity in Fe-based pnictides: The relevance of intra-band electron-boson scattering. <b>2009</b> , 85, 47008	11
2112	Growth of large single crystals of BaFe1.87Co0.13As2using a nucleation pole. <b>2009</b> , 22, 105006	10
2111	The metal-insulator transition in Fe(1.01-x)Cu(x)Se. <b>2009</b> , 21, 305701	63
2110	The magnetoresistance of a PrFeAsO1â⊠Fysuperconductor. <b>2009</b> , 22, 095015	18
2109	DOPING INDUCED ELECTRONIC PHASE SEPARATION AND COULOMB BUBBLES IN LAYERED SUPERCONDUCTORS. <b>2009</b> , 23, 4198-4215	2
2108	High-T c superconductivity induced by doping rare-earth elements into CaFeAsF. <b>2009</b> , 85, 67003	73
2107	Electronic structure of heavily electron-doped BaFe1.7Co0.3As2studied by angle-resolved photoemission. <b>2009</b> , 11, 025020	114
2106	Angular and field properties of the critical current and melting line of Co-doped SrFe2As2epitaxial films. <b>2009</b> , 22, 125011	23
2105	Possible high temperature superconductivity in a Ti-doped AâBcâBeâAsâD (A = Ca, Sr) system. <b>2009</b> , 22, 072001	41
2104	High-pressure growth of fluorine-free SmFeAsO1â⊠superconducting single crystals. <b>2009</b> , 22, 075023	19
2103	Feshbach resonance and mesoscopic phase separation near a quantum critical point in multiband FeAs-based superconductors. <b>2009</b> , 22, 014004	74

2102 Successive Phase Transitions under High Pressure in FeTe0.92. <b>2009</b> , 78, 083709	49
Antiferromagnetic Fluctuations in Fe(Se1-xTex)0.92(x= 0.75, 1) Observed by Inelastic Neutron Scattering. <b>2009</b> , 78, 103704	23
Anisotropic spin fluctuations and multiple superconducting gaps in hole-doped Ba 0.72 K 0.28 As 2 : NMR in a single crystal. <b>2009</b> , 87, 27012	3 Fe 2 63
Spin Susceptibility, Phase Diagram, and Quantum Criticality in the Eelctron-Doped High Tc Superconductor Ba(Fe1-xCox)2As2. <b>2009</b> , 78, 013711	153
2098 Anisotropy of the Upper Critical Field in a Co-Doped BaFe2As2 Single Crystal. <b>2009</b> , 78, 08471	9 102
2097 Superconductivity in Layered Pnictides BaRh2P2 and BaIr2P2. <b>2009</b> , 78, 023706	38
Abrupt Emergence of Pressure-Induced Superconductivity of 34 K in SrFe2As2: A Resistivity S under Pressure. <b>2009</b> , 78, 013709	itudy 101
2095 Resistivity and Upper Critical Field in KFe2As2 Single Crystals. <b>2009</b> , 78, 063702	80
2094 A structural study of the hole-doped superconductors Pr1â\SrxFeAsO. <b>2009</b> , 11, 083003	8
The structural and physical properties of Ba(1-x)Sr(x)Fe(2)As(2) $\mathbb{I}(0)$ alk all and Ba(1-x)Sr(x)Fe(1.8)Co(0.2)As(2) $\mathbb{I}(0)$ alk all all 2009, 21, 495701	8
2092 Elastic theory for the vortex-lattice melting in iron-based high-Tcsuperconductors. <b>2009</b> , 11, 0	3
2091 Magnetic impurities in the pnictide superconductor Ba1â\(\mathbb{U}\)KxFe2As2. <b>2009</b> , 11, 055002	14
2090 First Principles Study on FeAs Single Layers. <b>2009</b> , 22, 139-142	1
Interplay between magnetism and superconductivity and the appearance of laßecond superconducting transition in⊞-FeSe at high pressure. <b>2009</b> , 21, 415701	13
2088 Superconductivity induced by Ni doping in BaFe2As2single crystals. <b>2009</b> , 11, 025008	228
Synthesis ofLnFeAsO1âysuperconductors (Ln=La and Nd) using the high-pressure technique. 2087 11, 045002	<b>2009</b> , 5
Possible Multiple Gap Superconductivity with Line Nodes in Heavily Hole-Doped Superconductivity With Line Nodes in Heavily	
Superconducting gap symmetry of Ba 0.6 K 0.4 Fe 2 As 2 studied by angle-resolved photoemis spectroscopy. <b>2009</b> , 85, 67002	ssion 183

2084	CaFeAsF. <b>2009</b> , 11, 025012	43
2083	Competition of magnetism and superconductivity in underdoped (Ba1-xKx)Fe2As2. <b>2009</b> , 11, 025014	83
2082	Pairing in the iron arsenides: a functional RG treatment. <b>2009</b> , 11, 055058	61
2081	The band structure and Fermi surface of (Sr(3)Sc(2)O(5))Fe(2)As(2). <b>2009</b> , 21, 415702	1
2080	Metamagnetic transition in EuFe2As2single crystals. <b>2009</b> , 11, 025007	89
2079	Heavy-anion solvation of polarity fluctuations in pnictides. <b>2009</b> , 86, 17006	47
2078	Effect of tetrahedral distortion on the electronic properties of iron pnictides. 2009, 11, 013051	24
2077	The superconductor KxSr1-xFe2As2: normal state and superconducting properties. <b>2009</b> , 11, 025013	31
2076	Muon spin rotation study of magnetism and superconductivity in BaFe2â\CoxAs2and Pr1â\SrxFeAsO. <b>2009</b> , 11, 055050	40
2075	Pressure Effects on Superconductivity and Magnetism in FeSe1-xTex. <b>2009</b> , 78, 084710	26
2074	Superconductivity in some heavy rare-earth iron arsenide REFeAsO1-(RE = Ho, Y, Dy and Tb) compounds. <b>2009</b> , 11, 025005	28
2073	Competition/coexisitence of magnetism and superconductivity in iron pnictides probed by muon spin rotation. <b>2009</b> , 11, 035006	22
2072	Specific heat anomalies for [Formula: see text] in superconducting single crystal doped BaFe(2)As(2): comparison of different flux growth methods. <b>2009</b> , 21, 252201	22
2071	Possible Superconductivity above 25 K in Single-Crystalline Co-Doped BaFe2As2. <b>2009</b> , 78, 023702	96
2070	High-TC superconductivity related to deep inner orbital coupling in FeAs-based compounds. <b>2009</b> , 105, 07E317	
2069	Electronic Structure of Superconducting FeSe Studied by High-Resolution Photoemission Spectroscopy. <b>2009</b> , 78, 034708	34
2068	Relationship between Structure and Superconductivity in FeSe1-xTex. <b>2009</b> , 78, 074718	85
2067	Fermi Surface in BaNi2P2. <b>2009</b> , 78, 033706	20

2066 Superconductivity in fluoride-arsenide Sr 1-x La x FeAsF compounds. <b>2009</b> , 85, 17011	53
Three-Dimensional Electronic Structure of Superconducting Iron Pnictides Observed by Angle-Resolved Photoemission Spectroscopy. <b>2009</b> , 78, 123706	61
Quantum oscillations in antiferromagnetic CaFe(2)As(2) on the brink of superconductivity. <b>2009</b> , 21, 322202	16
Superconductivity up to 30 K in the vicinity of the quantum critical point in BaFe(2)(As(1-x)P(x))(2). <b>2009</b> , 21, 382203	226
2062 Research and Prospects of Iron-Based Superconductors. <b>2009</b> , 21, 4584-4592	139
2061 Superconductivity of powder-in-tube Sr0.6K0.4Fe2As2 wires. <b>2009</b> , 469, 717-720	64
Penetration depth, lower critical fields, and quasiparticle conductivity in Fe-arsenide superconductors. <b>2009</b> , 469, 590-598	15
2059 The synthesis and characterization of LiFeAs and NaFeAs. <b>2009</b> , 469, 326-331	110
2058 BaT2As2 single crystals (T=Fe, Co, Ni) and superconductivity upon Co-doping. <b>2009</b> , 469, 350-354	34
2057 High pressure studies on Fe-pnictide superconductors. <b>2009</b> , 469, 385-395	90
Normal state transport properties in single crystals of Ba1â\(\text{NxFe2As2}\) and NdFeAsO1â\(\text{WFx}\). <b>2009</b> , 469, 477-484	18
Structural, magnetic and superconducting phase transitions in CaFe2As2 under ambient and applied pressure. <b>2009</b> , 469, 404-412	106
2054 Missbauer spectroscopy studies of oxypnictides superconductors. <b>2009</b> , 469, 485-490	30
2053 Fermi surface of Ba1â⊠KxFe2As2 as probed by angle-resolved photoemission. <b>2009</b> , 469, 448-451	24
Single crystals of LnFeAsO1â¼Fx (Ln=La, Pr, Nd, Sm, Gd) and Ba1â¼RbxFe2As2: Growth, structure and superconducting properties. <b>2009</b> , 469, 370-380	110
Electronic properties of iron arsenic high temperature superconductors revealed by angle resolved photoemission spectroscopy (ARPES). <b>2009</b> , 469, 491-497	22
2050 Electronic structure, magnetism and superconductivity of layered iron compounds. <b>2009</b> , 469, 886-889	14
2049 First-principle calculation for the phonon structure on iron-based superconductors. <b>2009</b> , 469, 1024-1026	6

2048	Sn4As3 revisited: Solvothermal synthesis and crystal and electronic structure. <b>2009</b> , 182, 630-639	22
2047	Nickel deficiency in RENi2â⊠P2 (RE=La, Ce, Pr). Combined crystallographic and physical property studies. <b>2009</b> , 182, 1473-1480	17
2046	The Tetragonal to Orthorhombic Structural Phase Transition in Multiband FeAs-based Superconductors. <b>2009</b> , 22, 305-308	19
2045	Unity in the Diversity. <b>2009</b> , 22, 527-528	6
2044	The Microstrain-Doping Phase Diagram of the Iron Pnictides: Heterostructures at Atomic Limit. <b>2009</b> , 22, 589-593	25
2043	Electron-Conduction Mechanism and Specific Heat Above Transition Temperature in LaFeAsO and BaFe2As2 Superconductors. <b>2009</b> , 22, 785-789	8
2042	Tunneling Conductance of Ba1â⊠ K x Fe2As2â©aAs Junction. <b>2009</b> , 22, 719-722	2
2041	Quest for new materials: Inorganic chemistry plays a crucial role. <b>2009</b> , 121, 235-256	3
2040	Superconductivity in Ba1â⊠ Sm x FFeAs and Eu1â⊠ Sm x FFeAs systems. <b>2009</b> , 54, 1872-1875	1
2039	Band structure, Fermi surface, and superconducting gap in FeAs-based superconductors revealed by angle-resolved photoemission spectroscopy. <b>2009</b> , 4, 427-432	4
2038	The Layered Iron Arsenide Oxides Sr2CrO3FeAs and Ba2ScO3FeAs. <b>2009</b> , 635, 2242-2248	27
2037	Nearly isotropic superconductivity in (Ba,K)Fe(2)As(2). <b>2009</b> , 457, 565-8	420
2036	Similarities between structural distortions under pressure and chemical doping in superconducting BaFe2As2. <b>2009</b> , 8, 471-5	243
2035	A key role for unusual spin dynamics in ferropnictides. <b>2009</b> , 5, 141-145	237
2034	Spin waves and magnetic exchange interactions in CaFe2As2. <b>2009</b> , 5, 555-560	331
2033	Normal-state electrical resistivity and superconducting magnetic penetration depth in Eu0.5K0.5Fe2As2 polycrystals. <b>2009</b> , 89, 294-297	8
2032	Transport properties and the anisotropy of Ba1 âlk K x Fe2As2 single crystals in normal and superconducting states. <b>2009</b> , 90, 130-133	12
2031	Unconventional superconductivity originating from disconnected Fermi surfaces in the iron-based compound. <b>2009</b> , 404, 700-705	5

2030	Two gap superconductivity inBa0.55K0.45Fe2As2single crystals studied by the directional point-contact Andreev reflection spectroscopy. <b>2009</b> , 404, 3220-3222	1
2029	Electronic and magnetic properties of 3d transition-metal selenides from first principles. <b>2009</b> , 149, 505-509	19
2028	Superconductivity and single crystal growth of Ni0.05TaS2. <b>2009</b> , 149, 1296-1299	11
2027	Structural, electronic properties and intra-atomic bonding in new ThCr2Si2-like arsenides SrRu2As2, BaRu2As2, SrRh2As2 and BaRh2As2 from first principles calculations. <b>2009</b> , 149, 1860-1865	17
2026	Atomically-flat, chemically-stable, superconducting epitaxial thin film of iron-based superconductor, cobalt-doped BaFe2As2. <b>2009</b> , 149, 2121-2124	65
2025	Growth of NdFeAs(O1â⊠Fx) single crystals at ambient pressure and their transport properties. <b>2009</b> , 311, 358-361	20
2024	Elastic properties and chemical bonding in ternary arsenide SrFe2As2 and quaternary oxyarsenide LaFeAsO âlBasic phases for new 38âB5K superconductors from first principles. <b>2009</b> , 469, 15-19	32
2023	Novel superconducting characteristics and unusual normal-state properties in iron-based pnictide superconductors: 57FeNMR and 75AsNQR/NMR studies in REFeAsO1â¶ (RE=La, Pr, Nd) and Ba0.6K0.4Fe2As2. <b>2009</b> , 469, 559-565	23
2022	Specific heat and phase diagrams of single crystal iron pnictide superconductors. <b>2009</b> , 469, 575-581	17
2021	Anisotropic London penetration depth and superfluid density in single crystals of iron-based pnictide superconductors. <b>2009</b> , 469, 582-589	53
2020	Two classes of superconductors discovered in our material research: Iron-based high temperature superconductor and electride superconductor. <b>2009</b> , 469, 314-325	45
2019	Temperature dependence of the lower critical field Hc1 in SmFeASO0.9F0.1 and Ba0.6K0.4Fe2As2 iron-arsenide superconductors. <b>2009</b> , 469, 599-605	20
2018	Superconductivity, magnetism and crystal chemistry of Ba1â¼KxFe2As2. <b>2009</b> , 469, 332-339	55
2017	Pairing symmetry and pairing state in ferropnictides: Theoretical overview. <b>2009</b> , 469, 614-627	334
2016	Heteroepitaxial film growth of layered compounds with the ZrCuSiAs-type and ThCr2Si2-type structures: From Cu-based semiconductors to Fe-based superconductors. <b>2009</b> , 469, 657-666	37
2015	Doping âlDependent irreversible magnetic properties of Ba(Fe1âlCox)2As2 single crystals. <b>2009</b> , 469, 667-673	34
2014	Parent phase and superconductors in the fluorine derivative family. <b>2009</b> , 469, 381-384	15
2013	Ni2X2 (X = pnictide, chalcogenide, or B) based superconductors. <b>2009</b> , 469, 396-403	51

2012 Electronic structure of Fe-based superconductors. <b>2009</b> , 469, 418-424	117
Point contact Andreev reflection spectroscopy of superconducting energy gaps in 122-type family of iron pnictides. <b>2009</b> , 469, 507-511	58
Determination of superconducting gap of SmFeAsFxO1âld superconductors by Andreev reflection spectroscopy. <b>2009</b> , 469, 521-528	20
2009 Vortex imaging in Co-doped BaFe2As2. <b>2009</b> , 469, 529-534	27
2008 Optical and Raman spectroscopy studies on Fe-based superconductors. <b>2009</b> , 469, 545-558	44
2007 Scanning tunneling microscopy and spectroscopy on iron-pnictides. <b>2009</b> , 469, 535-544	38
2006 Superconductivity in the hole-doped oxy-arsenide RE1â\SrxFeAsO (RE=La, Pr). <b>2009</b> , 469, 894-897	5
2005 Transport properties of single crystal BaNi2P2. <b>2009</b> , 469, 905-907	1
2004 Magneto-optical imaging of iron-oxypnictide SmFeAsO1â⊠Fx and SmFeAsO1â☑. <b>2009</b> , 469, 915-920	27
2003 FeTe as a candidate material for new iron-based superconductor. <b>2009</b> , 469, 1027-1029	61
2002 Superconductivity induced by doping Ru in SrFe2â\RuxAs2. 2009, 469, 1921-1924	16
2001 The first-principles studying LaOMnSe: A possible parent compound of superconductor. <b>2009</b> , 374, 351-354	4
2000 Suppression of spin density wave by isoelectronic substitution in PrFe1-xRuxAsO. 2009, 182, 2326-2331	36
1999 Superconductivity in Ti-doped iron-arsenide compound Sr4Cr0.8Ti1.2O6Fe2As2. <b>2009</b> , 52, 1876-1878	7
Electronic structure and unusual exchange splitting in the spin-density-wave state of the BaFe2As2 parent compound of iron-based superconductors. <i>Physical Review Letters</i> , <b>2009</b> , 102, 107002	137
1997 Charge dynamics of the spin-density-wave state in BaFe2As2. <b>2009</b> , 67, 513-517	23
1996 Synthesis and physical properties of LaO1-xFxFeAs. <b>2009</b> , 70, 461-468	41
1995 Extreme sensitivity of superconductivity to stoichiometry in Fe1+Be. <b>2009</b> , 79,	530

1994	Structural phase transitions and superconductivity in Fe(1+delta)Se0.57Te0.43 at ambient and elevated pressures. <b>2009</b> , 131, 16944-52		96
1993	Superconductivity of FeSe0.89crystal with hexagonal and tetragonal structures. <b>2009</b> , 22, 075016		24
1992	Substitution Effects on FeSe Superconductor. <b>2009</b> , 78, 074712		280
1991	Coexistence of the spin-density wave and superconductivity in Ba 1â⊠ K x Fe 2 As 2. <b>2009</b> , 85, 17006		296
1990	Superconducting fluctuations in the reversible magnetization of the iron-pnictide Ba1â⊠KxFe2As2. <b>2009</b> , 80,		27
1989	Two-gap superconductivity in the Fe-1111 superconductor LaFeAsO1即 Fx: A point-contact Andreev-reflection study. <b>2009</b> , 7,		7
1988	Suppression of superconductivity in FeSe films under tensile strain. <b>2009</b> , 94, 242505		89
1987	Fermi surface nesting induced strong pairing in iron-based superconductors. <b>2009</b> , 106, 7330-3		294
1986	Angle-resolved photoemission spectroscopy of the Fe-Based Ba0.6K0.4Fe2As2 high temperature superconductor: evidence for an orbital selective electron-mode coupling. <i>Physical Review Letters</i> , <b>2009</b> , 102, 047003	7-4	65
1985	Determination of the phase diagram of the electron-doped superconductor Ba(Fe1â\(\mathbb{U}\)Cox)2As2. <b>2009</b> , 79,		447
1984	Absence of superconductivity in hole-doped BaFe2â\(\mathbb{Q}\)CrxAs2 single crystals. <b>2009</b> , 79,		94
1983	Decoupling of the superconducting and magnetic/structural phase transitions in electron-doped BaFe2As2. <b>2009</b> , 80,		174
1982	Superconducting and ferromagnetic phases induced by lattice distortions in stoichiometric SrFe2As2 single crystals. <i>Physical Review Letters</i> , <b>2009</b> , 103, 037005	7.4	86
1981	CaFe4As3: a metallic iron arsenide with anisotropic magnetic and charge-transport properties. <b>2009</b> , 131, 5405-7		29
1980	Zero-resistance superconducting phase in BaFe2As2 under high pressure. <b>2009</b> , 79,		54
1979	Absence of superconductivity in single-phase CaFe2As2 under hydrostatic pressure. <b>2009</b> , 79,		146
1978	Sr3Sc2Fe2As2O5 as a possible parent compound for FeAs-based superconductors. <b>2009</b> , 79,		124
1977	New iron-based arsenide oxides (Fe2As2)(Sr4M2O6)(M = Sc, Cr). <b>2009</b> , 22, 085001		69

1976	Spontaneous formation of a superconducting and antiferromagnetic hybrid state in SrFe2As2 under high pressure. <i>Physical Review Letters</i> , <b>2009</b> , 103, 257002	7.4	48
1975	First-Principles Study for the Anisotropy of Iron-Based Superconductors toward Power and Device Applications. <b>2009</b> , 78, 123712		42
1974	Structure, antiferromagnetism and superconductivity of the layered iron arsenide NaFeAs. <b>2009</b> , 2189	-91	178
1973	Superconductivity in SrPd2Ge2. <b>2009</b> , 79,		43
1972	Scanning tunneling spectroscopy and vortex imaging in the iron pnictide superconductor BaFe1.8Co0.2As2. <i>Physical Review Letters</i> , <b>2009</b> , 102, 097002	7.4	221
1971	Coexistence of competing antiferromagnetic and superconducting phases in the underdoped Ba(Fe0.953Co0.047)2As2 compound using x-ray and neutron scattering techniques. <i>Physical Review Letters</i> , <b>2009</b> , 103, 087001	7.4	271
1970	Band structure and fermi surface of an extremely overdoped iron-based superconductor KFe2As2. <i>Physical Review Letters</i> , <b>2009</b> , 103, 047002	7.4	182
1969	Effects of two gaps and paramagnetic pair breaking on the upper critical field of SmFeAsO0.85 and SmFeAsO0.8F0.2 single crystals. <b>2009</b> , 80,		79
1968	Anisotropy in the electrical resistivity and susceptibility of superconducting BaFe2As2 single crystals. <i>Physical Review Letters</i> , <b>2009</b> , 102, 117005	7.4	210
1967	Magnetic, thermal, and transport properties of layered arsenides BaRu2As2 and SrRu2As2. <b>2009</b> , 79,		29
	Tabananal barathada ankin sharabaral ahara bara 200 ay 100 Million ay ay ay 1 day 5 /4 00/2		
1966	Tetragonal-to-orthorhombic structural phase transition at 90 K in the superconductor Fe(1.01)Se. <i>Physical Review Letters</i> , <b>2009</b> , 103, 057002	7.4	371
		7.4	15
	Physical Review Letters, 2009, 103, 057002	7·4 7·4	
1965	Physical Review Letters, 2009, 103, 057002  Crystal structure of ternary germanides SrM2Ge2 (M=Ni and Ir). 2009, 487, 198-201  Electronic phase separation in the slightly underdoped iron pnictide superconductor		15
1965 1964	Crystal structure of ternary germanides SrM2Ge2 (M=Ni and Ir). 2009, 487, 198-201  Electronic phase separation in the slightly underdoped iron pnictide superconductor Ba1-xKxFe2As2. Physical Review Letters, 2009, 102, 117006		15 185
1965 1964 1963	Crystal structure of ternary germanides SrM2Ge2 (M=Ni and Ir). 2009, 487, 198-201  Electronic phase separation in the slightly underdoped iron pnictide superconductor Ba1-xKxFe2As2. Physical Review Letters, 2009, 102, 117006  Superconductivity in S-substituted FeTe. 2009, 94, 012503  Tunable (deltapi, deltapi)-type antiferromagnetic order in alpha-Fe(Te,Se) superconductors.	7.4	15 185 245
1965 1964 1963 1962	Crystal structure of ternary germanides SrM2Ge2 (M=Ni and Ir). 2009, 487, 198-201  Electronic phase separation in the slightly underdoped iron pnictide superconductor Ba1-xKxFe2As2. Physical Review Letters, 2009, 102, 117006  Superconductivity in S-substituted FeTe. 2009, 94, 012503  Tunable (deltapi, deltapi)-type antiferromagnetic order in alpha-Fe(Te,Se) superconductors. Physical Review Letters, 2009, 102, 247001	7.4	15 185 245 559
1965 1964 1963 1962	Crystal structure of ternary germanides SrM2Ge2 (M=Ni and Ir). 2009, 487, 198-201  Electronic phase separation in the slightly underdoped iron pnictide superconductor Ba1-xKxFe2As2. Physical Review Letters, 2009, 102, 117006  Superconductivity in S-substituted FeTe. 2009, 94, 012503  Tunable (deltapi, deltapi)-type antiferromagnetic order in alpha-Fe(Te,Se) superconductors. Physical Review Letters, 2009, 102, 247001  Anisotropic thermal expansion of Fe1.06Te and FeTe0.5Se0.5 single crystals. 2009, 80,	7.4	15 185 245 559

1958	Three-band s∃ Eliashberg theory and the superconducting gaps of iron pnictides. <b>2009</b> , 80,	51
1957	New compounds and structures in the solid state. <b>2009</b> , 105, 348	O
1956	FestkEperchemie 2008. <b>2009</b> , 57, 239-251	3
1955	Pressure evolution of the low-temperature crystal structure and bonding of the superconductor FeSe (Tc=37 K). <b>2009</b> , 80,	485
1954	Pressure-induced superconducting state of antiferromagnetic CaFe2As2. <b>2009</b> , 80,	55
1953	Synthesis, crystal structure, and chemical stability of the superconductor FeSe1â⊠. <b>2009</b> , 80,	124
1952	Bulk superconductivity at 14 K in single crystals of Fe1+yTexSe1â⊠. <b>2009</b> , 79,	360
1951	Superconductivity and magnetism in K-doped EuFe(2)As(2). <b>2009</b> , 21, 265701	29
1950	Response of superconductivity and crystal structure of LiFeAs to hydrostatic pressure. <b>2009</b> , 131, 2986-92	49
1949	Heat capacity measurements on FeAs-based compounds: a thermodynamic probe of electronic and magnetic states. <b>2009</b> , 11, 025010	33
1948	High-temperature superconductivity (T c onset at 34 K) in the high-pressure orthorhombic phase of FeSe. <b>2009</b> , 86, 27001	100
1947	Ir doping-induced superconductivity in the SmFeAsO system. <b>2009</b> , 131, 10338-9	29
1946	Tight-binding model for iron pnictides. <b>2009</b> , 80,	47
1945	High-resolution measurements of the thermal expansion of superconducting Co-doped BaFe2As2. <b>2009</b> , 79,	31
1944	Thermal expansion and anisotropic pressure derivatives of Tc in Ba(Fe1â\(\mathbb{U}\)Cox)2As2 single crystals. <b>2009</b> , 79,	54
1943	Magnetic and Transport Properties of FeAs Single Crystals. <b>2009</b> , 78, 104720	24
1942	Functional renormalization-group study of the doping dependence of pairing symmetry in the iron pnictide superconductors. <b>2009</b> , 80,	98
1941	Conducting solids. <b>2009</b> , 105, 436	1

1940	Three- to two-dimensional transition of the electronic structure in CaFe2As2: a parent compound for an iron arsenic high-temperature superconductor. <i>Physical Review Letters</i> , <b>2009</b> , 102, 167004	7.4	71
1939	Superconductivity inLnFePO (Ln= La, Pr and Nd) single crystals. 2009, 11, 025018		37
1938	Superconductivity induced by phosphorus doping and its coexistence with ferromagnetism in EuFe2(As0.7P0.3)(2). <i>Physical Review Letters</i> , <b>2009</b> , 102, 137002	7.4	224
1937	Pnictogen height as a possible switch between high-Tc nodeless and low-Tc nodal pairings in the iron-based superconductors. <b>2009</b> , 79,		580
1936	Measurement of anomalous phonon dispersion of CaFe2As2 single crystals using inelastic neutron scattering. <i>Physical Review Letters</i> , <b>2009</b> , 102, 217001	7.4	39
1935	Suppression of the structural phase transition and lattice softening in slightly underdoped Ba1â\( KxFe2As2\) with electronic phase separation. <b>2009</b> , 79,		35
1934	Effect of external pressure on the Fe magnetic moment in undoped LaFeAsO from density functional theory: Proximity to a magnetic instability. <b>2009</b> , 79,		35
1933	Effect of pressure on the iron arsenide superconductor LixFeAs (x=0.8,1.0,1.1). <b>2009</b> , 80,		60
1932	Superconductivity at 31 K in the âll11âltype iron arsenide superconductor Na 1âll FeAs induced by pressure. <b>2009</b> , 88, 47008		39
			_
1931	Superconducting FeSe1âNTex Single Crystals Grown by Optical Zone-Melting Technique. <b>2009</b> , 9, 4847-4	4851	54
	Superconducting FeSe1â\(\text{Tex Single Crystals Grown by Optical Zone-Melting Technique. 2009, 9, 4847-45.}\) Superconductivity at Tc~14 K in single-crystalline FeTe0.61Se0.39. 2009, 80,	4851	54 162
		4851	
1930	Superconductivity at Tc~14 K in single-crystalline FeTe0.61Se0.39. <b>2009</b> , 80,  Neutron scattering study of the interplay between structure and magnetism in Ba(Fe1â\( \text{VC}\) Cox)2As2.	4851	162
1930 1929	Superconductivity at Tc~14 K in single-crystalline FeTe0.61Se0.39. <b>2009</b> , 80,  Neutron scattering study of the interplay between structure and magnetism in Ba(Fe1â\(\text{MC}\)Cox)2As2. <b>2009</b> , 79,  Itinerant antiferromagnetism in BaCr2As2: Experimental characterization and electronic structure	4851	162 162
1930 1929 1928	Superconductivity at Tc~14 K in single-crystalline FeTe0.61Se0.39. <b>2009</b> , 80,  Neutron scattering study of the interplay between structure and magnetism in Ba(Fe1â\( \text{MCox} \))2As2. <b>2009</b> , 79,  Itinerant antiferromagnetism in BaCr2As2: Experimental characterization and electronic structure calculations. <b>2009</b> , 79,	4851	<ul><li>162</li><li>162</li><li>56</li></ul>
1930 1929 1928	Superconductivity at Tc~14 K in single-crystalline FeTe0.61Se0.39. 2009, 80,  Neutron scattering study of the interplay between structure and magnetism in Ba(Fe1â⊠Cox)2As2. 2009, 79,  Itinerant antiferromagnetism in BaCr2As2: Experimental characterization and electronic structure calculations. 2009, 79,  The peculiar physical properties and phase diagram of BaFe2-xCoxAs2single crystals. 2009, 11, 045003  Evolution of the bulk properties, structure, magnetic order, and superconductivity with Ni doping	7·4	<ul><li>162</li><li>162</li><li>56</li><li>93</li></ul>
1930 1929 1928 1927	Superconductivity at Tc~14 K in single-crystalline FeTe0.61Se0.39. 2009, 80,  Neutron scattering study of the interplay between structure and magnetism in Ba(Fe1â\( \text{SC}\) (2As2. 2009, 79,  Itinerant antiferromagnetism in BaCr2As2: Experimental characterization and electronic structure calculations. 2009, 79,  The peculiar physical properties and phase diagram of BaFe2-xCoxAs2single crystals. 2009, 11, 045003  Evolution of the bulk properties, structure, magnetic order, and superconductivity with Ni doping in CaFe2â\( \text{NixAs2}\). 2009, 80,		<ul><li>162</li><li>162</li><li>56</li><li>93</li><li>36</li></ul>

1922	Phase diagrams of Ba(Fe1â⊠Mx)2As2 single crystals (M=Rh and Pd). <b>2009</b> , 80,	151
1921	Jump in specific heat at the superconducting transition temperature in Ba(Fe1â⊠Cox)2As2 and Ba(Fe1â⊠Nix)2As2 single crystals. <b>2009</b> , 79,	137
1920	Superconductivity at 17 K in (Fe2P2)(Sr4Sc2O6): a new superconducting layered pnictide oxide with a thick perovskite oxide layer. <b>2009</b> , 22, 075008	204
1919	Preparation and superconductivity of iron selenide thin films. <b>2009</b> , 21, 235702	58
1918	Neutron scattering investigation of the magnetic order in single crystalline BaFe2As2. <b>2009</b> , 11, 055001	37
1917	Density functional study of excess Fe in Fe1+xTe: Magnetism and doping. <b>2009</b> , 79,	149
1916	Effects of pressure on the electronic and structural properties of LaOFeAs. <b>2009</b> , 106, 073910	8
1915	Evidence of magnetically driven structural phase transition in RFeAsO (R=La, Sm, Gd, and Tb): A low-temperature x-ray diffraction study. <b>2009</b> , 80,	31
1914	Response of the Crystal Structure and Electronic Properties to Calcium Substitution in NdFeAsO. <b>2009</b> , 21, 2967-2972	17
1913	Superconductivity up to 29 K in SrFe(2)As(2) and BaFe(2)As(2) at high pressures. <b>2009</b> , 21, 012208	361
1912	A new âll 11âltype iron pnictide superconductor LiFeP. <b>2009</b> , 87, 37004	70
1911	Zintl phase as dopant source in the flux synthesis of Ba(1-x)K(x)Fe(2)As(2) type superconductors. <b>2009</b> , 4965-7	13
1910	To What Extent Iron-Pnictide New Superconductors Have Been Clarified: A Progress Report. <b>2009</b> , 78, 062001	632
1909	Structural models of FeSe(x). <b>2009</b> , 21, 435702	4
1909 1908	Structural models of FeSe(x). 2009, 21, 435702  Upper Critical Fields of the 11-System Iron-Chalcogenide Superconductor FeSe0.25Te0.75. 2009, 78, 113701	78
	Upper Critical Fields of the 11-System Iron-Chalcogenide Superconductor FeSe0.25Te0.75. <b>2009</b> ,	
1908	Upper Critical Fields of the 11-System Iron-Chalcogenide Superconductor FeSe0.25Te0.75. <b>2009</b> , 78, 113701	78

1904	Electronic properties, band structure, and fermi surface instabilities of Ni1+/Ni2+ nickelate La3Ni2O6, isoelectronic with superconducting cuprates. <i>Physical Review Letters</i> , <b>2009</b> , 102, 046405	35
1903	Superconductivity at 23 K and low anisotropy in Rb-substituted BaFe2As2 single crystals. <b>2009</b> , 79,	52
1902	Substitution-induced superconductivity in SrFe2â⊠RuxAs2 (0â⊠âӢ). <b>2009</b> , 79,	68
1901	Superconductivity, magnetism, and stoichiometry of single crystals of Fe1+y(Te1â⊠Sx)z. <b>2009</b> , 80,	96
1900	AFe2As2(A = Ca, Sr, Ba, Eu) and SrFe2-xTMxAs2(TM = Mn, Co, Ni): crystal structure, charge doping, magnetism and superconductivity. <b>2009</b> , 11, 025023	126
1899	First-principles calculations of the electronic structure of tetragonal alpha-FeTe and alpha-FeSe crystals: evidence for a bicollinear antiferromagnetic order. <i>Physical Review Letters</i> , <b>2009</b> , 102, 177003 7.4	242
1898	Transition of stoichiometric Sr2VO3FeAs to a superconducting state at 37.2 K. <b>2009</b> , 79,	267
1897	Antiferromagnetism of SrFe2As2 Studied by Single-Crystal 75As-NMR. <b>2009</b> , 78, 063706	61
1896	Pressure-induced superconductivity in BaFe 2 As 2 single crystal. <b>2009</b> , 87, 17004	73
1895	Fabrication of Feâlleâß Superconducting Epitaxial Thin Films by Pulsed Laser Deposition. <b>2009</b> , 2, 073002	29
1894	Vortices in superconducting Ba(Fe0.93Co0.07)2As2 studied via small-angle neutron scattering and Bitter decoration. <b>2009</b> , 79,	46
1893	Interplay between magnetic properties and Fermi surface nesting in iron pnictides. <b>2009</b> , 79,	78
1892	Anomalous Pressure Dependence of the Superconducting Transition Temperature in FeSe1-xStudied by DC Magnetic Measurements. <b>2009</b> , 78, 093703	28
1891	Pressure-Induced Superconductivity in Iron Pnictide Compound SrFe2As2. <b>2009</b> , 78, 025001	68
1890	Fabrication of Iron-based Superconducting Wire. <b>2009</b> , 48, 520-521	
1889	Two-Dimensional Spin Density Wave State in LaFeAsO. <b>2009</b> , 78, 043705	37
1888	75As NMR Study of Hole-Doped Superconductor Ba1-xKxFe2As2 (Tc?38 K). <b>2009</b> , 78, 033704	98
1887	Full Gap Superconductivity in Ba0.6K0.4Fe2As2 Probed by Muon Spin Rotation. <b>2009</b> , 78, 023710	34

1886	Iron-based superconductors. <b>2009</b> , 62, 36-40	22
1885	Possible strong electron-lattice interaction and giant magneto-elastic effects in Fe-pnictides. <b>2009</b> , 87, 17007	9
1884	Polaron-like conduction in iron pnictides of the Ln-1111 and £122 families. <b>2009</b> , 88, 37004	7
1883	A novel nonâ <b>B</b> ermi-liquid state in the iron-pnictide FeCrAs. <b>2009</b> , 85, 17009	29
1882	Pairing symmetry and properties of iron-based high-temperature superconductors. <b>2009</b> , 85, 57007	36
1881	Isotope Effect in Multi-Band and Multi-Channel Attractive Systems and Inverse Isotope Effect in Iron-Based Superconductors. <b>2009</b> , 78, 094718	26
1880	Perturbation Theory of High-Tc Superconductivity in Iron Pnictides. <b>2009</b> , 78, 034716	28
1879	Evidence for coexistence of superconductivity and magnetism in single@rystals of Co-doped SrFe(2)As(2). <b>2009</b> , 21, 102203	13
1878	Structure and physical properties of the new layered oxypnictides Sr 4 Sc 2 O 6 M 2 As 2 (M=Fe and Co). <b>2009</b> , 86, 57007	23
1877	EuFe2As2 under High Pressure: An Antiferromagnetic Bulk Superconductor. <b>2009</b> , 78, 083701	103
• • • • • • • • • • • • • • • • • • • •	EuFe2As2 under High Pressure: An Antiferromagnetic Bulk Superconductor. <b>2009</b> , 78, 083701  Contrasting Pressure Effects in Sr2VFeAsO3and Sr2ScFePO3. <b>2009</b> , 78, 123707	103
1876		
1876	Contrasting Pressure Effects in Sr2VFeAsO3and Sr2ScFePO3. <b>2009</b> , 78, 123707	40
1876 1875	Contrasting Pressure Effects in Sr2VFeAsO3and Sr2ScFePO3. <b>2009</b> , 78, 123707  Multiorbital Effects on Antiferromagnetism in Fe Pnictides. <b>2009</b> , 78, 083704  New Series of Nickel-Based Pnictide Oxide Superconductors (Ni2Pn2)(Sr4Sc2O6) (Pn= P, As). <b>2009</b> ,	40
1876 1875 1874	Contrasting Pressure Effects in Sr2VFeAsO3and Sr2ScFePO3. <b>2009</b> , 78, 123707  Multiorbital Effects on Antiferromagnetism in Fe Pnictides. <b>2009</b> , 78, 083704  New Series of Nickel-Based Pnictide Oxide Superconductors (Ni2Pn2)(Sr4Sc2O6) (Pn= P, As). <b>2009</b> , 2, 063007  Strong-Coupling Spin-Singlet Superconductivity with Multiple Full Gaps in Hole-Doped	40 29 15
1876 1875 1874 1873	Contrasting Pressure Effects in Sr2VFeAsO3and Sr2ScFePO3. 2009, 78, 123707  Multiorbital Effects on Antiferromagnetism in Fe Pnictides. 2009, 78, 083704  New Series of Nickel-Based Pnictide Oxide Superconductors (Ni2Pn2)(Sr4Sc2O6) (Pn= P, As). 2009, 2, 063007  Strong-Coupling Spin-Singlet Superconductivity with Multiple Full Gaps in Hole-Doped Ba0.6K0.4Fe2As2Probed by57Fe-NMR. 2009, 78, 103702	40 29 15 96
1876 1875 1874 1873	Contrasting Pressure Effects in Sr2VFeAsO3and Sr2ScFePO3. 2009, 78, 123707  Multiorbital Effects on Antiferromagnetism in Fe Pnictides. 2009, 78, 083704  New Series of Nickel-Based Pnictide Oxide Superconductors (Ni2Pn2)(Sr4Sc2O6) (Pn= P, As). 2009, 2, 063007  Strong-Coupling Spin-Singlet Superconductivity with Multiple Full Gaps in Hole-Doped Ba0.6K0.4Fe2As2Probed by57Fe-NMR. 2009, 78, 103702  Electrical resistivity measurements under high pressure for FeTe0.92. 2010, 200, 012196	40 29 15 96

1868	Anomalous phonons in CaFe2As2explored by inelastic neutron scattering. <b>2010</b> , 251, 012008	2
1867	Superconductivity in SmFe 1-x M x ASO (M = Co, Rh, Ir). <b>2010</b> , 89, 67007	10
1866	Superconductivity and magnetism in Eu1â⊠KxFe2As2. <b>2010</b> , 200, 012060	7
1865	75As-NMR study of the iron pnictide Ba1â⊠KxFe2As2under high pressure. <b>2010</b> , 215, 012041	4
1864	Critical current characteristics and history dependence in superconducting SmFeAsOF bulk. <b>2010</b> , 234, 012028	2
1863	Synthesis of High-Density Polycrystalline (Ba, K)Fe2As2 Superconductor and Its Critical Properties. <b>2010</b> , 74, 453-459	1
1862	Origin of Tc Enhancement Induced by Doping Yttrium and Hydrogen into LaFeAsO-Based Superconductors: 57Fe-, 75As-, 139La-, and 1H-NMR Studies. <b>2010</b> , 79, 103703	17
1861	Magnetic and Structural Phase Transitions of EuFe2As2 Studied via Neutron and Resonant X-ray Scattering. <b>2010</b> , 79, 114708	14
1860	Effect of K Doping on Phonons in Ba1-xKxFe2As2. <b>2010</b> , 79, 014714	12
1859	Pressure-Induced Superconductivity in Eu0.5Ca0.5Fe2As2: Wide Zero-Resistivity Region Due to Suppression of Eu Magnetic Order and Chemical Pressure. <b>2010</b> , 79, 073704	8
1858	Evidence for Anisotropic Vortex Dynamics and Pauli Limitation in the Upper Critical Field of FeSe1-xTex. <b>2010</b> , 79, 053703	46
1857	Weak Superconducting Fluctuations and Small Anisotropy of the Upper Critical Fields in an Fe1.05Te0.85Se0.15 Single Crystal. <b>2010</b> , 79, 074706	21
1856	Spectroscopic Study of 75As and 139La NMR on Layered Structure Ferromagnet LaCoAsO. <b>2010</b> , 79, 054703	16
1855	Magnetic Properties of Single Crystals of Pseudobinary Fe1-xCoxTe0.85 System. <b>2010</b> , 57, 166-171	
1854	Iron pages of HTSC. <b>2010</b> , 111, 313-331	11
1853	Will the iron age of superconductivity become the M\( \text{S}\) sbauer age?. <b>2010</b> , 74, 330-334	1
1852	Electronic structure of Ti-doped Sr4Sc2Fe2As2O6 as a possible parent phase for the new FeAs superconductors. <b>2010</b> , 8,	5
1851	Tunneling spectroscopy of layered superconductors: intercalated Li0.48(C4H8O)xHfNCl and De-intercalated HfNCl0.7. <b>2010</b> , 73, 471-482	14

1850	Synthesis, structural and physical properties of affected -x. <b>2010</b> , 77, 101-107	12
1849	Towards a better understanding of superconductivity at high transition temperatures. <b>2010</b> , 188, 3-14	4
1848	Phase diagram of the NdFe1â⊠Rhx AsO superconductor. <b>2010</b> , 4, 67-69	2
1847	Density of phonon states in superconducting FeSe as a function of temperature and pressure. <b>2010</b> , 81,	34
1846	Crystal and electronic structure of FeSe at high pressure and low temperature. <b>2010</b> , 114, 12597-606	73
1845	Anisotropic fluctuations and quasiparticle excitations in FeSe0.5Te0.5. <b>2010</b> , 82,	27
1844	Pressure dependence of phonon modes across the tetragonal to collapsed-tetragonal phase transition in CaFe2As2. <b>2010</b> , 81,	13
1843	Pressure effects on FeSe family superconductors. <b>2010</b> , 470, S353-S355	13
1842	Air-exposure effects of superconductivity in Fe(Te, S). <b>2010</b> , 470, S340-S341	13
1841	Superfluid density of Ba(Fe1-xMx)2As2 from optical experiments. <b>2010</b> , 470, S399-S400	10
1840	Superconductivity in 4d and 5d transition metal layered pnictides BaRh2P2, BaIr2P2 and SrIr2As2. <b>2010</b> , 470, S296-S297	22
1839	75As NMR studies of superconducting Ba0.72K0.28Fe2As2. <b>2010</b> , 470, S495-S496	
1838	Large transport critical currents of powder-in-tube Sr0.6K0.4Fe2As2/Ag superconducting wires and tapes. <b>2010</b> , 470, 183-186	68
1837	New superconducting RbFe2As2: A first-principles investigation. <b>2010</b> , 470, 202-205	6
1836	Critical current properties of Ag added Sr0.6K0.4Fe2As2. <b>2010</b> , 470, S413-S415	1
1835	Two-dimensionality of electronic structure and strong Fermi surface nesting in highly anisotropic iron-based superconductors. <b>2010</b> , 470, 1002-1006	4
1834	MBE growth of FeSe and Sr1â⊠KxFe2As2. <b>2010</b> , 470, 1468-1472	31
1833	Effect of bond length and radius on superconducting transition temperature for FeAs-based superconductors. <b>2010</b> , 53, 59-63	3

1832	Heat treatment effects on the superconducting properties of Ag-doped SrKFeAs compounds. <b>2010</b> , 53, 1187-1193	3
1831	Cobalt-doping effects in single crystalline and polycrystalline EuFe2âর Co x As2 compounds. <b>2010</b> , 53, 1212-1215	5
1830	Low temperature properties of pnictide CrAs single crystal. <b>2010</b> , 53, 1207-1211	20
1829	Effect of annealing on superconductivity in Fe1+y (Te1â⊠ S x ) system. <b>2010</b> , 53, 1216-1220	4
1828	Structural and transport properties of Sr2VO3âlFeAs superconductors with different oxygen deficiencies. <b>2010</b> , 53, 1202-1206	18
1827	Superconductivity and normal state magnetoresistance in superconducting FeSe:Sb. 2010, 53, 1180-1186	2
1826	Electronic structures of ternary iron arsenides AFe2As2 (A = Ba, Ca, or Sr). <b>2010</b> , 5, 150-160	60
1825	High-Field Studies on Single Crystals of EuFe2As2. <b>2010</b> , 159, 601-605	11
1824	Orbital-Selective Mott Transitions: Heavy Fermions and Beyond. <b>2010</b> , 161, 203-232	54
1823	Critical Current Densities and Vortex Dynamics in Ba(Fe1â⊠ Co x )2As2 Single Crystals. <b>2010</b> , 23, 605-608	
1822	Structural and Physical Properties of Ca1â\\ Sr x Fe2As2 (0â\\\\\\\\\\\\\\\\\\\\\\\\\\\\\\\\\\\\	2
1821	Probing the Superconducting Gap from Tunneling Conductance on NdFeAsO0.7 with T C=51 K. <b>2010</b> , 23, 575-578	10
1820	The Doping Effect on the Lattices and Electronic Structure in Superconducting Fe-based Compounds Sr1â⊠ K x Fe2As2. <b>2010</b> , 23, 985-988	
1819	Magnetic Properties and Superconductivity in GdFeAsO1â⊠ F x. <b>2010</b> , 23, 625-628	6
1818	The Effects of Pressure on the âd 11â Euperconductor. <b>2010</b> , 23, 587-589	
1817	Multiple Superconducting Gaps and Anisotropic Spin Fluctuations in Hole-Doped and Electron-Doped Iron-Pnictides: NMR Studies. <b>2010</b> , 23, 609-612	
1816	Band structure and density of states in the normal state of FeSe, Fe2Se2, Fe2Se1 and Fe2SeTe superconductors. <b>2010</b> , 124, 876-879	2
1815	Synthesis of LaRhAsO and superconductivity within the LaFe1âNRhxAsO system. <b>2010</b> , 45, 392-395	15

1814	Direct Physical Imaging and Chemical Probing of LiFePO4 for Lithium-Ion Batteries. <b>2010</b> , 20, 4219-4232	37
1813	New oxypnictide superconductors: PrOFe1âto As. <b>2010</b> , 183, 338-343	12
1812	Critical properties of superconducting Ba1â⊠KxFe2As2. <b>2010</b> , 470, 8-11	7
1811	Characterization of FeSe single crystals. <b>2010</b> , 470, S497-S498	8
1810	Ni doping effect and phase diagram of Ni-doped BaFe2-xNixAs2. <b>2010</b> , 470, S447-S448	6
1809	Doping dependence of magnetic and transport properties in single crystalline Co-doped BaFe2As2. <b>2010</b> , 470, S408-S410	7
1808	Superconductivity induced by isovalent doping in single crystals of BaFe2(As1-xPx)2. <b>2010</b> , 470, S462-S463	3
1807	Superconductivity around quantum critical point in P-doped iron arsenides. <b>2010</b> , 470, S458-S459	5
1806	Evolution of Fermi surface and superconducting gap by electron doping in Ba(Fe,Co)2As2. <b>2010</b> , 470, S449-S451	
1805	Signature of excitonic effect in BaFe2As2 revealed by angle-resolved photoemission spectroscopy. <b>2010</b> , 470, S435-S437	
1804	Aliovalent ion-doped BaFe2As2: Single crystal growth and superconductivity. <b>2010</b> , 470, S513-S515	30
1803	Optical response of FeAs-based compounds. <b>2010</b> , 470, S326-S327	4
1802	75As-NMR study of hole-doped iron-based superconductor Ba1â⊠KxFe2As2. <b>2010</b> , 470, S464-S465	2
1801	Superconducting anisotropy in single-crystalline Ba(Fe0.93Co0.07)2As2 near Tc. <b>2010</b> , 470, S813-S814	2
1800	Bulk superconductivity at 2.6 K in undoped RbFe2As2. <b>2010</b> , 470, S328-S329	32
1799	Angle-resolved photoemission study of heavily electron-doped BaFe2â©o As2. <b>2010</b> , 470, S394-S396	
1798	Superconducting state of iron arsenide Ba1-xKxFe2As2: 57Fe and 75As NMR studies. <b>2010</b> , 470, S466-S467	3
1797	Superconductivity in ternary iron silicide YFe2-Bi2 single crystal. <b>2010</b> , 470, S404-S405	3

1796	A semimetal model of the normal state magnetic susceptibility and transport properties of Ba(Fe1âICox)2As2. <b>2010</b> , 470, 304-308	27
1795	Characterization of superconductivity in FeTe0.61Se0.39 single crystal with T~ 14 K. <b>2010</b> , 470, S391-S393	6
1794	Effects of Ni and Co doping on the physical properties of tetragonal FeSe0.5Te0.5 superconductor. <b>2010</b> , 470, 528-532	35
1793	Yttrium doped La1â⊠YxO0.9F0.1FeAs superconductors: Hall and thermopower studies. <b>2010</b> , 470, 511-515	1
1792	Physical properties of the new superconducting system Sr2VO3âEeAs (21311). <b>2010</b> , 470, S263-S266	2
1791	Pulsed laser deposition and in-field characterization of FeTe0.8S0.2 epitaxial thin films with enhanced superconducting properties. <b>2010</b> , 470, 1033-1037	5
1790	Growth of superconducting FeSe0.5Te0.5 thin films by pulsed-laser deposition. <b>2010</b> , 470, 1038-1041	8
1789	First-principles calculations for anisotropy of iron-based superconductors. <b>2010</b> , 470, 1066-1069	2
1788	Elastic properties of mono- and poly-crystalline PbO-type FeSe1â⊠Tex (x=0â₫.0): A first-principles study. <b>2010</b> , 470, 2072-2075	23
1787	Potential parent compound of superconductor: Sr2CuM2As2O2 (M=Mn, Fe). <b>2010</b> , 374, 4727-4731	4
1786	Structural and superconductivity study on ∃-FeSex. <b>2010</b> , 71, 495-498	27
1785	First-principles study on the lattice dynamics and thermodynamics properties of CaFe2As2. <b>2010</b> , 405, 4226-4230	1
1784	Impurities in FeAs-based superconductor, SrFe2As2, studied by first-principles calculations. <b>2010</b> , 173, 244-247	4
1783	Low-temperature fabrication of superconducting FeSe thin films by pulsed laser deposition. <b>2010</b> , 519, 1540-1545	32
1782	The crystal structure of. <b>2010</b> , 150, 383-385	60
1781	Upper critical fields and critical current density of BaFe2(As0.68P0.32)2 single crystal. <b>2010</b> , 150, 1178-1181	16
1780	Evolution of the hyperfine parameters of Fe in superconducting LiFeAs as observed by 57Fe MSsbauer spectroscopy. <b>2010</b> , 150, 1525-1528	7
1779	Kohlerâā rule in Ba1â⊠KxFe2As2. <b>2010</b> , 150, 1940-1943	6

Density functional calculations of the electronic structure and magnetism of the different phases 1778 of . 2010, 498, 281-286 Synthesis, Structure and Chemical Bonding of CaCo2Si2 and BaCo2Ge2 âlTwo New Compounds 13 with ThCr2Si2 Structure Type 2010, 636, 378-384 High resolution angle-resolved photoemission spectroscopy on Cu-based and Fe-based high-Tc 1776 7 superconductors. 2010, 207, 2674-2692 Different nature of instabilities in BaFe2As2 and BaNi2As2 as revealed by optical spectroscopy. **2010**, 247, 495-499 Anion height dependence of T c and the density of states in iron-based superconductors. 2010, 91, 518-522 38 Electronic structure of novel multiple-band superconductor SrPt2As2. 2010, 92, 751-755 16 1772 Template engineering of Co-doped BaFe2As2 single-crystal thin films. 2010, 9, 397-402 173 From (pi,0) magnetic order to superconductivity with (pi,pi) magnetic resonance in 224 Fe(1.02)Te(1-x)Se(x). **2010**, 9, 716-20 1770 Evolution of spin excitations into the superconducting state in FeTe1â\Sex. 2010, 6, 182-186 142 Integer and half-integer flux-quantum transitions in a niobiumâlion pnictide loop. 2010, 6, 260-264 120 Evidence for a Lifshitz transition in electron-doped iron arsenic superconductors at the onset of 1768 205 superconductivity. 2010, 6, 419-423 Electronic and Lattice Dynamical Properties of the Iron-Based Superconductors LiFeAs and NaFeAs. **2010**, 2010, 1-6 1766 Spin-Lattice Coupling and Superconductivity in Fe Pnictides. 2010, 2010, 1-7 27 Competition of Superconductivity and Charge Density Waves in Cuprates: Recent Evidence and 37 Interpretation. 2010, 2010, 1-40 The Phenomenology of Iron Pnictides Superconductors Explained in the Framework of -Wave Three-Band Eliashberg Theory. 2010, 2010, 1-6 Josephson junction in cobalt-doped BaFe2As2 epitaxial thin films on (La,Sr)(Al,Ta)O3 bicrystal 66 1763 substrates. 2010, 96, 142507 1762 Molecular Beam Epitaxy Growth of Superconducting Sr1-xKxFe2As2and Ba1-xKxFe2As2. 2010, 3, 093101 25 1761 Undeca-europium hexa-zinc dodeca-arsenide. 2010, 66, i24 16

1760	Sizable Residual Quasiparticle Density of States Induced by Impurity Scattering Effect in Ba(Fe 1âlx Co x ) 2 As 2 Single Crystals. <b>2010</b> , 27, 037402		33	
1759	The role of silver addition on the structural and superconducting properties of polycrystalline Sr0.6K0.4Fe2As2. <b>2010</b> , 23, 025027		30	
1758	Coexistence between superconducting and spin density wave states in iron-based superconductors: Ginzburgâllandau analysis. <b>2010</b> , 23, 054011		28	
1757	Disorder effects and current percolation in FeAs-based superconductors. <b>2010</b> , 23, 054006		10	
1756	Small-angle neutron scattering study of vortices in superconducting Ba(Fe0.93Co0.07)2As2. <b>2010</b> , 23, 054007		7	
1755	Influence of Pb addition on the superconducting properties of polycrystalline Sr0.6K0.4Fe2As2. <b>2010</b> , 23, 054010		19	
1754	Pressure-induced unconventional superconductivity near a quantum critical point in CaFe2As2. <b>2010</b> , 23, 054004		26	
1753	Growth and characterization of Nd(Fe1â⊠Cox)AsO single crystals. <b>2010</b> , 23, 054008		9	
1752	Low-temperature synthesis of SmFeAsO0.7F0.3 âllwires with a high transport critical current density. <b>2010</b> , 23, 075005		34	
1751	Crystal Growth and Characterization of FeAs-Based Superconductors. <b>2010</b> , 638-642, 1412-1415			
1750	Isotropic superconductivity in LaRu2P2with the ThCr2Si2-type structure. <b>2010</b> , 23, 115009		13	
1749	Observation of lateral long range order in superconducting FeTe thin films. <b>2010</b> , 19, 087403		1	
1748	Coexistence of Superconductivity and Charge Density Wave in SrPt2As2. <b>2010</b> , 79, 123710		82	
1747	Chemical Pressure and Physical Pressure in BaFe2(As1-xPx)2. <b>2010</b> , 79, 123706		49	
1746	Band structure of the heavily-electron-doped FeAs-based Ba(Fe,Co)2As2 superconductor suppresses antiferromagnetic correlations. <i>Physical Review Letters</i> , <b>2010</b> , 104, 177002	·4	12	
1745	In situ growth of superconducting NdFeAs(O,F) thin films by molecular beam epitaxy. <b>2010</b> , 97, 042509		55	
1744	Normal-state hourglass dispersion of the spin excitations in FeSexTe(1-x). <i>Physical Review Letters</i> , <b>2010</b> , 105, 157002	·4	29	
1743	Can the Mott insulator TiOCl be metallized by doping? A first-principles study. <i>Physical Review Letters</i> , <b>2010</b> , 104, 146402	·4	8	

1742	Antiferromagnetic ordering in the absence of structural distortion in Ba(Fe1â⊠Mnx)2As2. <b>2010</b> , 82,		81
1741	Distinct high-T transitions in underdoped Ba(1-x)KxFe2As2. <i>Physical Review Letters</i> , <b>2010</b> , 105, 107001	7.4	34
1740	Superconductivity in SnO: a nonmagnetic analog to Fe-based superconductors?. <i>Physical Review Letters</i> , <b>2010</b> , 105, 157001	7·4	32
1739	Anisotropic thermal expansion of AEFe2As2 (AE = Ba, Sr, Ca) single crystals. <b>2010</b> , 90, 1219-1227		13
1738	Synthesis, anisotropy, and superconducting properties of LiFeAs single crystal. <b>2010</b> , 96, 212508		59
1737	Ab initio description of disordered Sr(1-x)KxFe2As2 using the coherent potential approximation. <i>Physical Review Letters</i> , <b>2010</b> , 104, 177006	7.4	5
1736	Evidence from neutron diffraction for superconductivity in the stabilized tetragonal phase of CaFe2As2 under uniaxial pressure. <b>2010</b> , 81,		39
1735	Structural, magnetic, thermal, and electronic transport properties of single-crystal EuPd2Sb2. <b>2010</b> , 81,		12
1734	Electron-doping evolution of the low-energy spin excitations in the iron arsenide superconductor BaFe2â�NixAs2. <b>2010</b> , 81,		69
1733	Weak anisotropy of the superconducting upper critical field in Fe1.11Te0.6Se0.4 single crystals. <b>2010</b> , 81,		122
1732	Electron-hole asymmetry in Co- and Mn-doped SrFe2As2. <b>2010</b> , 82,		35
1731	Magnetic and superconducting transitions in Ba1â⊠KxFe2As2 studied by specific heat. <b>2010</b> , 81,		33
1730	Electronic structure of CsFe2Sb2 and its alloy with cobalt: A magnetic compound related to the iron superconductors. <b>2010</b> , 81,		2
1729	Electron spin resonance in EuFe2â⊠CoxAs2 single crystals. <b>2010</b> , 81,		32
1728	Nodes in the gap structure of the iron arsenide superconductor Ba(Fe1â⊠Cox)2As2 from c-axis heat transport measurements. <b>2010</b> , 82,		138
1727	Temperature versus doping phase diagrams for Ba(Fe1â¼TMx)2As2(TM=Ni,Cu,Cu/Co) single crystals. <b>2010</b> , 82,		169
1726	Magnetization distribution in the tetragonal phase of BaFe2As2. <b>2010</b> , 82,		7
1725	Anisotropic superconducting properties of optimally doped BaFe2(As0.65P0.35)2 under pressure. <b>2010</b> , 82,		15

1724	Physical and magnetic properties of Ba(Fe1â\(\mathbb{R}\)express Rux)2As2 single crystals. <b>2010</b> , 82,		93
1723	Suppression of magnetism in SrFe2â⊠RuxAs2: First-principles calculations. <b>2010</b> , 81,		9
1722	Superconductivity induced by doping platinum in BaFe2As2. <b>2010</b> , 81,		24
1721	Magnetic study of SmCoAsO showing a ferromagnetic-antiferromagnetic transition. <b>2010</b> , 82,		26
1720	Flux dynamics associated with the second magnetization peak in the iron pnictide Ba1â\(\text{KxFe2As2}\). <b>2010</b> , 82,		58
1719	Unconventional pairing in the iron arsenide superconductors. <b>2010</b> , 81,		174
1718	Neutron diffraction study of phase transitions and thermal expansion of SrFeAsF. 2010, 81,		18
1717	Signatures of pressure-induced superconductivity in insulating Bi1.98Sr2.06Y0.68CaCu2O8+[] <b>2010</b> , 81,		5
1716	Coupling between the structural and magnetic transition in CeFeAsO. <b>2010</b> , 81,		42
1715	Phase diagram and gap anisotropy in iron-pnictide superconductors. <b>2010</b> , 81,		137
1714	Lattice distortion and magnetic quantum phase transition in CeFeAs(1-x)P(x)O. <i>Physical Review Letters</i> , <b>2010</b> , 104, 017204	7.4	57
1713	Impurity scattering rate and coherence factor in vortex core of sign-reversing s-wave superconductors. <b>2010</b> , 82,		7
1712	Strong vortex pinning in Co-doped BaFe2As2 single crystal thin films. <b>2010</b> , 96, 142510		64
1711	Potassium-doped BaFe2As2 superconducting thin films with a transition temperature of 40 K. <b>2010</b> , 96, 202505		36
1710	Large D-2 theory of superconducting fluctuations in a magnetic field and its application to iron pnictides. <i>Physical Review Letters</i> , <b>2010</b> , 105, 037006	7.4	11
1709	Where are the extra d electrons in transition-metal-substituted iron pnictides?. <i>Physical Review Letters</i> , <b>2010</b> , 105, 157004	7.4	131
1708	Ultrafast pump-probe study of phase separation and competing orders in the underdoped (Ba,K)Fe2As2 superconductor. <i>Physical Review Letters</i> , <b>2010</b> , 104, 027003	7.4	81
1707	Heterojunction of Fe(Se1â⊠Tex) superconductor on Nb-doped SrTiO3. <b>2010</b> , 96, 122506		13

1706	NMR evidence of strongly correlated superconductivity in LiFeAs: Tuning toward a spin-density-wave ordering. <b>2010</b> , 82,		38
1705	Pair-breaking effects and coherence peak in the terahertz conductivity of superconducting BaFe2âØxCo2xAs2 thin films. <b>2010</b> , 82,		31
1704	Magnetic phase transitions in NdCoAsO. <b>2010</b> , 81,		42
1703	Competing ferromagnetism and superconductivity on FeAs layers in EuFe2(As0.73P0.27)2. <i>Physical Review Letters</i> , <b>2010</b> , 105, 207003	7.4	25
1702	2½ structure and charge inhomogeneity at the surface of superconducting BaFe2â½CoxAs2 (x=0âD.32). <b>2010</b> , 81,		32
1701	Electronic structure of Fe1.04Te0.66Se0.34. <b>2010</b> , 81,		98
1700	Strong coupling to magnetic fluctuations in the charge dynamics of iron-based superconductors. <b>2010</b> , 82,		23
1699	Magnetic ordering in blocking layer and highly anisotropic electronic structure of high-Tc iron-based superconductor Sr2VFeAsO3: LDA+U study. <b>2010</b> , 82,		22
1698	Strong reduction of the Korringa relaxation in the spin-density wave regime of EuFe2As2 observed by electron spin resonance. <b>2010</b> , 81,		24
1697	Theory of vortex structure in Josephson junctions with multiple tunneling channels: Vortex enlargement as a probe of ⊞s-wave superconductivity. <b>2010</b> , 81,		19
1696	Field-induced spin reorientation and giant spin-lattice coupling in EuFe2As2. 2010, 81,		43
1695	Different response of the crystal structure to isoelectronic doping in BaFe2(As1â⊠Px)2 and (Ba1â⊠Srx)Fe2As2. <b>2010</b> , 82,		63
1694	Magnetic fluctuations and superconductivity in iron pnictides as probed by electron spin resonance. <b>2010</b> , 82,		14
1693	Competing order and nature of the pairing state in the iron pnictides. <b>2010</b> , 82,		176
1692	Angle-resolved photoemission spectroscopy of the iron-chalcogenide superconductor Fe1.03Te0.7Se0.3: strong coupling behavior and the universality of interband scattering. <i>Physical Review Letters</i> , <b>2010</b> , 105, 197001	7.4	107
1691	Superconductivity and spin-density waves in multiband metals. <b>2010</b> , 81,		118
1690	Contrasting impurity scattering and pair-breaking effects by doping Mn and Zn in Ba0.5K0.5Fe2As2. <b>2010</b> , 81,		58
1689	Spin fluctuations and superconductivity in a three-dimensional tight-binding model for BaFe2As2. <b>2010</b> , 81,		180

## (2010-2010)

1688	Transition from antiferromagnetism to superconductivity in the compensated metallic state of Ba1â¼Kx(Fe1â¼Coy)2As2. <b>2010</b> , 82,	8	
1687	Anisotropic superconducting properties of single-crystalline FeSe0.5Te0.5. <b>2010</b> , 81,	10	08
1686	High-resolution angle-resolved photoemission spectroscopy study of the electronic structure of EuFe2As2. <b>2010</b> , 81,	26	6
1685	Cooperative effects of Coulomb and electron-phonon interactions in the two-dimensional 16-band dâß model for iron-based superconductors. <b>2010</b> , 82,	22	2
1684	Static and dynamical susceptibility of LaO1â⊠FxFeAs. <b>2010</b> , 81,	6	
1683	A75s NMR study of single crystals of the heavily overdoped pnictide superconductors Ba1â¼KxFe2As2 (x=0.7 and 1). <b>2010</b> , 81,	45	5
1682	Optical properties of the iron arsenic superconductor BaFe1.85Co0.15As2. <b>2010</b> , 82,	7 <sup>2</sup>	2
1681	Spin dynamics in electron-doped iron pnictide superconductors. <b>2010</b> , 82,	13	3
1680	Very strong intrinsic flux pinning and vortex avalanches in (Ba,K)Fe2As2 superconducting single crystals. <b>2010</b> , 82,	12	24
1679	High-pressure synthesis of the indirectly electron-doped iron pnictide superconductor $Sr1a\overline{M}LaxFe2As2$ with maximum $Tc=22$ K. <b>2010</b> , 82,	29	9
1678	Dual character of magnetism in EuFe2As2: Optical spectroscopic and density-functional calculation study. <b>2010</b> , 81,	40	0
1677	First-principles investigation of BaFe2As2(001). <b>2010</b> , 82,	7	
1676	Nodes versus minima in the energy gap of iron pnictide superconductors from field-induced anisotropy. <i>Physical Review Letters</i> , <b>2010</b> , 105, 187004	. 21	1
1675	Renormalization group flow, competing phases, and the structure of superconducting gap in multiband models of iron-based superconductors. <b>2010</b> , 82,	71	í
1674	Neutron spin resonance as a probe of the superconducting energy gap of BaFe1.9Ni0.1As2 superconductors. <b>2010</b> , 81,	32	2
1673	Pauli-limited upper critical field of Fe1+yTe1â⊠Sex. <b>2010</b> , 81,	10	02
1672	Strong carrier-scattering in iron-pnictide superconductors LnFeAsO1â¼ (Ln=La and Nd) obtained from charge transport experiments. <b>2010</b> , 81,	21	ſ
1671	Microstructure and superconductivity of Ir-doped BaFe2As2 superconductor. <b>2010</b> , 96, 012507	20	)

1670	Quasi-two-dimensional Fermi surfaces and coherent interlayer transport in KFeâAsâ\(\textit{Physical Review Letters}\), 2010, 105, 246403	7.4	12
1669	Andreev bound states in iron pnictide superconductors. <b>2010</b> , 81,		13
1668	Synthesis, structure, and properties of tetragonal Sr2M3As2O2 (M3=Mn3, Mn2Cu, and MnZn2) compounds containing alternating CuO2-type and FeAs-type layers. <b>2010</b> , 81,		26
1667	Ambegaokar-Baratoff relations for Josephson critical current in heterojunctions with multigap superconductors. <b>2010</b> , 81,		29
1666	Transfer of optical spectral weight in magnetically ordered superconductors. 2010, 82,		32
1665	Surface-driven electronic structure in LaFeAsO studied by angle-resolved photoemission spectroscopy. <b>2010</b> , 82,		33
1664	Spin reversal effect in hybrid s(⊞)-wave/p-wave Josephson junction. <b>2010</b> , 22, 225701		2
1663	Nematic electronic structure in the "parent" state of the iron-based superconductor Ca(Fe(1-x)Co(x))2As2. <b>2010</b> , 327, 181-4		397
1662	Theory of Josephson effects in iron-based multi-gap superconductor junctions. <b>2010</b> , 248, 012040		
1661	THE EVOLUTION OF HTS: Tc-EXPERIMENT PERSPECTIVES. <b>2010</b> , 24, 4102-4149		5
			3
1660	Effects on superconductivity of transition-metal doping in FeSe(0.5)Te(0.5). <b>2010</b> , 22, 245701		16
1659	Effects on superconductivity of transition-metal doping in FeSe(0.5)Te(0.5). <b>2010</b> , 22, 245701  75As NOR and NMR Studies of Superconductivity and Electron Correlations in Iron Arsenide LiFeAs		16
1659	Effects on superconductivity of transition-metal doping in FeSe(0.5)Te(0.5). <b>2010</b> , 22, 245701  75As NQR and NMR Studies of Superconductivity and Electron Correlations in Iron Arsenide LiFeAs. <b>2010</b> , 79, 083702		16 72
1659 1658 1657	Effects on superconductivity of transition-metal doping in FeSe(0.5)Te(0.5). <b>2010</b> , 22, 245701  75As NQR and NMR Studies of Superconductivity and Electron Correlations in Iron Arsenide LiFeAs. <b>2010</b> , 79, 083702  Structure and physical properties for a new layered pnictide-oxide: BaTiâAsâD. <b>2010</b> , 22, 075702  Control of magnetic ordering by altering Coâlo distances in La0.9R0.1Co2P2 (R=Ce, Pr, Nd, and Sm)		16 72 45
1659 1658 1657	Effects on superconductivity of transition-metal doping in FeSe(0.5)Te(0.5). <b>2010</b> , 22, 245701  75As NQR and NMR Studies of Superconductivity and Electron Correlations in Iron Arsenide LiFeAs. <b>2010</b> , 79, 083702  Structure and physical properties for a new layered pnictide-oxide: BaTiâAsâD. <b>2010</b> , 22, 075702  Control of magnetic ordering by altering CoâCo distances in La0.9R0.1Co2P2 (R=Ce, Pr, Nd, and Sm) phases with ThCr2Si2-type structures. <b>2010</b> , 107, 09E316		<ul><li>16</li><li>72</li><li>45</li><li>7</li></ul>
1659 1658 1657 1656	Effects on superconductivity of transition-metal doping in FeSe(0.5)Te(0.5). 2010, 22, 245701  75As NQR and NMR Studies of Superconductivity and Electron Correlations in Iron Arsenide LiFeAs. 2010, 79, 083702  Structure and physical properties for a new layered pnictide-oxide: BaTiâAsâD. 2010, 22, 075702  Control of magnetic ordering by altering CoâCo distances in La0.9R0.1Co2P2 (R=Ce, Pr, Nd, and Sm) phases with ThCr2Si2-type structures. 2010, 107, 09E316  Superconductivity in a new iron pnictide oxide (Fe2As2)(Sr4(Mg, Ti)2O6). 2010, 23, 045001		<ul> <li>16</li> <li>72</li> <li>45</li> <li>7</li> <li>46</li> </ul>

# (2010-2010)

1652	Distinct quasiparticle relaxation dynamics in an electron-doped superconductor, BaFe1.9Ni0.1As2. <b>2010</b> , 12, 123003	9
1651	Superconductivity at 15.6 K in calcium-doped Tb 1-x Ca x FeAsO: The structure requirement for achieving superconductivity in the hole-doped 1111 phase. <b>2010</b> , 89, 27002	8
1650	Comprehensive studies for the crystal structures and electronic properties of the superconducting system Fe(1 + $\mathbb{K}$ e(1 - x)Te(x) with $\mathbb{I}$ s approximately equal to 0.037 and x is approximately equal to 0.55. <b>2010</b> , 22, 505702	5
1649	Evidence for competing magnetic and superconducting phases in superconducting Eu 1-x Sr x Fe 2-y Co y As 2 single crystals. <b>2010</b> , 22, 235701	16
1648	Magneto-optical visualization of vortices penetration into Ba(Fe1.8Co0.2)As2. <b>2010</b> , 107, 09E155	4
1647	Efficient charge carriers induced by extra outer-shell electrons in iron-pnictides: a comparison between Ni- and Co-doped CaFeAsF. <b>2010</b> , 12, 083050	5
1646	Pressure-driven phase transitions in TiOCl and the family (Ca, Sr, Ba)Fe2As2. <b>2010</b> , 22, 164208	4
1645	Temperature-dependent Raman study of a CeFeAsO(0.9)F(0.1) superconductor: crystal field excitations, phonons and their coupling. <b>2010</b> , 22, 255402	8
1644	Magnetic lattice dynamics of the oxygen-free FeAs pnictides: how sensitive are phonons to magnetic ordering?. <b>2010</b> , 22, 315701	23
1643	Charge dynamics of Co-doped BaFe2As2. <b>2010</b> , 12, 073036	71
1642	Superconductivity of FeSe0.5Te0.5Thin Films Grown by Pulsed Laser Deposition. <b>2010</b> , 49, 023101	45
1641	A comparative study on the thermoelectric effect of parent oxypnictides LaTAsO (T = Fe, Ni). <b>2010</b> , 22, 072201	7
1640	Review of Fe Chalcogenides as the Simplest Fe-Based Superconductor. <b>2010</b> , 79, 102001	295
1639	Magnetic and structural properties of Ca(Fe1âผิCox)2P2 and Ca(Ni1âผิCox)2P2. <b>2010</b> , 81,	13
1638	Anion height dependence of Tcfor the Fe-based superconductor. <b>2010</b> , 23, 054013	379
1637	Gutzwiller density functional studies of FeAs-based superconductors: structure optimization and evidence for a three-dimensional Fermi surface. <i>Physical Review Letters</i> , <b>2010</b> , 104, 047002	58
1636	Comparison of Ab initio Low-Energy Models for LaFePO, LaFeAsO, BaFe2As2, LiFeAs, FeSe, and FeTe: Electron Correlation and Covalency. <b>2010</b> , 79, 044705	252
1635	Itinerant nature of magnetism in iron pnictides: A first-principles study. <b>2010</b> , 81,	31

1634	Phase separation and suppression of the structural and magnetic transitions in superconducting doped iron tellurides, Fe(1+x)Te(1-y)S(y). <b>2010</b> , 132, 13000-7		55
1633	Thermally activated energy and flux-flow Hall effect of Fe1+y(Te1+xSx)z. <b>2010</b> , 82,		43
1632	Unusual electronic structure and observation of dispersion kink in CeFeAsO parent compound of FeAs-based superconductors. <i>Physical Review Letters</i> , <b>2010</b> , 105, 027001	7.4	24
1631	Symmetry and disorder of the vitreous vortex lattice in overdoped BaFe2â\(\mathbb{Q}\)CoxAs2: Indication for strong single-vortex pinning. <b>2010</b> , 81,		43
1630	Superconductivity above 33 K in (Ca(â⊞ x)Na(x))Feâ∆sâ□2010, 22, 222203		29
1629	Critical properties of a dense polycrystalline (Ba, K)Fe2As2superconductor prepared by a combined process of melting and deformation. <b>2010</b> , 23, 045009		10
1628	Enhancement of the critical temperature of the pnictide superconductor LaFeAsO1â⊠Fx studied via A75s NMR under pressure. <b>2010</b> , 81,		33
1627	Orbital-dependent modifications of electronic structure across the magnetostructural transition in BaFe2As2. <i>Physical Review Letters</i> , <b>2010</b> , 104, 057002	7.4	148
1626	Weak superconducting pairing and a single isotropic energy gap in stoichiometric LiFeAs. <i>Physical Review Letters</i> , <b>2010</b> , 104, 187001	7.4	71
1625	The itinerant state of carriers in pnictide NaCu 2 P 2 : Role of distortion in CuP 4 tetrahedra. <b>2010</b> , 92, 57002		4
1624	Flux pinning in PrFeAsO0.9 and NdFeAsO0.9F0.1 superconducting crystals. 2010, 81,		93
1623	Formation of collapsed tetragonal phase in EuCoâAsâIunder high pressure. <b>2010</b> , 22, 425701		26
1622	Isolated infinity1[ZnPn2]4- chains in the Zintl phases Ba2ZnPn2 (Pn = As, Sb, Bi)synthesis, structure, and bonding. <b>2010</b> , 49, 5173-9		51
1621	Unified picture for magnetic correlations in iron-based superconductors. <i>Physical Review Letters</i> , <b>2010</b> , 105, 107004	7.4	140
1620	Orbital order and spontaneous orthorhombicity in iron pnictides. <b>2010</b> , 82,		178
1619	Tuning the superconducting and magnetic properties of FeySe0.25Te0.75 by varying the iron content. <b>2010</b> , 82,		88
1618	Doping-dependent specific heat study of the superconducting gap in Ba(Fe1â⊠Cox)2As2. <b>2010</b> , 81,		56
1617	Gap structure in the electron-doped ironâ∃rsenide superconductor Ba(Fe0.92Co0.08)2As2: low-temperature specific heat study. <b>2010</b> , 12, 023006		39

1616	Compositional control of the superconducting properties of LiFeAs. <b>2010</b> , 132, 10467-76	58
1615	General Theory of High-Tc Superconductors. <b>2010</b> , 1-47	Ο
1614	Self-energy effects and electron-phonon coupling in Fe-As superconductors. <b>2010</b> , 22, 115802	25
1613	Observation of Softened Fe Modes in K-Doped BaFe2As2 via 57Fe Nuclear Resonant Inelastic Scattering. <b>2010</b> , 79, 013706	7
1612	Observation of Dirac cone electronic dispersion in BaFe2As2. <i>Physical Review Letters</i> , <b>2010</b> , 104, 137001 <sub>7.4</sub>	196
1611	Highly Two-dimensional Electronic Structure and Strong Fermi-Surface Nesting of the Iron-Based Superconductor Sr2ScFePO3: A First-Principles Study. <b>2010</b> , 79, 013705	7
1610	Uniaxial-strain mechanical detwinning of CaFe2As2 and BaFe2As2 crystals: Optical and transport study. <b>2010</b> , 81,	231
1609	Selective Substitution of Cr in CaFe4As3 and Its Effect on the Spin Density Wave. <b>2010</b> , 22, 4996-5002	9
1608	Anomalous suppression of the orthorhombic lattice distortion in superconducting Ba(Fe1-xCox)2As2 single crystals. <i>Physical Review Letters</i> , <b>2010</b> , 104, 057006	337
1607	Tuning Ferro- and Metamagnetic Transitions in Rare-Earth Cobalt Phosphides La1â⊠PrxCo2P2. <b>2010</b> , 22, 1704-1713	40
1606	Appearance of pressure-induced superconductivity in BaFe2As2 under hydrostatic conditions and its extremely high sensitivity to uniaxial stress. <b>2010</b> , 81,	88
1605	Indifference of Superconductivity and Magnetism to Size-Mismatched Cations in the Layered Iron Arsenides Ba1â�NaxFe2As2. <b>2010</b> , 22, 4304-4311	33
1604	Materials Chemistry of BaFe2As2: A Model Platform for Unconventional Superconductivity. <b>2010</b> , 22, 715-723	68
1603	A new pnictide superconductor without iron. <b>2010</b> , 132, 908-9	31
1602	Collapsed tetragonal phase and superconductivity of BaFe2As2 under high pressure. <b>2010</b> , 82,	64
1601	Superconductivity at 23 K in Pt doped BaFeâAsâLingle crystals. <b>2010</b> , 22, 072204	44
1600	Ternary rare-earth iron arsenides RE12Fe57.5As41 (RE = La, Ce). <b>2010</b> , 49, 2325-33	17
1599	First-principles study of the magnetic, structural and electronic properties of LiFeAs. <b>2010</b> , 22, 046006	9

1598	Spin-phonon coupling and effect of pressure in the superconductor LiFeAs: Lattice dynamics from first-principles calculations. <b>2010</b> , 82,		27
1597	High upper critical fields and evidence of weak-link behavior in superconducting LaFeAsO1-xFx thin films. <i>Physical Review Letters</i> , <b>2010</b> , 104, 077001	4	68
1596	Evolution of superconductivity by oxygen annealing in FeTe 0.8 S 0.2. <b>2010</b> , 90, 57002		55
1595	The puzzle of high temperature superconductivity in layered iron pnictides and chalcogenides. <b>2010</b> , 59, 803-1061		1404
1594	Epitaxial LaFeAsO1â⊠Fxthin films grown by pulsed laser deposition. <b>2010</b> , 23, 022002		39
1593	Coherent interfacial bonding on the FeAs tetrahedron in Fe/Ba(Fe1â\(\mathbb{U}\)Cox)2As2 bilayers. <b>2010</b> , 97, 022506		53
1592	FeAs-Based Superconductivity: A Case Study of the Effects of Transition Metal Doping on BaFe2As2. <b>2010</b> , 1, 27-50		322
1591	Three-band superconductivity and the order parameter that breaks time-reversal symmetry. <b>2010</b> , 81,		154
1590	Superconductivity in the iron selenide KxFe2Se2 (0â�ata.0). <b>2010</b> , 82,		994
1589	Leggett mode in a strong-coupling model of iron arsenide superconductors. <b>2010</b> , 82,		20
1588	Synthesis and dislocations of 1111-type GdFePO superconductor. <b>2010</b> , 507, 93-96		4
1587	BaNiSn3-type ternary germanides SrMGe3 (M=Ir; Pd and Pt). <b>2010</b> , 508, 338-341		6
1586	Effects of nematic fluctuations on the elastic properties of iron arsenide superconductors. <i>Physical Review Letters</i> , <b>2010</b> , 105, 157003	4	283
1585	Electronic Structure Calculation by First Principles for Strongly Correlated Electron Systems. <b>2010</b> , 79, 112001		93
1584	Hole and electron contributions to the transport properties of Ba(Fe1â\(\text{Rux}\))2As2 single crystals. <b>2010</b> , 81,		95
1583	Critical current and vortex dynamics in single crystals of Ca(Fe1â\(\mathbb{R}\)Cox)2As2. <b>2010</b> , 82,		31
1582	Surface structures of ternary iron arsenides AFe2As2 (A=Ba, Sr, or Ca). <b>2010</b> , 81,		29
1581	Quantum criticality and nodal superconductivity in the FeAs-based superconductor KFe2As2.  Physical Review Letters, <b>2010</b> , 104, 087005	4	205

### (2010-2010)

1580	Significant reduction of electronic correlations upon isovalent Ru substitution of BaFe2As2.  Physical Review Letters, <b>2010</b> , 105, 087001  7-4	54
1579	Single crystal growth and characterizations of iron arsenide superconductor BaFe 2âlk Ni x As 2 (0.0 âlk âld.12). <b>2010</b> , 19, 026103	4
1578	Structural and physical properties of undoped and nickel-doped BaFe $2\hat{a}$ lk Ni x As 2 (x = 0, 0.04) single crystals. <b>2010</b> , 19, 086101	1
1577	Magnetism in Fe-based superconductors. <b>2010</b> , 22, 203203	264
1576	Doping-driven structural phase transition and loss of superconductivity in MxFe1â⊠Se[(M=Mn, Cu). <b>2010</b> , 82,	47
1575	Local antiferromagnetic correlations in the iron pnictide superconductors LaFeAsO1â\(\text{NF}\)x and Ca(Fe1â\(\text{NC}\)cox)2As2 as seen via normal-state susceptibility. <b>2010</b> , 81,	95
1574	Orbital character variation of the Fermi surface and doping dependent changes of the dimensionality in BaFe2âIdCoxAs2 from angle-resolved photoemission spectroscopy. <b>2010</b> , 81,	51
1573	Superconductivity in iron telluride thin films under tensile stress. <i>Physical Review Letters</i> , <b>2010</b> , 104, 017θΩ3	133
1572	Superconductivity in Ru-substituted polycrystalline BaFe2â\RuxAs2. <b>2010</b> , 81,	105
1571	Single-crystal growth and superconducting properties of LiFeAs. <b>2010</b> , 91, 67002	28
1570	MBsbauer studies of Ba(Fe(1-x)Ni(x))2As2. <b>2010</b> , 22, 355701	19
1569	Structural properties and superconductivity of SrFe(2)As(2 - x)P(x) (0.0 $\hat{a}$ $\hat{b}$ $\hat{a}$ $\hat{b}$ 0.3). <b>2010</b> , 22, 125702	29
1568	Local magnetic inhomogeneities in Ba(Fe1â⊠Nix)2As2 as seen via A75s NMR. <b>2010</b> , 82,	33
1567	Orbital ordering and unfrustrated ( ${\rm I\!D}$ ) magnetism from degenerate double exchange in the iron pnictides. <b>2010</b> , 82,	168
1566	Single Crystal Growth and Characterization of Superconducting LiFeAs. <b>2010</b> , 10, 4428-4432	46
1565	Lattice and magnetism in superconducting compounds Ca 1âlk K x Fe 2 As 2. <b>2010</b> , 19, 037401	2
1564	Structure and Physical Properties of the Layered Pnictide-Oxides: (SrF)2Ti2Pn2O (Pn = As, Sb) and (SmO)2Ti2Sb2O. <b>2010</b> , 22, 1503-1508	46
1563	Fabrication of superconducting oxypnictide thin films. <b>2010</b> , 90, 57005	18

1562	Shapiro steps as a direct probe of ⊞s-wave symmetry in multigap superconducting Josephson junctions. <b>2010</b> , 82,	20
1561	Precision microwave electrodynamic measurements of K- and Co-doped BaFe2As2. <b>2010</b> , 82,	25
1560	Fluctuation conductivity of single-crystalline BaFe1.8Co0.2As2 in the critical region. <b>2010</b> , 108, 063916	28
1559	Inelastic neutron scattering study of the resonance mode in the optimally doped pnictide superconductor LaFeAsO0.92F0.08. <b>2010</b> , 82,	44
1558	Quasiparticle scattering induced by charge doping of iron-pnictide superconductors probed by collective vortex pinning. <i>Physical Review Letters</i> , <b>2010</b> , 105, 267002	4 63
1557	High pressure study of BaFe2As2the role of hydrostaticity and uniaxial stress. <b>2010</b> , 22, 052201	62
1556	Electronic, magnetic and optical properties of two Fe-based superconductors and related parent compounds. <b>2010</b> , 23, 054005	13
1555	An overview on iron based superconductors. <b>2010</b> , 23, 073001	110
1554	Missbauer studies of spin density wave-superconducting Fe-As systems. <b>2010</b> , 217, 012121	5
1553	Evolution of the Fermi surface of BaFe2(As1-xPx){2} on entering the superconducting dome.  Physical Review Letters, <b>2010</b> , 104, 057008	ļ 179
1553 1552		179 17
	Physical Review Letters, <b>2010</b> , 104, 057008 7-4	
1552	Physical Review Letters, <b>2010</b> , 104, 057008  Incommensurate spin-density wave and magnetic lock-in transition in CaFe4As3. <b>2010</b> , 81,  Synthesis, crystal and electronic structures of the new quaternary phases A5Cd2Sb5F (A = Sr, Ba,	17
1552 1551	Incommensurate spin-density wave and magnetic lock-in transition in CaFe4As3. <b>2010</b> , 81,  Synthesis, crystal and electronic structures of the new quaternary phases A5Cd2Sb5F (A = Sr, Ba, Eu), and Ba5Cd2Sb5O(x) (0.5. <b>2010</b> , 39, 11335-43  Intercalation and superconductivity in ternary layer structured metal nitride halides (MNX: M = Ti,	17 14
1552 1551 1550	Incommensurate spin-density wave and magnetic lock-in transition in CaFe4As3. <b>2010</b> , 81,  Synthesis, crystal and electronic structures of the new quaternary phases A5Cd2Sb5F (A = Sr, Ba, Eu), and Ba5Cd2Sb5O(x) (0.5. <b>2010</b> , 39, 11335-43  Intercalation and superconductivity in ternary layer structured metal nitride halides (MNX: M = Ti, Zr, Hf; X = Cl, Br, I). <b>2010</b> , 20, 2922  Actinoid transition metal phosphides An2T12P7 (An = Th, U; T = Fe, Co, Ni) and arsenides	17 14 50
1552 1551 1550 1549	Incommensurate spin-density wave and magnetic lock-in transition in CaFe4As3. 2010, 81,  Synthesis, crystal and electronic structures of the new quaternary phases A5Cd2Sb5F (A = Sr, Ba, Eu), and Ba5Cd2Sb5O(x) (0.5. 2010, 39, 11335-43  Intercalation and superconductivity in ternary layer structured metal nitride halides (MNX: M = Ti, Zr, Hf; X = Cl, Br, I). 2010, 20, 2922  Actinoid transition metal phosphides An2T12P7 (An = Th, U; T = Fe, Co, Ni) and arsenides An2T12As7 (An = Th, U; T = Co, Ni) with Zr2Fe12P7 type structure. 2010, 39, 6067-73  Topotactic Redox Chemistry of NaFeAs in Water and Air and Superconducting Behavior with	17 14 50
1552 1551 1550 1549 1548	Incommensurate spin-density wave and magnetic lock-in transition in CaFe4As3. 2010, 81,  Synthesis, crystal and electronic structures of the new quaternary phases A5Cd2Sb5F (A = Sr, Ba, Eu), and Ba5Cd2Sb5O(x) (0.5. 2010, 39, 11335-43  Intercalation and superconductivity in ternary layer structured metal nitride halides (MNX: M = Ti, Zr, Hf; X = Cl, Br, I). 2010, 20, 2922  Actinoid transition metal phosphides An2T12P7 (An = Th, U; T = Fe, Co, Ni) and arsenides An2T12As7 (An = Th, U; T = Co, Ni) with Zr2Fe12P7 type structure. 2010, 39, 6067-73  Topotactic Redox Chemistry of NaFeAs in Water and Air and Superconducting Behavior with Stoichiometry Change. 2010, 22, 3916-3925  Field-dependent transport critical current in single crystals of Ba(Fe1 â\text{\text{M}TMx})2As2(TM = Co, Ni) superconductors. 2010, 23, 054002	17 14 50 10 26

## (2011-2010)

1544	Strong correlations and spin-density-wave phase induced by a massive spectral weight redistribution in ∃-Fe1.06Te. <b>2010</b> , 82,	44
1543	Possible magnetic order and suppression of superconductivity by V doping in Sr2VO3FeAs. <b>2010</b> , 82,	21
1542	Superconductivity and magnetism in platinum-substituted SrFe2As2 single crystals. 2010, 82,	19
1541	Heat capacity study of BaFe2As2: Effects of annealing. <b>2010</b> , 82,	52
1540	Microscopic study of the superconducting state of the iron pnictide RbFe2As2 via muon spin rotation. <b>2010</b> , 82,	26
1539	La2Sb, a layered superconductor with metal-metal bonds. <b>2011</b> , 47, 3778-80	9
1538	Raman evidence for the superconducting gap and spinaphonon coupling in the superconductor Ca(Fe0.95Co0.05)2As2. <b>2011</b> , 23, 255403	8
1537	Dependence of Epitaxial ${\rm Ba}{({\rm Fe}_{1-{\rm rm} x}}{\rm Co}_{\rm rm} x})}_{2}{\rm As}_{2}$ Thin Films Properties on ${\rm SrTiO}_{3}$ Template Thickness. <b>2011</b> , 21, 2882-2886	7
1536	Development of Powder-in-Tube Processed Iron Pnictide Wires and Tapes. <b>2011</b> , 21, 2878-2881	43
1535	Synthesis of ThCr2Si2-type arsenides from Bi flux. <b>2011</b> , 47, 5563-5	19
1534	Transport Properties of Iron-Based \$hbox{FeTe}_{0.5}hbox{Se}_{0.5}\$ Superconducting Wire. <b>2011</b> , 21, 2858-2861	23
1533	\$J_{rm c}\$ Scaling and Anisotropies in Co-Doped Ba-122 Thin Films. <b>2011</b> , 21, 2887-2890	20
1532	Estimation of Critical Current Densities in Polycrystalline ${\rm Sr}_{0.6}{\rm K}_{0.4}{\rm Fe}_{2}{\rm Sn}_{2}$ Superconductors. <b>2011</b> , 21, 2862-2865	
1531	Superconductivity and magnetism in FeSe thin films grown by metalâBrganic chemical vapor deposition. <b>2011</b> , 24, 015010	17
1530	Emergence of superconductivity in "32522" structure of (Ca3Al2O(5-y))(Fe2Pn2) (Pn = As and P). <b>2011</b> , 133, 9630-3	34
1529	Nonequilibrium quasiparticle relaxation dynamics in single crystals of hole- and electron-doped BaFe2As2. <b>2011</b> , 84,	23
1528	Eight-coordinated arsenic in the Zintl phases RbCd4As3 and RbZn4As3: synthesis and structural characterization. <b>2011</b> , 50, 8375-83	31
1527	Growth and transport studies of BaMn2As2 thin filmsa). <b>2011</b> , 29, 031210	2

1526	Pressure and chemical substitution effects in the local atomic structure of BaFe2As2. <b>2011</b> , 83,	33
1525	Pressure-induced isostructural phase transition and correlation of FeAs coordination with the superconducting properties of 111-type Na(1-x)FeAs. <b>2011</b> , 133, 7892-6	51
1524	Phase transition and superconductivity of SrFe(2)As(2) under high pressure. <b>2011</b> , 23, 122201	37
1523	Absence of superconductivity in LiCu2P2. <b>2011</b> , 133, 1751-3	8
1522	MgF2 Doping of SmFeAsO Superconductors Prepared by Mechanical Alloying and Rapid Annealing. <b>2011</b> , 23, 3039-3044	5
1521	Structure of vacancy-ordered single-crystalline superconducting potassium iron selenide. <b>2011</b> , 83,	125
1520	Microstructure and ordering of iron vacancies in the superconductor system KyFexSe2 as seen via transmission electron microscopy. <b>2011</b> , 83,	214
1519	Anisotropic magnetism, superconductivity, and the phase diagram of Rb1â\Fe2â\JSe2. <b>2011</b> , 84,	53
1518	Systematic growth of BaFe2 â⊠NixAs2large crystals. <b>2011</b> , 24, 065004	48
	taran da tanàna ao amin'ny faritr'i Nord-Nord-Nandana ao amin'ny faritr'i Austra, ao amin'ny faritr'i Austra,	
1517	Block spin ground state and three-dimensionality of (K,Tl)(y)Fe(1.6)Se2. <i>Physical Review Letters</i> , 7.4	65
1517 1516		8
	2011, 107, 056401  Suppression of superconductivity in Fe chalcogenides by annealing: A reverse effect to pressure.	
1516	2011, 107, 056401  Suppression of superconductivity in Fe chalcogenides by annealing: A reverse effect to pressure. 2011, 84,  Improvement of superconducting properties of FeSe0.5Te0.5single crystals by Mn substitution.	8
1516 1515	2011, 107, 056401  Suppression of superconductivity in Fe chalcogenides by annealing: A reverse effect to pressure. 2011, 84,  Improvement of superconducting properties of FeSe0.5Te0.5single crystals by Mn substitution. 2011, 24, 045009	8
1516 1515 1514	Suppression of superconductivity in Fe chalcogenides by annealing: A reverse effect to pressure.  2011, 84,  Improvement of superconducting properties of FeSe0.5Te0.5single crystals by Mn substitution.  2011, 24, 045009  Phase separation and superconductivity in Fe(1+x)Te(0.5)Se(0.5). 2011, 47, 11297-9	8 33 21
1516 1515 1514 1513	2011, 107, 056401  Suppression of superconductivity in Fe chalcogenides by annealing: A reverse effect to pressure. 2011, 84,  Improvement of superconducting properties of FeSe0.5Te0.5single crystals by Mn substitution. 2011, 24, 045009  Phase separation and superconductivity in Fe(1+x)Te(0.5)Se(0.5). 2011, 47, 11297-9  Theory of high-TCsuperconductivity: transition temperature. 2011, 23, 295701	8 33 21 18
1516 1515 1514 1513 1512	Suppression of superconductivity in Fe chalcogenides by annealing: A reverse effect to pressure.  2011, 84,  Improvement of superconducting properties of FeSe0.5Te0.5single crystals by Mn substitution.  2011, 24, 045009  Phase separation and superconductivity in Fe(1+x)Te(0.5)Se(0.5). 2011, 47, 11297-9  Theory of high-TCsuperconductivity: transition temperature. 2011, 23, 295701  Physical properties of SrSn(4) single crystals. 2011, 23, 455703	8 33 21 18

1508	SmFeAsO1âMFx. <b>2011</b> , 84,	26
1507	Anisotropic phase diagram and superconducting fluctuations of single-crystalline SmFeAsO0.85F0.15. <b>2011</b> , 83,	42
1506	Room temperature antiferromagnetic order in superconducting $X(y)Fe(2-x)Seal(X = Rb, K)$ : a neutron powder diffraction study. <b>2011</b> , 23, 156003	36
1505	Electronic structure of optimally doped pnictide Ba0.6K0.4Fe2As2: a comprehensive angle-resolved photoemission spectroscopy investigation. <b>2011</b> , 23, 135701	76
1504	Structureâproperty relationships of iron arsenide superconductors. <b>2011</b> , 21, 13726	74
1503	Magnetic field effect on static antiferromagnetic order and spin excitations in the underdoped iron arsenide superconductor BaFe1.92Ni0.08As2. <b>2011</b> , 83,	28
1502	Electronic structures and magnetic order of ordered-Fe-vacancy ternary iron selenides TlFe1.5Se2 and AFe1.5Se2 (A=K, Rb, or Cs). <i>Physical Review Letters</i> , <b>2011</b> , 106, 087005	82
1501	Analysis of local chemical and structural inhomogeneities in FeySe1â⊠Tex single crystals. <b>2011</b> , 99, 192504	14
1500	Coexistence of antiferromagnetic ordering and superconductivity in the Ba(Fe0.961Rh0.039)2As2 compound studied by M\(\mathbb{B}\)sbauer spectroscopy. <b>2011</b> , 84,	16
1499	Magnetic exchange interactions in BaMn2As2: A case study of the J1-J2-Jc Heisenberg model. <b>2011</b> , 84,	108
1499 1498		108
1498	, 84,  Cyclotron resonance and mass enhancement by electron correlation in KFe2As2. <i>Physical Review</i>	
1498	Cyclotron resonance and mass enhancement by electron correlation in KFe2As2. <i>Physical Review Letters</i> , <b>2011</b> , 107, 166402	10
1498 1497	Cyclotron resonance and mass enhancement by electron correlation in KFe2As2. <i>Physical Review Letters</i> , <b>2011</b> , 107, 166402  Superconductivity and anomalous transport in SrPd2Ge2 single crystals. <b>2011</b> , 83,  Large Transport Critical Current Densities of Ag Sheathed (Ba,K)Fe2As2+Ag Superconducting Wires	10
1498 1497 1496	Cyclotron resonance and mass enhancement by electron correlation in KFe2As2. <i>Physical Review Letters</i> , <b>2011</b> , 107, 166402  Superconductivity and anomalous transport in SrPd2Ge2 single crystals. <b>2011</b> , 83,  Large Transport Critical Current Densities of Ag Sheathed (Ba,K)Fe2As2+Ag Superconducting Wires Fabricated by anEx-situPowder-in-Tube Process. <b>2011</b> , 4, 043101	10 21 102
1498 1497 1496 1495	Cyclotron resonance and mass enhancement by electron correlation in KFe2As2. <i>Physical Review Letters</i> , <b>2011</b> , 107, 166402  7-4  Superconductivity and anomalous transport in SrPd2Ge2 single crystals. <b>2011</b> , 83,  Large Transport Critical Current Densities of Ag Sheathed (Ba,K)Fe2As2+Ag Superconducting Wires Fabricated by anEx-situPowder-in-Tube Process. <b>2011</b> , 4, 043101  Ternary and higher pnictides; prospects for new materials and applications. <b>2011</b> , 40, 4099-118  Vanadium fluoroarsenatesfolding sheets into highly corrugated layers and crystalline arrays of	10 21 102 42
1498 1497 1496 1495	Cyclotron resonance and mass enhancement by electron correlation in KFe2As2. <i>Physical Review Letters</i> , <b>2011</b> , 107, 166402  Superconductivity and anomalous transport in SrPd2Ge2 single crystals. <b>2011</b> , 83,  Large Transport Critical Current Densities of Ag Sheathed (Ba,K)Fe2As2+Ag Superconducting Wires Fabricated by anEx-situPowder-in-Tube Process. <b>2011</b> , 4, 043101  Ternary and higher pnictides; prospects for new materials and applications. <b>2011</b> , 40, 4099-118  Vanadium fluoroarsenatesfolding sheets into highly corrugated layers and crystalline arrays of large inorganic tubes. <b>2011</b> , 47, 6132-4  Structural chemistry of superconducting pnictides and pnictide oxides with layered structures.	10 21 102 42 3

1490	Resistivity and Hall effect of LiFeAs: Evidence for electron-electron scattering. 2011, 84,	33
1489	Hydrogen in layered iron arsenides: Indirect electron doping to induce superconductivity. <b>2011</b> , 84,	96
1488	Pressure and K doping induced superconductivity in BaFe2As2. <b>2011</b> , 273, 012096	1
1487	Interplay between magnetism and superconductivity in iron-chalcogenide superconductors: crystal growth and characterizations. <b>2011</b> , 74, 124503	86
1486	Spin-glass behavior in LaFe(x)Co(2-x)P2 solid solutions: interplay between magnetic properties and crystal and electronic structures. <b>2011</b> , 50, 10274-83	24
1485	Ternary rare-earth arsenides REZn3As3 (RE = La-Nd, Sm) and RECd3As3 (RE = La-Pr). <b>2011</b> , 50, 11152-61	22
1484	Common Fermi-surface topology and nodeless superconducting gap of K0.68Fe1.79Se2 and (Tl0.45K0.34)Fe1.84Se2 superconductors revealed via angle-resolved photoemission. <b>2011</b> , 83,	70
1483	Synthesis and crystal growth of Cs(0.8)(FeSe(0.98))(2): a new iron-based superconductor with $T(c) = 27$ K. <b>2011</b> , 23, 052203	236
1482	Fe-based superconductivity with T c = 31 K bordering an antiferromagnetic insulator in (Tl,K) Fe x Se 2. <b>2011</b> , 94, 27009	352
1481	Chemistry and high temperature superconductivity. <b>2011</b> , 21, 4756	17
•	Chemistry and high temperature superconductivity. <b>2011</b> , 21, 4756  Materials and Novel Superconductivity in Iron Pnictide Superconductors. <b>2011</b> , 2, 121-140	17
1480		
1480	Materials and Novel Superconductivity in Iron Pnictide Superconductors. <b>2011</b> , 2, 121-140  Magnetoelastic effects in iron telluride. <b>2011</b> , 83,	141
1480 1479	Magnetoelastic effects in iron telluride. 2011, 83,  Anomalous optical phonons in FeTe chalcogenides: Spin state, magnetic order, and lattice	141
1480 1479 1478	Materials and Novel Superconductivity in Iron Pnictide Superconductors. <b>2011</b> , 2, 121-140  Magnetoelastic effects in iron telluride. <b>2011</b> , 83,  Anomalous optical phonons in FeTe chalcogenides: Spin state, magnetic order, and lattice anharmonicity. <b>2011</b> , 83,	141 22 41
1480 1479 1478	Materials and Novel Superconductivity in Iron Pnictide Superconductors. 2011, 2, 121-140  Magnetoelastic effects in iron telluride. 2011, 83,  Anomalous optical phonons in FeTe chalcogenides: Spin state, magnetic order, and lattice anharmonicity. 2011, 83,  Orbital-independent superconducting gaps in iron pnictides. 2011, 332, 564-7	141 22 41 122
1480 1479 1478 1477	Materials and Novel Superconductivity in Iron Pnictide Superconductors. 2011, 2, 121-140  Magnetoelastic effects in iron telluride. 2011, 83,  Anomalous optical phonons in FeTe chalcogenides: Spin state, magnetic order, and lattice anharmonicity. 2011, 83,  Orbital-independent superconducting gaps in iron pnictides. 2011, 332, 564-7  Alcoholic beverages induce superconductivity in FeTe1 â\subseteq Sx. 2011, 24, 055008  Transport properties and microstructure of mono- and seven-core wires of FeSe1	141 22 41 122 42

1472	In-plane anisotropy of electrical resistivity in strain-detwinned SrFe2As2. <b>2011</b> , 83,	49
1471	Superconductivity at 32 K in single-crystalline RbxFe2âySe2. <b>2011</b> , 83,	272
1470	Common crystalline and magnetic structure of superconducting A2Fe4Se5 (A=K,Rb,Cs,Tl) single crystals measured using neutron diffraction. <i>Physical Review Letters</i> , <b>2011</b> , 107, 137003	191
1469	Electronic and magnetic structures of the ternary iron selenides AFe2Se2 (A=Cs, Rb, K, or Tl). <b>2011</b> , 84,	51
1468	Phase separation in superconducting and antiferromagnetic Rb0.8Fe1.6Se2 probed by M\(\mathbb{g}\)sbauer spectroscopy. <b>2011</b> , 84,	96
1467	Spectroscopic scanning tunneling microscopy insights into Fe-based superconductors. <b>2011</b> , 74, 124513	148
1466	Superconductivity in copper-oxygen compounds. <b>2011</b> , 226,	6
1465	As-NMR/NQR Study of CaFe2As2under Pressure. <b>2011</b> , 80, SA116	
1464	Effect of Substitution of Ca2+for Eu2+on Pressure-Induced Superconductivity in EuFe2As2. <b>2011</b> , 80, SA117	4
1463	Local structural studies of Ba(1-x)K(x)Fe2As2 using atomic pair distribution function analysis. <b>2011</b> , 23, 112202	5
1462	Quasiclassical Eilenberger approach to the vortex state in pnictide superconductors. <b>2011</b> , 303, 012113	1
1461	Magnetization distribution in the tetragonal Ba(Fe $1\hat{a}$ M Co x ) 2 As 2 , x=0.066 probed by polarized neutron diffraction. <b>2011</b> , 93, 32001	2
1460	Superconductivity in Sr(Pd1â⊠Nix)2Ge2. <b>2011</b> , 273, 012089	11
1459	Relation between superconductivity and tetragonal phase stabilized by uniaxial pressure in CaFe2As2. <b>2011</b> , 273, 012102	
1458	Uniform chemical pressure effect in solid solutions Ba1-xSrxFe2As2and Sr1â⊠CaxFe2As2. <b>2011</b> , 273, 012104	8
1457	Competing orders in underdoped (Ba1â¼Kx)Fe2As2. <b>2011</b> , 273, 012107	2
1456	Superconducting State in the Ternary Germanide Y2AlGe3with Related ThCr2Si2-Type Structure. <b>2011</b> , 80, 014716	3
1455	Superconductivity at 38 K in Iron-Based Compound with PlatinumâArsenide Layers Ca10(Pt4As8)(Fe2-xPtxAs2)5. <b>2011</b> , 80, 093704	103

1454	Magnetization hysteresis and time decay measurements in FeSe0.50Te0.50: Evidence for fluctuation in mean free path induced pinning. <b>2011</b> , 84,	32
1453	Determination of the Upper Critical Field of a Single Crystal LiFeAs: The Magnetic Torque Study up to 35 Tesla. <b>2011</b> , 80, 013706	45
1452	Ferromagnetic quantum critical point induced by dimer-breaking in SrCo2(Ge1âNPx)2. <b>2011</b> , 7, 207-210	60
1451	Observation of a ubiquitous three-dimensional superconducting gap function in optimally doped Ba0.6K0.4Fe2As2. <b>2011</b> , 7, 198-202	87
1450	Structural, electronic, and magnetic properties of layered cobalt pnictide oxides (Co2As2)(Sr4Sc2O6) and (Co2P2)(Sr4Sc2O6) from first principles. <b>2011</b> , 13, 837-842	1
1449	RE8Rh17Sb14 (REI±ILa, Ce, Pr, Nd) with a CaBe2Ge2-related superstructure through rhodiumâllntimony-ordering and vacancy formation. <b>2011</b> , 13, 1740-1747	6
1448	Electrodeposition of nano-dimensioned FeSe. <b>2011</b> , 519, 8397-8400	20
1447	Superconductivity of the platinum doped 122 iron arsenide SrFe2â⊠PtxAs2. <b>2011</b> , 471, 600-602	1
1446	Scanning tunneling microscopy on iron-chalcogenide superconductor Fe(Se,Te) single crystal. <b>2011</b> , 471, 622-624	7
1445	Microwave surface impedance measurements of LiFeAs, LiFe(As,P) and FeSe1â⊠Tex single crystals. <b>2011</b> , 471, 630-633	2
1444	Terahertz conductivity measurement of FeSe0.5Te0.5 and Co-doped BaFe2As2 thin films. <b>2011</b> , 471, 634-638	8
1443	Magneto-optical imaging of polycrystalline FeTe1â⊠Sex prepared at various conditions. <b>2011</b> , 471, 651-655	5
1442	Electronic structure of LaFe2X2 (X = Si,Ge). <b>2011</b> , 471, 656-658	8
1441	Ginzburgâllandau theory of multi-band superconductivity and applications to Fe pnictides. <b>2011</b> , 471, 675-678	3
1440	Synthesis and superconductivity of MgB2/FeâBeâTe composites. <b>2011</b> , 471, 721-724	
1439	Critical current density and vortex dynamics in uranium irradiated Co-doped BaFe2As2. <b>2011</b> , 471, 790-793	15
1438	MBE growth of Fe-based superconducting films. <b>2011</b> , 471, 1167-1173	23
1437	A study of the doping dependence of Tc in Ba1â\(\textbf{\mathbb{R}}\)KxFe2As2 and Sr1â\(\textbf{\mathbb{R}}\)KxFe2As2 films grown by molecular beam epitaxy. <b>2011</b> , 471, 1177-1180	14

1436	Epitaxial films of FeTe1â\Sx fabricated by second harmonic Nd:YAG pulsed laser deposition. <b>2011</b> , 471, 1185-1188	10
1435	The role of correlations in the high-pressure phase of FeSe. <b>2011</b> , 23, 205601	5
1434	Superconductivity in PbO-type Fe chalcogenides. <b>2011</b> , 226,	15
1433	Iron-vacancy superstructure and possible room-temperature antiferromagnetic order in superconducting CsyFe2â⊠Se2. <b>2011</b> , 83,	86
1432	Physical properties of FeSe0.5Te0.5 single crystals grown under different conditions. <b>2011</b> , 79, 289-299	71
1431	Physical properties, crystal and magnetic structure of layered Fe1.11Te1- x Se x superconductors. <b>2011</b> , 82, 113-121	6
1430	Revised phase diagram for the FeTe1â⊠Sex system with fewer excess Fe atoms. <b>2011</b> , 84,	70
1429	Superconductivity in iron compounds. <b>2011</b> , 83, 1589-1652	1137
1428	Pressure effects on two superconducting iron-based families. <b>2011</b> , 74, 124502	92
1427	Competing energy scales in high-temperature superconductors: Ultrafast pumpâßrobe studies. <b>2011</b> , 5, 1-9	6
1426	Magnetic and Missbauer Studies of Ba(Fe1â⊠ Ni x )2As2 Single Crystals. <b>2011</b> , 24, 1363-1369	3
1425	Observation of Multiple Gap Structures Using NdFeAsO1â¼ F x âGaAs Tunneling Junction. <b>2011</b> , 24, 1491-149	510
1424	A Comparative Study of Fe1+⊡re1â⊠ Se x Single Crystals Grown by Bridgman and Self-flux Techniques. <b>2011</b> , 24, 183-187	18
1423	Electronic Structure of BaFe2â⊠ Co x As2 Revealed by Angle-Resolved Photoemission Spectroscopy. <b>2011</b> , 24, 1133-1136	3
1422	Single Crystal Growth and Effect of Doping on Structural, Transport and Magnetic Properties of A1 $\hat{a}$ K x Fe2As2 (A = Ba, Sr). <b>2011</b> , 24, 1773-1785	20
1421	Scaling of the Temperature Dependent Resistivity and Hall Effect in Ba(Fe1â⊠ Co x )As2. <b>2011</b> , 24, 2285-2292	5
1420	EuGa2Sb2: a new Zintl phase with four-bonded gallium and three-bonded antimony in a complex three-dimensional [Ga2Sb2] polyanion. <b>2011</b> , 142, 875-880	13
1419	Pulsed laser deposition conditions and superconductivity of FeSe thin films. <b>2011</b> , 104, 311-318	25

1418 Upper critical field of the 122-type iron pnictide superconductors. <b>2011</b> , 72, 423-425	6
1417 The orbital characters and kz dispersions of bands in iron-pnictide NaFeAs. <b>2011</b> , 72, 479-482	10
1416 Variation of physical properties in the nominal Sr4V2O6Fe2As2. <b>2011</b> , 471, 143-149	16
Structural, magnetic and electronic properties of the iron-chalcogenide AxFe2âySe2 (A=K, Cs, Rb, and Tl, etc.) superconductors. <b>2011</b> , 6, 410-428	33
1414 Universal behavior of the upper critical field in iron-based superconductors. <b>2011</b> , 6, 463-473	36
1413 Magnetic excitation and thermodynamics of BaFe2As2. <b>2011</b> , 111, 3565-3570	5
1412 Charge transfer effects on the Fermi surface of Ba0.5K0.5Fe2As2. <b>2011</b> , 523, 259-264	
On the multi-orbital band structure and itinerant magnetism of iron-based superconductors. <b>2011</b> , 523, 8-50	111
1410 A theoretical approach to iron-based superconductors. <b>2011</b> , 523, 580-581	
1409 Iron-Based Superconductors with Extended FeX4 (X = As and Se) Tetrahedra. <b>2011</b> , 2011, 3868-3876	6
Supraleitung bis zu 35 K in den Eisen-Platinarseniden (CaFe1â\PtxAs)10Pt4â\JAs8 mit schichtartigem Aufbau. <b>2011</b> , 123, 9362-9366	1
1407 Recovery of a parentlike state in Ba(1-x)K(x)Fe(1.86)Co(0.14)As2. <b>2011</b> , 50, 7919-23	17
Superconductivity up to 35 K in the iron platinum arsenides (CaFe(1-x)Pt(x)As)10Pt(4-y)As8 with layered structures. <b>2011</b> , 50, 9195-9	83
Superconductivity up to 35 K in the iron platinum arsenides (CaFe(1-x)Pt(x)As)10Pt(4-y)As8 with layered structures. <b>2011</b> , 50, 9195-9  NMR studies on iron-pnictide superconductors: and. <b>2011</b> , 12, 515-531	2
layered structures. <b>2011</b> , 50, 9195-9	
layered structures. <b>2011</b> , 50, 9195-9  1405 NMR studies on iron-pnictide superconductors: and. <b>2011</b> , 12, 515-531  Electronic band structure and Fermi surface of new low-temperature Ni-based superconductors:	2
layered structures. 2011, 50, 9195-9  1405 NMR studies on iron-pnictide superconductors: and. 2011, 12, 515-531  Electronic band structure and Fermi surface of new low-temperature Ni-based superconductors: 3.3K (Ni2P2)(Sr4Sc2O6) and 2.7K (Ni2As2)(Sr4Sc2O6) from first principles. 2011, 406, 676-682  Stability, structural, elastic, and electronic properties of polymorphs of the superconducting	3

1400 As-NMR/NQR study of pressure-induced superconductivity in CaFe2As2. <b>2011</b> , 72, 501-504	3
1399 Novel superconducting phases in copper oxides and iron-oxypnictides: NMR studies. <b>2011</b> , 72, 486-	<b>491</b>
Multiple superconducting gap and anisotropic spin fluctuations in iron arsenides: Comparison with nickel analog. <b>2011</b> , 72, 492-496	1
1397 Structural and physical properties of SrMn2As2. <b>2011</b> , 72, 457-459	9
Doping effect on the carrier scattering in iron-pnictide superconductors studied by charge transport. <b>2011</b> , 72, 407-409	1
1395 Pnicogen-bridged antiferromagnetic superexchange interactions in iron pnictides. <b>2011</b> , 72, 319-32	23 5
Syntheses, and crystal and electronic structures of the new Zintl phases Na2ACdSb2 and K2ACdSb2 (A=Ca, Sr, Ba, Eu, Yb): Structural relationship with Yb2CdSb2 and the solid solutions Sr2â\(\text{A}\text{X}\text{CdSb2}\), Ba2â\(\text{A}\text{X}\text{CdSb2}\) and Eu2â\(\text{A}\text{Y}\text{b}\text{X}\text{CdSb2}\). <b>2011</b> , 184, 432-440	
1393 Synthesis and electronic properties of LnRhAsO and LnIrAsO compositions. <b>2011</b> , 184, 1972-1976	5
1392 Enhanced superconductivity by correlations between two Kondo impurities. <b>2011</b> , 406, 1738-1743	1
Single crystal growth and physical properties of superconducting ferro-pnictides Ba(Fe, Co)2As2 grown using self-flux and Bridgman techniques. <b>2011</b> , 314, 341-348	23
1390 Investigation of thermal behavior and crystal growth of iron pnictides using Sn flux. <b>2011</b> , 316, 85-8	39 1
Superconductivity and thermal properties of sulphur doped FeTe with effect of oxygen post annealing. <b>2011</b> , 471, 77-82	32
Electronic band structure and Fermi surface of new 3.7 K superconductor LiCu2P2 from first-principles calculations. <b>2011</b> , 471, 226-228	5
1387 Scaling of the temperature-dependent resistivity in SrFe2â⊠NixAs2. <b>2011</b> , 471, 237-241	7
New ternary ThCr2Si2-type ironâlelenide superconducting materials: Synthesis, properties and simulations. <b>2011</b> , 471, 409-427	49
Structural, electronic properties and inter-atomic bonding in layered ironâpnictide oxides (Fe2As2)(Sr4O6), where M are Mg and Ti. <b>2011</b> , 375, 2075-2078	2
1384 The flux pinning force and vortex phase diagram of single crystal. <b>2011</b> , 151, 216-218	34
1383 Effects of spin structures on Fermi surface topologies in BaFe2As2. <b>2011</b> , 151, 272-275	3

1382	The stable structures of iron pnictides AFeAs (A □ lalkali and alkaline-earth metals): A first principles study. <b>2011</b> , 151, 446-450	6
1381	Enhanced superconducting properties in. <b>2011</b> , 151, 557-560	16
1380	The magnetism for NN AFM ground state in Fe-based superconductor: Sr1â\(\text{K}\)KxFe2As2. <b>2011</b> , 151, 667-670	2
1379	Magnetization and characteristic fields in Nd0.8Ba0.2FeAsO0.6F0.4 with binary doping. <b>2011</b> , 151, 956-959	1
1378	First-order phase transitions in CaFeâAsâIsingle crystal: a local probe study. <b>2011</b> , 23, 145701	17
1377	Superconductivity at 22 K in Ir-doped CaFe 2â⊠ Ir x As 2 single crystals. <b>2011</b> , 96, 47005	11
1376	Anisotropic charge dynamics in detwinned Ba(Fe 1-x Co x ) 2 As 2. <b>2011</b> , 93, 37002	113
1375	Pressure effect on superconductivity of AxFe2Se2(A= K and Cs). <b>2011</b> , 13, 033008	28
1374	Proximity fingerprint of s ⊞ -superconductivity. <b>2011</b> , 96, 27014	13
1373	Spin glassiness and power law scaling in anisotropic triangular spin-1/2 antiferromagnets. <b>2011</b> , 93, 67001	3
1372	Synthesis and properties of La-doped CaFe 2 As 2 single crystals with T c =42.7 K. <b>2011</b> , 95, 67002	34
1371	57Fe and151Eu M\(\mathbb{B}\)sbauer spectroscopy and magnetization studies of Eu(Fe0.89Co0.11)2As2and Eu(Fe0.9Ni0.1)2As2. <b>2011</b> , 13, 023033	22
1370	The electronic structure of LaCo 2 B 2. <b>2011</b> , 95, 17001	2
1369	Orbital-transverse density-wave instabilities in iron-based superconductors. <b>2011</b> , 93, 37009	3
1368	Enhancement of the upper critical field in codoped iron-arsenic high-temperature superconductors. <b>2011</b> , 110, 123906	5
1367	Magnetic order in orbital models of the iron pnictides. <b>2011</b> , 23, 246001	21
1366	Anisotropic intrinsic spin Hall effect in quantum wires. <b>2011</b> , 23, 465301	1
1365	Electronic correlations in iron-pnictide superconductors and beyond: lessons learned from optics. <b>2011</b> , 13, 023011	25

1364	(75)As NMR study of antiferromagnetic fluctuations in Ba(Fe(1-x)Ru(x))(2)As(2). 2011, 23, 475701		2
1363	Pressure Dependence of Superconducting Transition Temperature on Perovskite-Type Fe-Based Superconductors and NMR Study of Sr2VFeAsO3. <b>2011</b> , 80, 014712		8
1362	The synthesis, and crystal and magnetic structure of the iron selenide BaFe2Se3 with possible superconductivity at $Tc = 11 \text{ K. } 2011, 23, 402201$		37
1361	Neutron scattering studies of spin excitations in hole-doped Ba(0.67)K(0.33)Fe(2)As(2) superconductor. <b>2011</b> , 1, 115		65
1360	Superconductivity induced by doping Rh in CaFe2â⊠RhxAs2. <b>2011</b> , 13, 033020		9
1359	Anisotropy in transport and magnetic properties of K0.64Fe1.44Se2. <b>2011</b> , 83,		39
1358	Se77 NMR investigation of the KxFe2â�JSe2 high-Tc superconductor (Tc=33 K). <b>2011</b> , 83,		71
1357	Magnetic ordering and structural distortion in Ru-doped BaFe2As2 single crystals studied by neutron and x-ray diffraction. <b>2011</b> , 83,		59
1356	Effects of chemical doping and pressure on CaFe4As3. <b>2011</b> , 84,		4
1355	Measurement of a sign-changing two-gap superconducting phase in electron-doped Ba(Fe(1-x)Co(x))2As2 single crystals using scanning tunneling spectroscopy. <i>Physical Review Letters</i> , 7. <b>2011</b> , 106, 087004	4	50
1354	Magnetic and quasiparticle excitation spectra of an itinerant J1-J2 model for iron-pnictide superconductors. <i>Physical Review Letters</i> , <b>2011</b> , 106, 117002	4	6
1353	Ternary iron selenide K0.8Fe1.6Se2 is an antiferromagnetic semiconductor. <b>2011</b> , 83,		81
1352	Synthesis, structure, and magnetic properties of the layered iron oxychalcogenide Na2Fe2Se2O. <b>2011</b> , 84,		27
1351	Spin-glass behavior of semiconducting KxFe2âyS2. <b>2011</b> , 83,		46
1350	Evidence of multiple nodeless energy gaps in superconducting Ba0.6K0.4Fe2As2 single crystals from scanning tunneling spectroscopy. <b>2011</b> , 83,		23
1349	Spin fluctuations and unconventional pairing in KFe2As2. <b>2011</b> , 84,		50
1348	Infrared spectrum and its implications for the electronic structure of the semiconducting iron selenide K0.83Fe1.53Se2. <b>2011</b> , 83,		43
1347	Pressure-induced changes in the magnetic and valence state of EuFe2As2. <b>2011</b> , 84,		56

1346	Different effects of Ni and Co substitution on the transport properties of BaFe2As2. <b>2011</b> , 83,		24
1345	Combined effects of pressure and Ru substitution on BaFe2As2. <b>2011</b> , 84,		44
1344	Possible origin of the nonmonotonic doping dependence of the in-plane resistivity anisotropy of Ba(Fe1â☑Tx)2As2 (T=Co, Ni and Cu). <b>2011</b> , 84,		86
1343	London penetration depth in iron-based superconductors. <b>2011</b> , 74, 124505		127
1342	Electronic band structure of SrCu4As2 and KCu4As2: Metals with diversely doped CuAs layers. <b>2011</b> , 84,		2
1341	Critical current densities in ultrathin Ba(Fe,Co)2As2 microbridges. <b>2011</b> , 83,		25
1340	Fe57 MBsbauer study of magnetic ordering in superconducting K0.80Fe1.76Se2.00 single crystals. <b>2011</b> , 83,		76
1339	Coexistence of light and heavy carriers associated with superconductivity and antiferromagnetism in CeNi0.8Bi2 with a Bi square net. <i>Physical Review Letters</i> , <b>2011</b> , 106, 057002	7.4	44
1338	Quasiclassical description of a superconductor with a spin density wave. <b>2011</b> , 83,		15
1337	Pressure- and temperature-induced structural phase transitions of CaFe2As2 and BaFe2As2 studied in the Hundâll rule correlation picture. <b>2011</b> , 83,		18
1336	Macroscopic quantum tunneling in multigap superconducting Josephson junctions: Enhancement of escape rate via quantum fluctuations of the Josephson-Leggett mode. <b>2011</b> , 83,		13
1335	Nematic phase without Heisenberg physics in FeAs planes. <b>2011</b> , 84,		16
1334	Transport properties and anisotropy of Rb1â⊠Fe2âÿSe2 single crystals. <b>2011</b> , 83,		94
1333	Electronic structure of detwinned BaFe2As2 from photoemission and first principles. <b>2011</b> , 83,		50
1332	Interplay of antiferromagnetism, ferromagnetism, and superconductivity in EuFe2(As1âNPx)2 single crystals. <b>2011</b> , 83,		103
1331	Andreev reflection spectroscopy of the new Fe-based superconductor EuAsFeO0.85F0.15: Evidence of strong anisotropy in the order parameter. <b>2011</b> , 37, 280-286		4
1330	Effects of nonhydrostatic pressure on the structural and magnetic properties of BaFe2As2. <b>2011</b> , 83,		16
1329	Suppressed superconductivity in charge-doped Li(Fe1â\(\text{\beta}\)Cox)As single crystals. <b>2011</b> , 84,		13

1328	Physical and magnetic properties of Ba(Fe1âMMnx)2As2 single crystals. <b>2011</b> , 84,		45
1327	Anisotropic magnetic order of the Eu sublattice in single crystals of EuFe2â⊠CoxAs2 (x=0,0.2) studied by means of magnetization and magnetic torque. <b>2011</b> , 84,		23
1326	Eliashberg approach to infrared anomalies induced by the superconducting state of Ba0.68K0.32Fe2As2 single crystals. <b>2011</b> , 84,		60
1325	Effect of Co substitution on the magnetic order in Ca(Fe1â\(\mathbb{U}\)Cox)2As2 single crystals studied by neutron diffraction. <b>2011</b> , 83,		11
1324	Thermoelectric studies of KxFe2âySe2 indicating a weakly correlated superconductor. <b>2011</b> , 83,		22
1323	Anisotropy in BaFe2Se3 single crystals with double chains of FeSe tetrahedra. <b>2011</b> , 84,		64
1322	Variable temperature study of the crystal and magnetic structures of the giant magnetoresistant materials LMnAsO( $L = La, Nd$ ). <b>2011</b> , 83,		52
1321	Phonon softening near the structural transition in BaFe2As2 observed by inelastic x-ray scattering. <b>2011</b> , 84,		34
1320	Mixed-state Hall effect and flux pinning in Ba(Fe1â⊠Cox)2As2 single crystals (x=0.08 and 0.10). <b>2011</b> , 83,		18
1319	Pressure-restored superconductivity in Cu-substituted FeSe. <b>2011</b> , 84,		14
1319	Anisotropic upper critical field and possible Fulde-Ferrel-Larkin-Ovchinnikov state in the stoichiometric pnictide superconductor LiFeAs. <b>2011</b> , 83,		102
1318	Anisotropic upper critical field and possible Fulde-Ferrel-Larkin-Ovchinnikov state in the		
1318	Anisotropic upper critical field and possible Fulde-Ferrel-Larkin-Ovchinnikov state in the stoichiometric pnictide superconductor LiFeAs. <b>2011</b> , 83,  Crystal and magnetic structures of the superconductor CeNi0.8Bi2. <b>2011</b> , 83,  Co-substitution effects on the Fe valence in the BaFe2As2 superconducting compound: a study of	7-4	102
1318	Anisotropic upper critical field and possible Fulde-Ferrel-Larkin-Ovchinnikov state in the stoichiometric pnictide superconductor LiFeAs. <b>2011</b> , 83,  Crystal and magnetic structures of the superconductor CeNi0.8Bi2. <b>2011</b> , 83,  Co-substitution effects on the Fe valence in the BaFe2As2 superconducting compound: a study of	7-4	102
1318 1317 1316	Anisotropic upper critical field and possible Fulde-Ferrel-Larkin-Ovchinnikov state in the stoichiometric pnictide superconductor LiFeAs. <b>2011</b> , 83,  Crystal and magnetic structures of the superconductor CeNi0.8Bi2. <b>2011</b> , 83,  Co-substitution effects on the Fe valence in the BaFe2As2 superconducting compound: a study of hard x-ray absorption spectroscopy. <i>Physical Review Letters</i> , <b>2011</b> , 107, 267402	7.4	102 18 47
1318 1317 1316 1315	Anisotropic upper critical field and possible Fulde-Ferrel-Larkin-Ovchinnikov state in the stoichiometric pnictide superconductor LiFeAs. 2011, 83,  Crystal and magnetic structures of the superconductor CeNi0.8Bi2. 2011, 83,  Co-substitution effects on the Fe valence in the BaFe2As2 superconducting compound: a study of hard x-ray absorption spectroscopy. <i>Physical Review Letters</i> , 2011, 107, 267402  Antiferromagnetism in semiconducting KFe0.85Ag1.15Te2 single crystals. 2011, 84,  Static magnetic order of Sr4A2O6Fe2As2 (A = Sc and V) revealed by Missbauer and muon spin	7.4	102 18 47
1318 1317 1316 1315 1314	Anisotropic upper critical field and possible Fulde-Ferrel-Larkin-Ovchinnikov state in the stoichiometric pnictide superconductor LiFeAs. 2011, 83,  Crystal and magnetic structures of the superconductor CeNi0.8Bi2. 2011, 83,  Co-substitution effects on the Fe valence in the BaFe2As2 superconducting compound: a study of hard x-ray absorption spectroscopy. <i>Physical Review Letters</i> , 2011, 107, 267402  Antiferromagnetism in semiconducting KFe0.85Ag1.15Te2 single crystals. 2011, 84,  Static magnetic order of Sr4A2O6Fe2As2 (A = Sc and V) revealed by Missbauer and muon spin relaxation spectroscopies. 2011, 84,	7.4	102 18 47 19

1310	Exotic d-wave superconducting state of strongly hole-doped K(x)Ba(1-x)Fe2As2. <i>Physical Review Letters</i> , <b>2011</b> , 107, 117001	7.4	132
1309	What controls the phase diagram and superconductivity in Ru-substituted BaFe2As2?. <i>Physical Review Letters</i> , <b>2011</b> , 107, 267002	7.4	59
1308	LaCo2B2: a Co-based layered superconductor with a ThCr2Si2-type structure. <i>Physical Review Letters</i> , <b>2011</b> , 106, 237001	7.4	29
1307	Layered transition-metal pnictide SrMnBi2 with metallic blocking layer. <b>2011</b> , 84,		59
1306	Effect of annealing on the specific heat of Ba(Fe1â⊠Cox)2As2. <b>2011</b> , 83,		50
1305	Charge compensation effect in Pr1â∏SryFe1â⊠CoxAsO codoped with Sr and Co. <b>2011</b> , 83,		9
1304	Noncollinear spin-density-wave antiferromagnetism in FeAs. <b>2011</b> , 83,		47
1303	Theoretical investigation of optical conductivity in Ba(Fe1â\( Cox)\) 2As2. <b>2011</b> , 83,		18
1302	The electron-pairing mechanism of iron-based superconductors. <b>2011</b> , 332, 200-4		195
1301	Iron displacements and magnetoelastic coupling in the antiferromagnetic spin-ladder compound BaFe2Se3. <b>2011</b> , 84,		101
1300	Electronic band structure, Fermi surface, and elastic properties of polymorphs of the 5.2 K iron-free superconductor SrPt2As2 from first-principles calculations. <b>2011</b> , 83,		39
1299	Magnetic phase diagram of CeAu2Ge2: High magnetic anisotropy due to crystal electric field. <b>2011</b> , 84,		7
1298	Superconductivity and magnetic properties of single crystals of K0.75Fe1.66Se2 and Cs0.81Fe1.61Se2. <b>2011</b> , 83,		92
1297	Model of vortex states in hole-doped iron-pnictide superconductors. <i>Physical Review Letters</i> , <b>2011</b> , 106, 027004	7.4	28
1296	Different response of superconductivity to the transition-metal impurities in K0.8Fe2â�Jâ�MxSe2 (M = Cr, Mn, Co, Zn). <b>2011</b> , 84,		31
1295	Large magnetoresistance effects in LnCoAsO (Ln= Nd, Sm) with a ferromagnetic-antiferromagnetic transition. <b>2011</b> , 84,		13
1294	High transport critical current densities in textured Fe-sheathed Sr1â⊠KxFe2As2+Sn superconducting tapes. <b>2011</b> , 99, 242506		64
1293	Competing magnetic ground states in nonsuperconducting Ba(Fe1â\(\mathbb{R}\)Crx)2As2 as seen via neutron diffraction. <b>2011</b> , 83,		61

1292	Raman scattering study of electron-doped PrxCa1â\(\mathbb{R}\)Fe2As2 superconductors. <b>2011</b> , 84,		14
1291	Theory of mixed-state effect on NMR relaxation measurements in iron pnictide superconductors. <b>2011</b> , 84,		3
1290	Enhanced critical current properties in Ba0.6K0.4+xFe2As2 superconductor by overdoping of potassium. <b>2011</b> , 98, 042508		22
1289	Phase diagram of superconductivity and antiferromagnetism in single crystals of Sr(Fe1â\(\mathbb{U}\)Cox)2As2 and Sr1â\(\mathbb{E}\)Euy(Fe0.88Co0.12)2As2. <b>2011</b> , 83,		27
1288	Phonon, two-magnon, and electronic Raman scattering of Fe1+yTe1â⊠Sex. <b>2011</b> , 83,		40
1287	Anisotropic Hc2 of K0.8Fe1.76Se2 determined up to 60 T. <b>2011</b> , 83,		50
1286	Magnetic and electrical properties and carrier doping effects on the iron-based host compound Sr2ScFeAsO3. <b>2011</b> , 83,		6
1285	Calorimetric evidence of strong-coupling multiband superconductivity in Fe(Te0.57Se0.43) single crystal. <b>2011</b> , 83,		46
1284	Muon-spin rotation measurements of the magnetic penetration depth in the iron-based superconductor Ba1â⊠RbxFe2As2. <b>2011</b> , 84,		18
1283	Character of the structural and magnetic phase transitions in the parent and electron-doped BaFe2As2 compounds. <b>2011</b> , 83,		123
1282	Evolution of correlation strength in KxFe2âŪSe2 superconductor doped with S. <b>2011</b> , 84,		13
1281	Soft and isotropic phonons in PrFeAsO1â¶. <b>2011</b> , 84,		17
1280	Linear decrease of critical temperature with increasing Zn substitution in the iron-based superconductor BaFe1.89âØxZn2xCo0.11As2. <b>2011</b> , 84,		47
	Standard Laboratory of Capada 2 2014 04		
1279	Structural and physical properties of CaFe4As3. <b>2011</b> , 84,		6
1279	Nodeless energy gaps of single-crystalline Ba0.68K0.32Fe2As2 as seen via As75 NMR. <b>2011</b> , 83,		53
1278	Nodeless energy gaps of single-crystalline Ba0.68K0.32Fe2As2 as seen via As75 NMR. <b>2011</b> , 83,	7.4	53

1274 Large miscibility gap in the Ba(MnxFe1â⊠)2As2 system. <b>2011</b> , 84,	24
Effect of doping on structural and superconducting properties in Ca1â\(\mathbb{\text{N}}\) NaxFe2As2 single crystal (x=0.5, 0.6, 0.75). <b>2011</b> , 84,	s <sub>23</sub>
Effect of the isoelectronic substitution of Sb for As on the magnetic and structural properties of LaFe(As1â\Sbx)O. <b>2011</b> , 84,	9
Comparative study of the electronic and magnetic properties of BaFe2As2 and BaMn2As2 using Gutzwiller approximation. <b>2011</b> , 84,	the <sup>23</sup>
Specific heat in KFe2As2 in zero and applied magnetic field. <b>2011</b> , 83,	33
Ambient- and low-temperature synchrotron x-ray diffraction study of BaFe2As2 and CaFe2As2 all high pressures up to 56 GPa. <b>2011</b> , 83,	t 91
1268 Doping dependence of the superconductivity of (Ca1â⊠Nax)Fe2As2. <b>2011</b> , 84,	27
1267 Finite-temperature signatures of gap anisotropy in optical conductivity of ferropnictides. <b>2011</b> , 8	34, 4
1266 Transport properties of the new Fe-based superconductor KxFe2Se2 (Tc=33 K). <b>2011</b> , 98, 042511	129
Phase diagram of pressure-induced superconductivity in EuFe2As2 probed by high-pressure resistivity up to 3.2 GPa. <b>2011</b> , 83,	41
High-pressure study of superconducting and nonsuperconducting single crystals of the same nominal composition Rb0.8Fe2Se2. <b>2011</b> , 84,	10
1263 Elastic stiffness of single-crystalline FeSe measured by picosecond ultrasonics. <b>2011</b> , 110, 07350	5 5
Orthorhombic fluctuations in tetragonal AFe2As2 (A=Sr and Eu). <b>2011</b> , 84,	9
Fermi surface, structural and electronic properties of ThCr2Si2-type charge-balanced KFe2AsSe: parent system for the group of mixed pnictide-chalcogenide superconductors. <b>2011</b> , 84,	A 1
Small anisotropy in iron-based superconductors induced by electron correlation. <b>2011</b> , 84,	4
1259 Self-assembled oxide nanopillars in epitaxial BaFe2As2 thin films for vortex pinning. <b>2011</b> , 98, 04	12509 40
High-field properties of pure and doped MgB2 and Fe-based superconductors. <b>2011</b> , 36, 626-630	) 2
1257 Tuning the ground state of BaFe2As2: Phase diagrams and empirical trends. <b>2011</b> , 36, 620-625	16

1256	High T(c) electron doped Ca10(Pt3As8)(Fe2As2)5 and Ca10(Pt4As8)(Fe2As2)5 superconductors with skutterudite intermediary layers. <b>2011</b> , 108, E1019-26	117
1255	A new iron pnictide oxide (Fe2As2)(Ca5(Mg, Ti)4Oy) and a new phase in the FeâAsâCaâMgâIIiâD system. <b>2011</b> , 24, 085020	11
1254	Superconducting properties of FeSe wires and tapes prepared by a gas diffusion technique. <b>2011</b> , 24, 065022	32
1253	Upper critical fields and superconducting anisotropy of K 0.70 Fe 1.55 Se 1.01 S 0.99 and K 0.76 Fe 1.61 Se 0.96 S 1.04 single crystals. <b>2011</b> , 95, 57006	10
1252	Anisotropic magnetism, resistivity, London penetration depth and magneto-optical imaging of superconducting K0.80Fe1.76Se2single crystals. <b>2011</b> , 24, 065006	22
1251	Chemistry and electronic structure of iron-based superconductors. <b>2011</b> , 36, 614-619	33
1250	Superconductivity and magnetic properties in SmFe 1â⊠ Co x AsO (x=0 to 1). <b>2011</b> , 96, 17007	8
1249	A New Noncentrosymmetric Superconducting Phase in the LiâRhâB System. <b>2011</b> , 80, 013702	3
1248	In-plane electronic anisotropy of underdoped âll 22âlFe-arsenide superconductors revealed by measurements of detwinned single crystals. <b>2011</b> , 74, 124506	193
1247	Symmetry-breaking orbital anisotropy observed for detwinned Ba(Fe1-xCox)2As2 above the spin density wave transition. <b>2011</b> , 108, 6878-6883	409
1246	Scaling of the temperature-dependent resistivity in 122 iron-pnictide superconductors. <b>2011</b> , 24, 105004	6
1245	Structural stability and electronic properties of the new superconductor (Ca4Al2O6 â☑)(Fe2As2) from first-principles study. <b>2011</b> , 24, 105014	4
1244	Physical property and electronic structure characterization of bulk superconducting Bi3Ni. 2011,	29
	24, 085002	<u>-9</u>
1243	An anomalous tail effect in the resistivity transition and weak-link behavior of superconducting NdFeAsO0.88F0.12. <b>2011</b> , 24, 085011	9
1243	An anomalous tail effect in the resistivity transition and weak-link behavior of superconducting	
	An anomalous tail effect in the resistivity transition and weak-link behavior of superconducting NdFeAsO0.88F0.12. <b>2011</b> , 24, 085011  Analysis of interdiffusion between SmFeAsO0.92F0.08and metals forex situfabrication of superconducting wire. <b>2011</b> , 24, 075024	9
1242	An anomalous tail effect in the resistivity transition and weak-link behavior of superconducting NdFeAsO0.88F0.12. <b>2011</b> , 24, 085011  Analysis of interdiffusion between SmFeAsO0.92F0.08and metals forex situfabrication of superconducting wire. <b>2011</b> , 24, 075024	9

1238	Low-temperature synthesis of FeTe0.5Se0.5polycrystals with a high transport critical current density. <b>2011</b> , 24, 075025	24
1237	Hall sign reversal and electrical transport properties of single crystalline SrPd2Ge2. <b>2011</b> , 109, 07E109	2
1236	Unusual superconducting state at 49 K in electron-doped CaFe2As2 at ambient pressure. <b>2011</b> , 108, 15705-9	110
1235	Microwave Surface Impedance Measurements of LiFeAs Single Crystals. <b>2011</b> , 80, 013704	37
1234	Direct observation of nanometer-scale amorphous layers and oxide crystallites at grain boundaries in polycrystalline Sr1â⊠KxFe2As2 superconductors. <b>2011</b> , 98, 222504	31
1233	Electronic behavior of superconducting SmFeAsO0.75. <b>2011</b> , 109, 083914	8
1232	ANALYSIS OF MAGNETIC CRITICAL FIELDS IN IRON-BASED SmFeAsO0.85 HIGH-Tc SUPERCONDUCTOR. <b>2011</b> , 25, 1939-1948	3
1231	Crystal structure, physical properties and superconductivity inAxFe2Se2single crystals. <b>2011</b> , 13, 053011	39
1230	One-step method to grow Ba0.6K0.4Fe2As2single crystals without fluxing agent. <b>2011</b> , 24, 065002	16
1229	Distinct fermi surface topology and nodeless superconducting gap in a (Tl0.58Rb0.42)Fe1.72Se2 superconductor. <i>Physical Review Letters</i> , <b>2011</b> , 106, 107001	191
1229 1228	superconductor. <i>Physical Review Letters</i> , <b>2011</b> , 106, 107001	9
	superconductor. <i>Physical Review Letters</i> , <b>2011</b> , 106, 107001	
1228	superconductor. <i>Physical Review Letters</i> , <b>2011</b> , 106, 107001  Effect of pressure on a âll 11âltype iron pnictide superconductor. <b>2011</b> , 31, 7-12	9
1228	Superconductivity and upper fields in Na-doped iron arsenides Eu1â\(\text{NaxFe2As2.}\) 2012, 14, 033011  Structural Quantum Criticality and Superconductivity in Iron-Based Superconductor	9
1228 1227 1226	Effect of pressure on a âll 11âltype iron pnictide superconductor. 2011, 31, 7-12  Superconductivity and upper fields in Na-doped iron arsenides Eu1âllNaxFe2As2. 2012, 14, 033011  Structural Quantum Criticality and Superconductivity in Iron-Based Superconductor Ba(Fe1-xCox)2As2. 2012, 81, 024604  A Possible New Parent Compound Sr4Al2O6Fe2As2 with High-TC Superconductivity. 2012, 81, 024713	9 10 155
1228 1227 1226 1225	Superconductor. <i>Physical Review Letters</i> , <b>2011</b> , 106, 107001  Effect of pressure on a âll 11âltype iron pnictide superconductor. <b>2011</b> , 31, 7-12  Superconductivity and upper fields in Na-doped iron arsenides Eu1âll NaxFe2As2. <b>2012</b> , 14, 033011  Structural Quantum Criticality and Superconductivity in Iron-Based Superconductor Ba(Fe1-xCox)2As2. <b>2012</b> , 81, 024604  A Possible New Parent Compound Sr4Al2O6Fe2As2 with High-TC Superconductivity. <b>2012</b> , 81, 024713	9 10 155 3
1228 1227 1226 1225	Effect of pressure on a âl 11â Etype iron pnictide superconductor. 2011, 31, 7-12  Superconductivity and upper fields in Na-doped iron arsenides Eu1â NaxFe2As2. 2012, 14, 033011  Structural Quantum Criticality and Superconductivity in Iron-Based Superconductor Ba(Fe1-xCox)2As2. 2012, 81, 024604  A Possible New Parent Compound Sr4Al2O6Fe2As2 with High-TC Superconductivity. 2012, 81, 024713  Frontiers of Research on Iron-Based Superconductors toward Their Application. 2012, 51, 010005	9 10 155 3 21

1220	Mixed-state effect on quasiparticle interference in iron-based superconductors. 2012, 100, 37002	7
1219	Vortices and Chirality in Multi-Band Superconductors. <b>2012</b> , 81, 024712	52
1218	Magnetism and superconductivity in Eu0.2Sr0.8(Fe0.86Co0.14)2As2 probed by 75As NMR. 2012, 24, 045702	2
1217	Superconductivity and phase diagram in Ru-doped SrFe 2â⊠ Ru x As 2 single crystals. <b>2012</b> , 97, 17008	1
1216	Ultrafast dynamics and phonon softening in Fe1+ySe1â⊠Texsingle crystals. <b>2012</b> , 14, 103053	16
1215	Chemical pressure and electron doping effects in SrPd2Ge2 single crystals. <b>2012</b> , 111, 07E117	4
1214	Quasiparticle relaxation across the multiple superconducting gaps in the electron-doped BaFe1.85Co0.15As2. <b>2012</b> , 111, 07E134	3
1213	Theoretical study of point-contact Andreev reflection spectroscopy for ferromagnetic-metal/multi-band superconductor junctions. <b>2012</b> , 111, 07C518	1
1212	Flux distribution in Fe-based superconducting materials by magneto-optical imaging. <b>2012</b> , 111, 07E143	3
1211	Anisotropies and Homogeneities of Superconducting Properties in Ironâ <b>P</b> latinumâ <b>A</b> rsenide Ca10(Pt3As8)(Fe1.79Pt0.21As2)5. <b>2012</b> , 81, 114723	5
1210	High energy pseudogap and its evolution with doping in Fe-based superconductors as revealed by optical spectroscopy. <b>2012</b> , 24, 294202	30
1209	Electrochemical Synthesis of Iron-Based Superconductor FeSe Films. <b>2012</b> , 81, 043702	20
1208	Flux pinning and vortex transitions in doped BaFe2As2 single crystals. <b>2012</b> , 100, 072603	30
1207	Evolution of transport properties of BaFe2â\RuxAs2 in a wide range of isovalent Ru substitution. <b>2012</b> , 85,	34
1206	Evolution of normal and superconducting properties of single crystals of Na1âEeAs upon interaction with environment. <b>2012</b> , 85,	28
1205	Electronic structure of single-crystalline Sr(Fe1â\(\mathbb{R}\)Cox)2As2 probed by x-ray absorption spectroscopy: Evidence for effectively isovalent substitution of Fe2+ by Co2+. <b>2012</b> , 86,	22
1204	Phase diagram of Ba1â⊠KxFe2As2. <b>2012</b> , 85,	140
1203	Phase coexistence in Cs0.8Fe1.6Se2 as seen by x-ray mapping of reciprocal space. <b>2012</b> , 86,	16

1202	Phase diagram as a function of doping level and pressure in the Eu1â⊠LaxFe2As2 system. <b>2012</b> , 85,	11
1201	Superconducting properties and magneto-optical imaging of Ba0.6K0.4Fe2As2PIT wires with Ag addition. <b>2012</b> , 25, 035019	22
1200	Evolution of Eu2+ spin dynamics in Ba1â\(\text{EuxFe2As2}\). <b>2012</b> , 86,	14
1199	Local magnetic anisotropy in BaFe2As2: A polarized inelastic neutron scattering study. <b>2012</b> , 86,	48
1198	Superfluid density and superconducting gaps of RbFe2As2 as a function of hydrostatic pressure. <b>2012</b> , 86,	14
1197	Phase diagram and calorimetric properties of NaFe1â\(\mathbb{U}\)CoxAs. <b>2012</b> , 85,	65
1196	Anisotropic Hc2 up to 92 T and the signature of multiband superconductivity in Ca10(Pt4As8)((Fe1âष्यPtx)2As2)5. <b>2012</b> , 85,	27
1195	Doping dependence of Hall coefficient and evolution of coherent electronic state in the normal state of the Fe-based superconductor Ba1â⊠KxFe2As2. <b>2012</b> , 85,	33
1194	Magnetically polarized Ir dopant atoms in superconducting Ba(Fe1â⊠Irx)2As2. <b>2012</b> , 85,	7
1193	Identical effects of indirect and direct electron doping of superconducting BaFe2As2 thin films. <b>2012</b> , 85,	41
1192	Phase transition of square-lattice antiferromagnets at finite temperature. <b>2012</b> , 86,	17
1191	Structural analysis and superconductivity of CeFeAsO1â⊠Hx. <b>2012</b> , 85,	47
1190	Temperature dependence of the paramagnetic spin excitations in BaFe2As2. <b>2012</b> , 86,	21
1189	Fluxon dynamics of a long Josephson junction with two-gap superconductors. <b>2012</b> , 85,	5
1188	Transport and magnetic properties of La-doped CaFe2As2. <b>2012</b> , 85,	14
1187	Mixed-valence-driven heavy-fermion behavior and superconductivity in KNi2Se2. <b>2012</b> , 86,	63
1186	Optical conductivity of superconducting K0.8Fe2â�Se2 single crystals: Evidence for a Josephson-coupled phase. <b>2012</b> , 85,	19
1185	Effects of Ru substitution on electron correlations and Fermi-surface dimensionality in Ba(Fe1â�Rux)2As2. <b>2012</b> , 86,	31

# (2012-2012)

1184	Electronic properties of 3d transitional metal pnictides: A comparative study by optical spectroscopy. <b>2012</b> , 86,	40
1183	Evidence for filamentary superconductivity nucleated at antiphase domain walls in antiferromagnetic CaFe2As2. <b>2012</b> , 85,	39
1182	Structural collapse and superconductivity in rare-earth-doped CaFe2As2. <b>2012</b> , 85,	134
1181	Single crystal growth and superconductivity of Ca(Fe1â⊠ Co x )2As2. <b>2012</b> , 92, 3113-3120	6
1180	Phase transitions in spin-orbital models with spin-space anisotropies for iron pnictides: Monte Carlo simulations. <b>2012</b> , 85,	28
1179	Vortex images on Ba1â⊠KxFe2As2 observed directly by magnetic force microscopy. <b>2012</b> , 85,	19
1178	Metamagnetic transition in Ca1â $\square$ SrxCo2As2(x = 0 and 0.1) single crystals. <b>2012</b> , 85,	28
1177	Doping dependence of the electronic structure in phosphorus-doped ferropnictide superconductor BaFe2(As1â�Px)2 studied by angle-resolved photoemission spectroscopy. <b>2012</b> , 86,	38
1176	Superconducting phase transitions induced by chemical potential in (2+1)-dimensional four-fermion quantum field theory. <b>2012</b> , 86,	11
1175	Fermi-surface topology and low-lying electronic structure of the iron-based superconductor Ca10(Pt3As8)(Fe2As2)5. <b>2012</b> , 85,	30
1174	Enhancement of critical current density and vortex activation energy in proton-irradiated Co-doped BaFe2As2. <b>2012</b> , 86,	57
1173	Gradual suppression of antiferromagnetism in BaFe2(As1â⊠Px)2: Zero-temperature evidence for a quantum critical point. <b>2012</b> , 85,	12
1172	Raman scattering study of the lattice dynamics of superconducting LiFeAs. 2012, 85,	14
1171	Competition between stripe and checkerboard magnetic instabilities in Mn-doped BaFe2As2. <b>2012</b> , 86,	40
1170	Control of magnetic, nonmagnetic, and superconducting states in annealed Ca(Fe1â\( Cox)2As2. <b>2012</b> , 85,	49
1169	Multiband effects on EFeSe single crystals. <b>2012</b> , 85,	46
1168	High-resolution x-ray scattering studies of structural phase transitions in Ba(Fe1â⊠Crx)2As2. <b>2012</b> , 85,	7
1167	Superconductivity and structural variation of the electron-correlated layer systems $Sr(Pd1a\Pi Tx)2Ge2$ (T = Co, Ni, Rh; 0?x?1). <b>2012</b> , 85,	12

1166 Single-crystal growth and optical conductivity of SrPt2As2 superconductors. <b>2012</b> , 85,	15
1165 Impurity states in multiband s-wave superconductors: Analysis of iron pnictides. <b>2012</b> , 86,	21
Dimer impurity scattering, reconstructed Fermi-surface nesting, and density-wave diagnostiron pnictides. <b>2012</b> , 85,	stics in 7
Role of different negatively charged layers in Ca10(FeAs)10(Pt4As8) and superconductivit in electron-doped (Ca0.8La0.2)10(FeAs)10(Pt3As8). <b>2012</b> , 86,	y at 30 K
1162 Electron spin resonance in Eu-based iron pnictides. <b>2012</b> , 86,	11
Structural, thermal, magnetic, and electronic transport properties of the LaNi2(Ge1â\(\mathbb{U}\)Px)2  2012, 85,	system. 69
Muon spin rotation study of magnetism and superconductivity in Ba(Fe1â⊠Cox)2As2 single <b>2012</b> , 86,	e crystals.
Collapsed tetragonal phase in Ca(Fe1â\(\mathbb{R}\)Cox)2As2 stabilized by pressure: Structural studies single-crystal neutron diffraction. <b>2012</b> , 85,	s using 2
Observation of a phase transition at 55 K in single-crystal CaCu1.7As2. <b>2012</b> , 86,	10
Continuous critical temperature enhancement with gradual hydrogen doping in LaFeAsO0 $(x=0-0.85)$ . <b>2012</b> , 86,	0.85Hx 3
Superconductivity suppression of Ba0.5K0.5Fe2â@xM2xAs2 single crystals by substitution transition metal (M = Mn, Ru, Co, Ni, Cu, and Zn). <b>2012</b> , 85,	of 7º
Stability of the Fe electronic structure through temperature-, doping-, and pressure-inductions in the BaFe2As2 superconductors. <b>2012</b> , 86,	ed 4
Local structure of the superconductor K0.8Fe1.6+xSe2: Evidence of large structural disord 85,	ler. <b>2012</b> ,
1153 Experimental and theoretical electronic structure of EuRh2As2. <b>2012</b> , 85,	O
1152 Weakly ferromagnetic metallic state in heavily doped Ba1â⊠KxMn2As2. <b>2012</b> , 85,	29
1151 Doping dependence of antiferromagnetism in models of the pnictides. <b>2012</b> , 85,	8
1150 Magnetism and crystalline electric field effect in ThCr2Si2-type CeNi2As2. <b>2012</b> , 86,	18
1149 Effect of tensile stress on the in-plane resistivity anisotropy in BaFe2As2. <b>2012</b> , 85,	49

1148	Magnetic excitations in underdoped Ba(Fe1â⊠Cox)2As2 with x=0.047. <b>2012</b> , 86,	28
1147	Anomalous dependence of c-axis polarized Fe B1g phonon mode with Fe and Se concentrations in Fe1+yTe1â⊠Sex. <b>2012</b> , 85,	24
1146	Magnetic phase transitions and large mass enhancement in single crystal CaFe 4 As 3. <b>2012</b> , 21, 017402	2
1145	RAMAN SCATTERING IN IRON-BASED SUPERCONDUCTORS. <b>2012</b> , 26, 1230020	9
1144	Enhancement of superconducting properties in FeSe wires using a quenching technique. <b>2012</b> , 111, 013912	17
1143	High critical current density and low anisotropy in textured SrâFxKxFeâAsâLapes for high field applications. <b>2012</b> , 2, 998	62
1142	Evolution of the 251 cm âll infrared phonon mode with temperature in Ba 0.6 K 0.4 Fe 2 As 2. <b>2012</b> , 21, 077403	4
1141	Pairing symmetry in the iron-pnictide superconductor KFe 2 As 2. <b>2012</b> , 99, 57006	10
1140	Effect of starting materials on the superconducting properties of SmFeAsO1âNFxtapes. <b>2012</b> , 25, 035013	12
1139	Transport properties and anisotropy in rare-earth doped CaFe2As2single crystals withTcabove 40 K. <b>2012</b> , 25, 045007	17
1138	Evolution of Tetragonal Phase in the FeSe Wire Fabricated by a Novel Chemical-Transformation Powder-in-Tube Process. <b>2012</b> , 51, 010101	2
1137	Electronic and magnetic phase diagram in K(x)Fe(2-y)Se(2) superconductors. <b>2012</b> , 2, 212	102
1136	Pulsed laser deposition of BaFe2(As,P)2superconducting thin films with high critical current density. <b>2012</b> , 25, 105015	22
1135	Angular effects on upper critical field in LiFeAs using two-band Ginzburgâllandau theory. <b>2012</b> , 25, 095007	3
1134	Mn local moments prevent superconductivity in iron pnictides Ba(Fe 1â⊠ Mn x ) 2 As 2. <b>2012</b> , 99, 17002	42
1133	Microstructure and superconducting properties of Ag-sheathed (Ba, K)Fe2As2+ Ag superconducting wires fabricated by anex situpowder-in-tube process. <b>2012</b> , 25, 125010	4
1132	Growth of superconducting SmFeAs(O, F) epitaxial films by F diffusion. <b>2012</b> , 25, 035007	22
1131	Rare earth substitution in lattice-tuned Sr0.3Ca0.7Fe2As2solid solutions. <b>2012</b> , 25, 084014	1

1130	75 As Nuclear Magnetic Resonance Studies on Ba(Fe 1âlk Ni x ) 2 As 2 Single Crystals under High Pressure. <b>2012</b> , 29, 017401	1
1129	The influence of the sintering process on the superconducting property of Ba0.6K0.44Fe2As2.2. <b>2012</b> , 25, 035015	4
1128	Inverse-photoemission spectroscopy of iron-based superconductors NdFeAsO1â∃nd Ba(Fe1â⊠Cox)2As2. <b>2012</b> , 391, 012137	
1127	Elastic Anomalies Associated with superconducting phase transitions in Iron-based Superconductor Ba(Fe1â⊠Cox)2As2. <b>2012</b> , 400, 022037	
1126	Iron based superconductors processing and properties. <b>2012</b> , 57, 311-327	20
1125	Calorimetric study of the superconducting and normal state properties of Ca(Fe1â⊠Cox)2As2. <b>2012</b> , 391, 012120	3
1124	Powder x-ray diffraction of BaFe2As2under hydrostatic pressure. <b>2012</b> , 400, 022017	3
1123	Effect of Co-doping on the resistivity and thermopower of SmFe1-xCoxAsO (0.0â⊠âŪ.3). <b>2012</b> , 2, 042137	1
1122	Superconductivity in fluorine and yttrium co-doped SmFeAsO. <b>2012</b> , 111, 093912	5
1121	Local magnetic inhomogeneities observed via75As NMR in Ba(Fe1â⊠Nix)2As2withH0? c-axis. <b>2012</b> , 344, 012022	O
1120	Magnetic properties of layered compoundsLnCoAsO (Ln= lanthanoids) with itinerant-electron ferromagnetism. <b>2012</b> , 344, 012025	0
1119	Variation of superconductivity in the pseudoternary layer systems $Sr(T12MT'x)2Ge2(T,T'=transition metals)$ . <b>2012</b> , 391, 012131	2
1118	Cyclotron Resonance in Fe-based Superconductor KFe2As2. <b>2012</b> , 400, 022054	
1117	Magnetic spectrum of theJ1âIJ2model for pnictides. <b>2012</b> , 391, 012139	
1116	Spin glass instead of superconductivity in Ba(Fe1â⊠Crx/2Nix/2)2As2. <b>2012</b> , 400, 032115	1
1115	Superconductivity in Pt Doped BaFe2As2. <b>2012</b> , 81, 064704	7
1114	Review of NMR Studies on Iron-Based Superconductors. <b>2012</b> , 275-355	
1113	Unidirectional Electronic Structure in the Parent State of Iron-Chalcogenide Superconductor Fe1+ <b>I</b> Ie. <b>2012</b> , 81, 074714	14

## (2012-2012)

1112	Spin-Density-Wave Gap with Dirac Nodes and Two-Magnon Raman Scattering in BaFe2As2. <b>2012</b> , 81, 024718	16
1111	Field-Induced Magnetostructural Transitions in Antiferromagnetic Fe1+yTe1-xSx. <b>2012</b> , 81, 063703	6
1110	ANOMALOUS ELASTIC BEHAVIOR AND ITS CORRELATION WITH SUPERCONDUCTIVITY IN IRON-BASED SUPERCONDUCTOR Ba(Fe1-xCox)2As2. <b>2012</b> , 26, 1230011	14
1109	Physical properties of AxFe2âyS2 (A=K, Rb, and Cs) single crystals. <b>2012</b> , 85,	13
1108	Superconducting properties of single-crystalline AxFe2âŪSe2 (A=Rb, K) studied using muon spin spectroscopy. <b>2012</b> , 85,	59
1107	A possible approach from BCS through HTS to RTS with three examples. <b>2012</b> , 482, 33-44	7
1106	Nematic orders in iron-based superconductors. <b>2012</b> , 481, 215-222	29
1105	Hydrostatic-pressure tuning of magnetic, nonmagnetic, and superconducting states in annealed Ca(Fe1â☑Cox)2As2. <b>2012</b> , 86,	41
1104	Evolution of the band structure of superconducting NaFeAs from optimally doped to heavily overdoped Co substitution using angle-resolved photoemission spectroscopy. <b>2012</b> , 86,	18
1103	MgFeGe as an isoelectronic and isostructural analog of the superconductor LiFeAs. <b>2012</b> , 85,	12
1102	High pressure neutron and synchrotron X-ray diffraction studies of tetragonal LaFeAsO0.9F0.1. <b>2012</b> , 32, 405-411	2
1101	First-principles calculations of the electronic structure of iron-pnictide EuFe2(As,P)2 superconductors: Evidence for antiferromagnetic spin order. <b>2012</b> , 86,	19
1100	ZrCuSiAs type layered oxypnictides: A bird's eye view of LnMPnO compositions. <b>2012</b> , 40, 41-56	27
1099	Atomic and electronic structures of FeSe monolayer and bilayer thin films on SrTiO3 (001): First-principles study. <b>2012</b> , 85,	73
1098	Progress in wire fabrication of iron-based superconductors. <b>2012</b> , 25, 113001	128
1097	Intrinsic crystal phase separation in the antiferromagnetic superconductor Rb(y)Fe(2-x)Se2: a diffraction study. <b>2012</b> , 24, 435701	26
1096	Effects of particle irradiations on vortex states in iron-based superconductors. <b>2012</b> , 25, 084008	8o
1095	Theoretical Study of Point-Contact Andreev Reflection Spectroscopy for Ferromagnetic Metal/Insulator/D-Wave Superconductor Junctions. <b>2012</b> , 48, 2827-2830	

1094	Crystal and electronic structures of metallic Ba2Pd5Ge4. <b>2012</b> , 41, 12920-5	1
1093	Crystallographic and magnetic phase transitions in the layered ruthenium oxyarsenides TbRuAsO and DyRuAsO. <b>2012</b> , 51, 8502-8	2
1092	Symmetry breaking via orbital-dependent reconstruction of electronic structure in detwinned NaFeAs. <b>2012</b> , 85,	113
1091	Structural phase transitions in SrRh2As2. <b>2012</b> , 85,	15
1090	Thin Film Growth and Device Fabrication of Iron-Based Superconductors. <b>2012</b> , 81, 011011	47
1089	Artificial and self-assembled vortex-pinning centers in superconducting Ba(Fe1â\(\mathbb{R}\)Cox)2As2 thin films as a route to obtaining very high critical-current densities. <b>2012</b> , 86,	39
1088	Structural Phase Separation in K0.8Fe1.6+xSe2 Superconductors. <b>2012</b> , 116, 17847-17852	58
1087	U(1) slave-spin theory and its application to Mott transition in a multiorbital model for iron pnictides. <b>2012</b> , 86,	62
1086	Ternary arsenides A2Zn2As3 (A = Sr, Eu) and their stuffed derivatives A2Ag2ZnAs3. <b>2012</b> , 51, 2621-8	26
1085	Multiband superconductivity in Co-doped SrFe2As2investigated using local magnetic imaging. <b>2012</b> , 25, 045011	
1084	BiS2-based layered superconductor Bi4O4S3. <b>2012</b> , 86,	336
1083	Two-dome structure in electron-doped iron arsenide superconductors. <b>2012</b> , 3, 943	174
1082	Disappearance of superconductivity in the solid solution between (Ca4Al2O6)(Fe2As2) and (Ca4Al2O6)(Fe2P2) superconductors. <b>2012</b> , 134, 15181-4	7
1081	Simultaneous measurement of pressure evolution of crystal structure and superconductivity in FeSe 0.92 using designer diamonds. <b>2012</b> , 99, 26002	10
1080	Similar zone-center gaps in the low-energy spin-wave spectra of Na1âHeAs and BaFe2As2. <b>2012</b> , 86,	31
1080		31
1079	86,  Effect of iron content and potassium substitution in A0.8Fe1.6Se2 (A=K, Rb, Tl) superconductors: A	

1076 A common thread: The pairing interaction for unconventional superconductors. <b>2012</b> , 84, 1383-1417	825
1075 Iron based superconductors: Pnictides versus chalcogenides. <b>2012</b> , 324, 3481-3486	35
Crystal structure, electrical resistivity, and X-ray photoelectron spectroscopy of BaAg2As2. <b>2012</b> , 194, 113-118	4
Structural, electronic, elastic properties and chemical bonding in LaNi2P2 and LaNi2Ge2 from first principles. <b>2012</b> , 26, 1-7	9
First-principles study of Fe-based superconductors: A comparison of screened hybrid functional with gradient corrected functional. <b>2012</b> , 55, 284-294	4
1071 Fabrication of binary FeSe superconducting wires by diffusion process. <b>2012</b> , 111, 112620	37
1070 Strongly correlated materials. <b>2012</b> , 24, 4896-923	90
1069 Resonant inelastic X-ray scattering (RIXS) on magnetic EuCo2P2-based systems. <b>2012</b> , 96, 44-48	6
1068 Superconductivity at Tc = 44 K in LixFe2Se2(NH3)y. <b>2012</b> , 85, 1	85
Fe K-edge X-ray resonant magnetic scattering from Ba(Fe1â⊠ Co x )2As2 superconductors. <b>2012</b> , 208, 157-164	1
Unconventional multiband superconductivity with nodes in single-crystalline SrFe2(As0.65P0.35)2 as seen via 31P NMR and specific heat. <b>2012</b> , 85,	20
Fully-gapped superconductivity in Ba0.55K0.45Fe1.95Co0.05As2: A low-temperature specific heat study. <b>2012</b> , 85,	3
Polarized neutron scattering studies of magnetic excitations in electron-overdoped superconducting BaFe1.85Ni0.15As2. <b>2012</b> , 85,	25
1063 Electron doping evolution of the anisotropic spin excitations in BaFe2â\NixAs2. <b>2012</b> , 86,	40
Neutron scattering study of underdoped Ba1â\(\mathbb{R}\)KxFe2As2 (x=0.09 and 0.17) self-flux-grown single crystals and the universality of the tricritical point. <b>2012</b> , 85,	3
1061 Paraconductivity of the K-doped SrFe2As2superconductor. <b>2012</b> , 14, 043001	11
Iron-based superconductors: Magnetism, superconductivity, and electronic structure (Review Article). <b>2012</b> , 38, 888-899	159
1059 Properties of FeSe nanobridges prepared by using a focused ion beam. <b>2012</b> , 61, 1430-1434	3

1058	Fabrication of BaKFeAs intergrain nanobridges by using a focused ion beam. 2012, 61, 1449-1452		4
1057	Hydrostatic and uniaxial pressure dependence of superconducting transition temperature of KFe2As2 single crystals. <b>2012</b> , 86,		24
1056	Upper critical field, critical current density and thermally activated flux flow in CaFFe0.9Co0.1As superconductor. <b>2012</b> , 25, 045004		8
1055	Challenges in intermetallics: synthesis, structural characterization, and transitions. <b>2012</b> , 41, 14225-35		9
1054	Physics and chemistry of layered chalcogenide superconductors. <b>2012</b> , 13, 054303		71
1053	Phonon density of states and the search for a resonance mode in LaFeAsO0.85F0.15(Tc= 26 K). <b>2012</b> , 340, 012074		2
1052	Magnetic and transport properties of iron-platinum arsenide Ca10(Pt4â⅓s8)(Fe2â⅓PtxAs2)5 single crystal. <b>2012</b> , 85,		19
1051	Thermodynamic phase diagram, phase competition, and uniaxial pressure effects in BaFe2(As1â\( \text{Px}\)2 studied by thermal expansion. <b>2012</b> , 86,		37
1050	Penetration and de-pinning of vortices in sub-micrometer Ba(Fe,Co)2As2 thin film bridges. <b>2012</b> , 479, 164-166		2
1049	Synthesis and characterization of (Ba, Sr)Fe2(As, P)2 iron pnictide superconductors. <b>2012</b> , 483, 67-70		4
1048	Superconducting and thermoelectric properties of new layered superconductor Bi4O4S3. <b>2012</b> , 483, 94-96		41
1047	Magnetothermoelectric effects in Fe1+dTe1-xSex. <b>2012</b> , 483, 21-25		10
1046	Evidence of a spin resonance mode in the iron-based superconductor Ba(0.6)K(0.4)Fe2As2 from scanning tunneling spectroscopy. <i>Physical Review Letters</i> , <b>2012</b> , 108, 227002	·4	45
1045	Magnetic X-Ray Scattering. <b>2012</b> , 1		1
1044	Clarification as to why alcoholic beverages have the ability to induce superconductivity in Fe1+dTe1â\(\mathbb{B}\)Sx. <b>2012</b> , 25, 084025		21
1043	BaFe2Se2O as an iron-based Mott insulator with antiferromagnetic order. <b>2012</b> , 86,		21
1042	Crystal growth and physical properties of SrCu2As2, SrCu2Sb2, and BaCu2Sb2. <b>2012</b> , 85,		61
1041	Pressure-induced superconductivity in Ba0.5Sr0.5Fe2As2. <b>2012</b> , 24, 495702		1

1040	Pressure Dependence of Superconductivity in FeSe studied by DC Magnetic Measurements. <b>2012</b> , 400, 022075	1
1039	Iron chalcogenide superconductors at high magnetic fields. <b>2012</b> , 13, 054305	29
1038	Conductivity and incommensurate antiferromagnetism of Fe 1.02 Se 0.10 Te 0.90 under pressure. <b>2012</b> , 98, 37002	1
1037	Metastable superconducting state in quenched K x Fe2ây Se2. <b>2012</b> , 92, 2553-2562	34
1036	Growth of single-crystal Ca10(Pt4As8)(Fe(1.8)Pt(0.2)As2)5 nanowhiskers with superconductivity up to 33 K. <b>2012</b> , 134, 4068-71	10
1035	Superconductivity and magnetism in 11-structure iron chalcogenides in relation to the iron pnictides. <b>2012</b> , 13, 054304	24
1034	Competition and cooperation of pinning by extrinsic point-like defects and intrinsic strong columnar defects in BaFe2As2 thin films. <b>2012</b> , 86,	38
1033	Metastable 11 K superconductor Na(1-y)Fe(2-x)As2. <b>2012</b> , 51, 8161-7	20
1032	High-pressure structural phase transitions in chromium-doped BaFe2As2. <b>2012</b> , 377, 012016	4
1031	High, magnetic field independent critical currents in (Ba,K)Fe2As2 crystals. <b>2012</b> , 101, 012601	70
1030	75As NMR-NQR study in superconducting LiFeAs. <b>2012</b> , 85, 1	24
1029	MULTIPLE SUPERCONDUCTING GAPS, ANISOTROPIC SPIN FLUCTUATIONS AND SPIN-ORBIT COUPLING IN IRON-PNICTIDES. <b>2012</b> , 26, 1230008	4
1028	Inelastic neutron-scattering measurements of incommensurate magnetic excitations on superconducting LiFeAs single crystals. <i>Physical Review Letters</i> , <b>2012</b> , 108, 117001	63
1027	Improved transport critical current in Ag and Pb co-doped BaxK1â⊠Fe2As2superconducting tapes. <b>2012</b> , 25, 035020	16
1026	Electronic origin of high-temperature superconductivity in single-layer FeSe superconductor. <b>2012</b> , 3, 931	427
1025	Development of viable solutions for the synthesis of sulfur bearing single crystals. <b>2012</b> , 92, 2436-2447	23
1024	Magnetic structure of quasi-one-dimensional antiferromagnetic TaFe1+yTe3. <b>2012</b> , 85,	7
1023	Pairing Mechanism in Fe-Based Superconductors. <b>2012</b> , 3, 57-92	376

1022	Angle-Resolved Photoemission Studies of Quantum Materials. <b>2012</b> , 3, 129-167	59
1021	Satellites and large doping and temperature dependence of electronic properties in hole-doped BaFe2As2. <b>2012</b> , 8, 331-337	150
1020	Ba2Ti2Fe2As4O: A new superconductor containing Fe2As2 layers and Ti2O sheets. <b>2012</b> , 134, 12893-6	62
1019	Synthesis and Superconductivity of CeNi0.8Bi2: New Entrant in Superconductivity Kitchen?. <b>2012</b> , 25, 723-724	1
1018	Hole doping in BaFe2As2: The case of Ba1â⊠NaxFe2As2 single crystals. <b>2012</b> , 85,	34
1017	Current status of iron-based superconductors. <b>2012</b> , 208, 123-131	2
1016	EuRu2As2: A New Ferromagnetic Metal with Collapsed ThCr2Si2-Type Structure. 2012, 25, 441-445	6
1015	Scaling of the Temperature Dependent Resistivity in 11 Iron-Pnictide Superconductors. <b>2012</b> , 25, 1753-1759	1
1014	A Simple Fabrication of FeSe Superconductors with High Upper Critical Field. <b>2012</b> , 25, 1781-1785	8
1013	One-dimensional Electronic Order in Fe1.07Te Probed by Scanning Tunneling Spectroscopy. <b>2012</b> , 25, 1273-1276	1
1012	Trace element-incorporating octacalcium phosphate porous beads via polypeptide-assisted nanocrystal self-assembly for potential applications in osteogenesis. <b>2012</b> , 8, 1586-96	26
1011	Rapid microwave synthesis of the iron arsenides NdFeAsO and NdFe0.9Co0.1AsO. <b>2012</b> , 47, 798-800	10
1010	Electronic structure and chemical bonding of $\oplus$ - and $\oplus$ eIr2Si2 intermediate valence compounds. <b>2012</b> , 186, 81-86	5
1009	Synthesis, physical properties and electronic structure of Sr1â⊠LaxCu2Pn2 (Pn=P, As, Sb). <b>2012</b> , 187, 323-327	3
1008	Large elastic anomalies and strong electron-lattice coupling in iron-based superconductor Ba(Fe1â⊠Cox)2As2. <b>2012</b> , 152, 680-687	5
1007	Relationship between crystal structure and superconductivity in iron-based superconductors. <b>2012</b> , 152, 644-648	62
1006	Fabrication and transport properties of ex situ powder-in-tube (PIT) processed (Ba,K)Fe2As2 superconducting wires. <b>2012</b> , 152, 740-746	32
1005	Superconducting compounds with metallic square net. <b>2012</b> , 152, 666-670	6

1004	Angle-resolved photoemission study on the superconducting iron-pnictides of BaFe2(As,P)2 with low energy photons. <b>2012</b> , 152, 695-700	7
1003	A few points on iron-based superconductors. <b>2012</b> , 152, 660-665	4
1002	Ironâβlatinumâ⊞rsenide superconductors Ca10(PtnAs8)(Fe2â⊠PtxAs2)5. <b>2012</b> , 152, 635-639	28
1001	Impurity effects on the Fe-based superconductor A(Fe1â�Coy)2As2 (A=Ba and Sr). <b>2012</b> , 152, 671-679	18
1000	High- superconductivity in the LaFeAsO1â⊠Fx system based on inelastic neutron scattering measurements. <b>2012</b> , 152, 653-659	2
999	Superconductivity in PbO-type tetragonal FeSe nanoparticles. <b>2012</b> , 152, 649-652	24
998	Phase diagram and oxygen annealing effect of FeTe1â⊠Sex iron-based superconductor. <b>2012</b> , 152, 1135-1138	57
997	Irreversible magnetization in isovalently doped Ba(Fe1-xRux)2As2. <b>2012</b> , 27, 104-107	1
996	Charge stripe structure in FeTe. <b>2012</b> , 407, 1796-1798	3
995	Electronic structure and phonon spectrum of binary iron-based superconductor FeSe in both nonmagnetic and striped antiferromagnetic phases. <b>2012</b> , 472, 29-33	9
994	Structural properties of BaFe1.8Ni0.2As2 under pressure. <b>2012</b> , 474, 1-4	7
993	Irreversibility line of Ba1â⊠KxFe2As2 (Tc=36.9K) superconductor studied with ac-susceptibility measurements. <b>2012</b> , 476, 68-72	5
992	Superconducting and excitonic quantum phase transitions in doped Dirac electronic systems. <b>2012</b> , 376, 779-784	14
991	The electronic structure and magnetism of KxFe2Se2. <b>2012</b> , 376, 1072-1077	5
990	Symmetry analysis of the structural and magnetic phase transitions in 122 iron arsenides. <b>2012</b> , 68, 209-12	10
989	Enhancement of Superconductivity in Quenched ∃-FeSe Flakes. <b>2013</b> , 26, 3349-3353	3
988	Scaling of the Temperature Dependent Resistivity in 111 Iron-Pnictide Superconductors. <b>2013</b> , 26, 2727-2734	1
987	A Structural and Electronic Properties DFT Study of BaFe2As2 and Two Derived Substitution Compounds. <b>2013</b> , 26, 2403-2409	

986	Superconductivity at 35.5 K in K-Doped CaFe2As2. 2013, 26, 2121-2124	13
985	Anisotropy Parameters of Critical Fields in LiFeAs Using Two-Band Ginzburgâllandau Theory. <b>2013</b> , 26, 1903-1907	1
984	Theoretical Analysis of Isotope Effect Exponent of Diboride and Iron-Based Superconductors: Three-Square-Well Model Approach. <b>2013</b> , 26, 1195-1198	2
983	Superconductivity induced by hydrogen anion substitution in 1111-type iron arsenides. <b>2013</b> , 17, 49-58	24
982	Vortex phase transition and isotropic flux dynamics in K0.8Fe2Se2 single crystal lightly doped with Mn. <b>2013</b> , 103, 052602	20
981	Magnetic Properties of FeAs Single Crystal. <b>2013</b> , 26, 1185-1188	6
980	Pressure-induced phase transitions and correlation between structure and superconductivity in iron-based superconductor Ce(O(0.84)F(0.16))FeAs. <b>2013</b> , 52, 8067-73	6
979	Fermi surface in KFe2As2 determined via de HaasâNan Alphen oscillation measurements. <b>2013</b> , 87,	47
978	Effects of pressure on the electronic structures of LaOFeP. <b>2013</b> , 377, 1479-1485	
977	Evidence of strong correlations and coherence-incoherence crossover in the iron pnictide superconductor KFe2As2. <i>Physical Review Letters</i> , <b>2013</b> , 111, 027002	117
977 976	·	117
	superconductor KFe2As2. <i>Physical Review Letters</i> , <b>2013</b> , 111, 027002	,
976	superconductor KFe2As2. <i>Physical Review Letters</i> , <b>2013</b> , 111, 027002  7.4  Finite temperature and pressure molecular dynamics for BaFe2As2. <b>2013</b> , 88,	8
976 975	Finite temperature and pressure molecular dynamics for BaFe2As2. 2013, 88,  Superconductivity in 122 antimonide SrPt2Sb2. 2013, 26, 075001	8
976 975 974	Finite temperature and pressure molecular dynamics for BaFe2As2. 2013, 88,  Superconductivity in 122 antimonide SrPt2Sb2. 2013, 26, 075001  Quantum criticality in electron-doped BaFe2-xNixAs2. 2013, 4, 2265  Angular dependence of the resistive upper critical field of the iron-based superconductor Fe1+D	8
976 975 974 973	Finite temperature and pressure molecular dynamics for BaFe2As2. 2013, 88,  Superconductivity in 122 antimonide SrPt2Sb2. 2013, 26, 075001  Quantum criticality in electron-doped BaFe2-xNixAs2. 2013, 4, 2265  Angular dependence of the resistive upper critical field of the iron-based superconductor Fe1+II (Te,Se) in high magnetic fields. 2013, 62, 1997-2000  Analysis of the critical current density and flux pinning properties in iron-based Ba0.55K0.45Fe2As2	8
976 975 974 973	Finite temperature and pressure molecular dynamics for BaFe2As2. 2013, 88,  Superconductivity in 122 antimonide SrPt2Sb2. 2013, 26, 075001  Quantum criticality in electron-doped BaFe2-xNixAs2. 2013, 4, 2265  Angular dependence of the resistive upper critical field of the iron-based superconductor Fe1+II (Te,Se) in high magnetic fields. 2013, 62, 1997-2000  Analysis of the critical current density and flux pinning properties in iron-based Ba0.55K0.45Fe2As2 high-T c superconductor. 2013, 62, 2011-2015	8 18 78

## (2013-2013)

968	Enhanced density of states in Li(Fe1 $\frac{1}{2}$ MCox)As single crystals near x = 0.06 as implied by transport properties. <b>2013</b> , 495, 130-133	2
967	Electronic, elastic and thermal properties of SrCu2As2 via first principles calculation. <b>2013</b> , 570, 156-161	8
966	Iron-based superconductors in high magnetic fields. <b>2013</b> , 14, 94-105	11
965	Influence of microstructure on superconductivity in KxFeâEySeâEand evidence for a new parent phase KâEeâBeâD <b>2013</b> , 4, 1897	85
964	Crystal, magnetic, and electronic structures, and properties of new BaMnPnF (Pn = As, Sb, Bi). <b>2013</b> , 3, 2154	21
963	Crystal chemistry and structural design of iron-based superconductors. <b>2013</b> , 22, 087410	32
962	Hidden (ID) instability as an itinerant origin of bicollinear antiferromagnetism in Fe1+xTe. <b>2013</b> , 87,	13
961	Superconducting phases in potassium-intercalated iron selenides. <b>2013</b> , 135, 2951-4	138
960	Ba13Si6Sn8As22: a quaternary Zintl phase containing adamantane-like [Si4As10] clusters. <b>2013</b> , 52, 11836-42	9
959	Absence of superconductivity in the hole-doped Fe pnictide Ba(Fe1âkMnx)2As2: Photoemission and x-ray absorption spectroscopy studies. <b>2013</b> , 88,	22
958	Weak magnetism and the Mott state of vanadium in superconducting Sr2VO3FeAs. 2013, 88,	10
957	Molecular beam epitaxy and superconductivity of stoichiometric FeSe and KxFe2âySe2crystalline films. <b>2013</b> , 22, 086801	11
956	Vortex-glass phase transition and enhanced flux pinning in C4+-irradiated BaFe1.9Ni0.1As2superconducting single crystals. <b>2013</b> , 26, 095014	20
955	Functional renormalization group for multi-orbital Fermi surface instabilities. <b>2013</b> , 62, 453-562	126
954	Spin-density-wave-induced anomalies in the optical conductivity of AFe2As2, (A=Ca, Sr, Ba) single-crystalline iron pnictides. <b>2013</b> , 88,	22
953	Pressure-induced superconductivity in EuFe2As2 without a quantum critical point: Magnetotransport and upper critical field measurements under high pressure. <b>2013</b> , 88,	10
952	Magnetic catalysis effect in the (2+1)-dimensional Gross-Neveu model with Zeeman interaction. <b>2013</b> , 88,	7
951	Effect of excess Fe on magnetic properties and crystallographic phases in Fe1+IIe. 2013, 484, 19-21	7

950	Unusual pressure effects on the superconductivity of indirectly electron-doped (Ba1â\(\mathbb{U}\)Lax)Fe2As2 epitaxial films. <b>2013</b> , 88,		16
949	Coexistence of cluster spin glass and superconductivity in Ba(Fe(1-x)Co(x))2As2 for 0.060â⊠âŪ.071. <i>Physical Review Letters</i> , <b>2013</b> , 111, 207201	7.4	52
948	Doping effect of Cu and Ni impurities on the Fe-based superconductor Ba 0.6 K 0.4 Fe 2 As 2. <b>2013</b> , 104, 37007		12
947	Chemical excision of tetrahedral FeSe(2) chains from the superconductor FeSe: synthesis, crystal structure, and magnetism of Fe(3)Se(4)(en)(2). <b>2013</b> , 135, 19111-4		31
946	Upper critical field of isoelectron substituted SrFe2(As1â⊠Px)2. <b>2013</b> , 87,		11
945	Effect of heavy-ion irradiation on superconductivity in Ba0.6K0.4Fe2As2. <b>2013</b> , 87,		16
944	New layered iron sulfide NaFe(1.6)S2: synthesis and characterization. 2013, 52, 12860-2		12
943	New superconductor SrPt2Ge2 with Tc=10.2K. <b>2013</b> , 493, 93-95		9
942	Tartaric acid in red wine as one of the key factors to induce superconductivity in FeTe0.8S0.2. <b>2013</b> , 487, 16-18		8
941	Doping dependence of correlation effects in K1 âlk Fe2 âly Se2 superconductors: LDAâl+ DMFT investigation. <b>2013</b> , 117, 926-932		7
940	75As NMR local probe study of magnetism in (Eu1â⊠Kx)Fe2As2. <b>2013</b> , 86, 1		1
939	Phosphide oxides RE2AuP2O (RE = La, Ce, Pr, Nd): synthesis, structure, chemical bonding, magnetism, and 31P and 139La solid state NMR. <b>2013</b> , 52, 2094-102		12
938	Magnetic properties and spin dynamics in Ba(Fe(1-x)Mn(x))2As2 compounds studied by 57Fe MBsbauer spectroscopy. <b>2013</b> , 25, 135703		1
937	Bulk synthesis of iron-based superconductors. <b>2013</b> , 17, 59-64		32
936	Tunneling spectra and superconducting gaps observed by scanning tunneling microscopy near the grain boundaries of FeSe0.3Te0.7 films. <b>2013</b> , 495, 74-78		2
935	Phase diagram and annealing effect for Fe1+Te1-xSx single crystals. <b>2013</b> , 25, 385701		6
934	Superconducting properties of Ca1â⊠RExFe2As2 (RE: Rare Earths). <b>2013</b> , 484, 31-34		12
933	Superconducting Properties and Phase Diagram of Indirectly Electron-Doped \$(hbox{Sr}_{1 - x}hbox{La}_{x})hbox{Fe}_{2}hbox{As}_{2}\$ Epitaxial Films Grown by Pulsed Laser Deposition. <b>2013</b> , 23, 7300405-7300405		13

932	Conductance spectrum and superconducting gap structures observed in c-axis FeSe0.46Te0.54/Au junctions. <b>2013</b> , 114, 123912		3
931	Spin, charge, and orbital orderings in iron-based superconductors. <b>2013</b> , 22, 087402		4
930	Probing the anisotropic vortex lattice in the Fe-based superconductor KFe2As2 using small-angle neutron scattering. <b>2013</b> , 88,		6
929	Electronâphonon coupling in cuprate and iron-based superconductors revealed by Raman scattering. <b>2013</b> , 22, 087103		17
928	Spin-phonon coupling in K0.8Fe1.6Se2 and KFe2Se2: Inelastic neutron scattering and ab initio phonon calculations. <b>2013</b> , 87,		13
927	Enhancement of the superconducting transition temperature of FeSe by intercalation of a molecular spacer layer. <b>2013</b> , 12, 15-9		324
926	Interband quasiparticle scattering in superconducting LiFeAs reconciles photoemission and tunneling measurements. <i>Physical Review Letters</i> , <b>2013</b> , 110, 017006	·4	13
925	Solid Phase Epitaxial Growth of Fe(Te, S) Thin Films and Their Superconducting Properties. <b>2013</b> , 23, 7500104-7500104		4
924	The iron-age of superconductivity: structural correlations and commonalities among the various families having -Fe-Pn- slabs (Pn = P, As and Sb). <b>2013</b> , 42, 569-98		25
923	Muon-Spin Rotation and Magnetization Studies of Chemical and Hydrostatic Pressure Effects in EuFe2(As1 $\hat{a}$ M P x )2. <b>2013</b> , 26, 285-295		14
922	Enhanced transport critical current density in textured Sr0.6K0.4Fe2As2 + Ag tapes by an intermediate sintering process of precursors. <b>2013</b> , 490, 37-42		7
921	First-principles study on iron-pnictide superconductors Ca(Fe1â⊠Cox)2As2. <b>2013</b> , 154, 11-14		6
920	Theoretical investigation of isotope effect of the iron-based superconductors. 2013, 485, 71-74		1
919	New diluted ferromagnetic semiconductor with Curie temperature up to 180 K and isostructural to the '122' iron-based superconductors. <b>2013</b> , 4, 1442		128
918	Modulated crystal structure of Pr2SbO2. <b>2013</b> , 69, 547-55		7
917	Phase diagram and physical properties of NaFe1â⊠CuxAs single crystals. <b>2013</b> , 88,		32
916	Superconductivity in Ca1-xLaxFeAs2: A Novel 112-Type Iron Pnictide with Arsenic Zigzag Bonds. <b>2013</b> , 82, 123702		124
915	Large transportJcin Sn-added SmFeAsO1â⊠Fxtapes prepared by anex situPIT method. <b>2013</b> , 26, 075017		12

914	The antimonide oxides REZnSbO and REMnSbO (RE = Ce, Pr) âlĀn XPS study. <b>2013</b> , 17, 122-127	72
913	Critical current density and grain boundary property of BaFe2(As,P)2 thin films. 2013, 494, 181-184	35
912	Metalâlhsulator transition in Na-doped post-spinel CdRh2O4. <b>2013</b> , 563, 119-123	4
911	Calculation of the transport critical current density of c-axis textured 122 iron-based superconductors. <b>2013</b> , 485, 149-153	1
910	Quasi-periodic magnetic flux jumps in the superconducting state of Ba0.5K0.5Fe1.9M0.1As2 (M = Fe, Co, Ni, Cu, and Zn). <b>2013</b> , 495, 192-197	3
909	Superconducting properties of LiFe1â⊠CuxAs single crystals. <b>2013</b> , 493, 141-142	5
908	Upper fields and critical current density of K0.58Fe1.56Se2 single crystals grown by one step technique. <b>2013</b> , 492, 18-20	8
907	Effects of heating condition and Sn addition on the microstructure and superconducting properties of Sr0.6K0.4Fe2As2 tapes. <b>2013</b> , 495, 48-54	26
906	Effects of oxide precursors on superconducting properties of polycrystalline SmFeAsO1â⊠Fx. <b>2013</b> , 495, 198-201	
905	Effect of Sb and Si doping on the superconducting properties of FeSe0.9. <b>2013</b> , 485, 137-144	16
904	New ternary phosphides and arsenides. Syntheses, crystal structures, physical properties of Eu2ZnP2, Eu2Zn2P3 and Eu2Cd2As3. <b>2013</b> , 205, 116-121	13
903	Uniaxial pressure effects on the transport properties in Ba(Fe1â\(\mathbb{R}\)Cox)2As2 single crystals. <b>2013</b> , 494, 62-64	2
902	Hydrostatic pressure (8 GPa) dependence of electrical resistivity of BaCo2As2 single crystal. <b>2013</b> , 48, 4329-4331	3
901	Effect of pressure on structural, electronic and bonding properties of CaTM2Pn2 (TM=Ni, Pd; Pn=P, As) compounds: A full potential computational study. <b>2013</b> , 561, 268-275	8
900	Discovery of the Ca4Al2O6Fe2Pn2 â屆l-42622(Pn)â屆nd Ca3Al2O5Fe2Pn2 â屆l-32522(Pn)â[[Pn=As, P) superconductors. <b>2013</b> , 484, 12-15	6
899	Magnetic ordering and electron correlation of iron-based superconductor (Ca3Al2O5â☑)(Fe2As2) from first-principles study. <b>2013</b> , 172, 41-48	
898	Effect of doping on the magnetostructural ordered phase of iron arsenides: a comparative study of the resistivity anisotropy in doped BaFe2As2 with doping into three different sites. <b>2013</b> , 135, 3158-63	39

## (2013-2013)

896	Modelling the electronic structure and magnetic properties of LiFeAs and FeSe using hybrid-exchange density functional theory. <b>2013</b> , 161, 23-28	5
895	Type II superconductivity in SrPd2Ge2. <b>2013</b> , 26, 015010	5
894	Dependence of carrier doping on the impurity potential in transition-metal-substituted FeAs-based superconductors. <i>Physical Review Letters</i> , <b>2013</b> , 110, 107007	63
893	Fabrication and transport properties of Sr0.6K0.4Fe2As2 multifilamentary superconducting wires. <b>2013</b> , 102, 082602	25
892	Two-band superconductivity in doped SrTiO3 films and interfaces. <b>2013</b> , 87,	44
891	Charge density wave fluctuations, heavy electrons, and superconductivity in KNi2S2. <b>2013</b> , 87,	38
890	Magnetic anisotropy in hole-doped superconducting Ba0.67K0.33Fe2As2 probed by polarized inelastic neutron scattering. <b>2013</b> , 87,	27
889	Artificially engineered superlattices of pnictide superconductors. <b>2013</b> , 12, 392-6	62
888	Scanningâ <b>l</b> unneling microscopy and break-junction spectroscopy on the superconducting Fe(Se, Te) single crystal. <b>2013</b> , 484, 22-26	4
887	Scanning-tunneling microscopy/spectroscopy and break-junction tunneling spectroscopy of FeSe1â⊠Tex. <b>2013</b> , 39, 265-273	6
886	Bismuth-based candidates for topological insulators: Chemistry beyond Bi2Te3. <b>2013</b> , 7, 39-49	31
885	Quasiparticle Dynamics in FeSe Superconductors Studied by Femtosecond Spectroscopy. <b>2013</b> , 26, 1213-1215	2
884	Strong enhancement of the critical current at the antiferromagnetic transition in ErNi2B2C single crystals. <b>2013</b> , 87,	7
883	Ternary K2Zn5As4-type pnictides Rb2Cd5As4 and Rb2Zn5Sb4, and the solid solution Rb2Cd5(As,Sb)4. <b>2013</b> , 69, 455-9	13
882	Synthesis, structure and chemical bonding of CaFe2â⊠RhxSi2 (x=0, 1.32, and 2) and SrCo2Si2. <b>2013</b> , 203, 232-239	9
881	Structural complexity meets transport and magnetic anisotropy in single crystalline Ln30Ru4Sn31 (Ln = Gd, Dy). <b>2013</b> , 135, 2748-58	8
88o	Iron-Based Superconductors. <b>2013</b> , 19-44	
879	Structural and physical properties diversity of new CaCu5-type related europium platinum borides. <b>2013</b> , 52, 4185-97	8

878	Atomic and electronic structures of single-layer FeSe on SrTiO3(001): The role of oxygen deficiency. <b>2013</b> , 87,	76
877	Crystals, magnetic and electronic properties of a new ThCr2Si2-type BaMn2Bi2 and K-doped compositions. <b>2013</b> , 204, 32-39	29
876	FIRST PRINCIPLES STUDY ON IRON PNICTIDE SUPERCONDUCTOR Ca0.88Pr0.12Fe2As2. <b>2013</b> , 27, 1350100	
875	New Member of BiS2-Based Superconductor NdO1-xFxBiS2. <b>2013</b> , 82, 033708	222
874	Phase diagram and electronic indication of high-temperature superconductivity at 65 K in single-layer FeSe films. <b>2013</b> , 12, 605-10	585
873	Search for superconductivity in LaNiP2 (P=Bi, Sb) thin films grown by reactive molecular beam epitaxy. <b>2013</b> , 484, 171-174	5
872	Ginzburg-Landau theory for multiband superconductors: Microscopic derivation. 2013, 87,	59
871	Temperature dependence of the anisotropy parameter of the LiFeAs upper critical field in the two-band Ginzburg-Landau theory. <b>2013</b> , 58, 888-891	1
870	The flux pinning mechanism, and electrical and magnetic anisotropy in Fe1.04Te0.6Se0.4 superconducting single crystal. <b>2013</b> , 113, 17E115	15
869	Charge stripe structure in Fe1+xTe by STM. <b>2013</b> , 167, 10-13	4
868	SUPERCONDUCTIVITY PHENOMENON INDUCED BY EXTERNAL IN-PLANE MAGNETIC FIELD IN (2 + 1)-DIMENSIONAL GROSSâNEVEU TYPE MODEL. <b>2013</b> , 28, 1350096	7
867	Unusual temperature dependence of band dispersion in Ba(Fe(1-x)Ru(x))2As2 and its consequences for antiferromagnetic ordering. <i>Physical Review Letters</i> , <b>2013</b> , 110, 067002	40
866	Magnetic ordering in tetragonal 3d metal arsenides M2As (M = Cr, Mn, Fe): an ab initio investigation. <b>2013</b> , 52, 3013-21	4
865	Review on cerium intermetallic compounds: A bird's eye outlook through DFT. <b>2013</b> , 41, 55-85	25
864	Effect of Substitution and Heat Treatment Route on Polycrystalline FeSe0.5Te0.5 Superconductors. <b>2013</b> , 26, 2369-2374	13
863	Superconductivity in Ca10(Ir4As8)(Fe2As2)5 with Square-Planar Coordination of Iridium. <b>2013</b> , 3, 3101	23
862	Quaternary aluminum silicides grown in Al flux: RE5Mn4Al(23-x)Si(x) (RE = Ho, Er, Yb) and Er44Mn55(AlSi)237. <b>2013</b> , 52, 9931-40	4
861	Crystal and magnetic structure of CaCo1.86As2 studied by x-ray and neutron diffraction. <b>2013</b> , 88,	41

## (2013-2013)

860	Doping dependence of spin excitations and its correlations with high-temperature superconductivity in iron pnictides. <b>2013</b> , 4, 2874	82
859	Syntheses, crystal structure and physical properties of new Zintl phases Ba3T2As4 (T=Zn, Cd). <b>2013</b> , 198, 6-9	18
858	New quantum matters: Build up versus high pressure tuning. <b>2013</b> , 56, 2337-2350	6
857	Comparative study of electronic structure of new superconductors (Sr, Ca)Pd2As2 and related compound BaPd2As2. <b>2013</b> , 98, 24-27	5
856	Influence of spin-phonon coupling on antiferromagnetic spin fluctuations in FeSe under pressure: First-principles calculations with van der Waals corrections. <b>2013</b> , 88,	16
855	Resonant inelastic x-ray scattering at the Fe L3 edge of the one-dimensional chalcogenide BaFe2Se3. <b>2013</b> , 88,	18
854	First-principles Wannier function analysis of the electronic structure of PdTe: weaker magnetism and superconductivity. <b>2013</b> , 25, 405601	4
853	New Frontiers Opened Up Through Function Cultivation in Transparent Oxides. 2013, 455-487	1
852	Zigzag Chain Structure Transition and Orbital Fluctuations in Ni-Based Superconductors. <b>2013</b> , 82, 094704	4
851	Evidence of two superconducting phases in Ca1â\(\mathbb{\text{LaxFe2As2}}\). <b>2013,</b> 3, 102120	18
850	Spin wave excitations in AFe1.5Se2 (A = K, Tl): analytical study. <b>2013</b> , 25, 036004	4
849	Ultralow-Dissipative Conductivity by Dirac Fermions in BaFe2As2. <b>2013</b> , 82, 043709	8
848	Versatile fluoride substrates for Fe-based superconducting thin films. <b>2013</b> , 102, 142601	44
847	Magnetic scattering and electron pair breaking by rare-earth-ion substitution in BaFe2As2epitaxial films. <b>2013</b> , 15, 073019	18
846	Electronic phase diagram of disordered Co doped BaFe2As2â[1 <b>2013</b> , 26, 025014	25
845	High Pressure Low Temperature Studies on 1-2-2 Iron-based Superconductors Using Designer Diamond Cells. <b>2013</b> , 1582, 1	
844	Weak-link behaviour observed in iron-based superconductors with thick perovskite-type blocking layers. <b>2013</b> , 26, 105020	4
843	Fermi Surface and Band Structure of (Ca,La)FeAs 2 Superconductor from Angle-Resolved Photoemission Spectroscopy. <b>2013</b> , 30, 127402	16

842	Upper critical fields and anisotropy of Ca1â⊠LaxFe2As2single crystals. <b>2013</b> , 26, 095003		8
841	Quenched Fe moment in the collapsed tetragonal phase of Ca1â\(\mathbb{R}\)PrxFe2As2. <b>2013</b> , 22, 057401		11
840	Experimental Investigation of the Electronic Structure of Ca 0.83 La 0.17 Fe 2 As 2. <b>2013</b> , 30, 017402		11
839	Critical current density and magnetic phase diagrams of BaFe1.29Ru0.71As2single crystals. <b>2013</b> , 26, 015009		11
838	Enhancement in transport critical current density ofex situPIT Ag/(Ba, K)Fe2As2tapes achieved by applying a combined process of flat rolling and uniaxial pressing. <b>2013</b> , 26, 115007		20
837	Mechanochemical synthesis of pnictide compounds and superconducting Ba0.6K0.4Fe2As2bulks with high critical current density. <b>2013</b> , 26, 074003		38
836	Microstructural properties of K 0.8 Fe 1.6 S 2 , K 0.8 Fe 1.75 Se 2-y S y (0 â⅓ âЉ) and K 0.8 Fe 1.5+x S 2 (0. <b>2013</b> , 103, 37010		4
835	Strange Inter-Layer Properties of Ba(Fe1-xCox)2As2 Appearing in Ultrasonic Measurements. <b>2013</b> , 82, 114604		18
834	Superconductivity in HfCuGe 2: A non-magnetic analog of the 1111 iron pnictides. 2013, 101, 67001		4
833	Microstructure and transport critical current in Sr0.6K0.4Fe2As2superconducting tapes prepared by cold pressing. <b>2013</b> , 26, 075003		22
832	Strikingly dissimilar effect of Mn and Zn dopants imposed on local structural distortion of Ba0.5K0.5Fe2As2 superconductor. <b>2013</b> , 20, 455-9		3
831	Enhancement of Critical Current Densities in (Ba,K)Fe2As2by 320 MeV Au Irradiation in Single Crystals and by High-Pressure Sintering in Powder-in-Tube Wires. <b>2013</b> , 6, 123101		20
830	Superconductivity under pressure in RFeAsO1â $\overline{M}$ Fx (R = La, Ceâ $\overline{M}$ m) by dc magnetization measurements. <b>2013</b> , 87,		15
829	Crystallographic, electronic, thermal, and magnetic properties of single-crystal SrCo2As2. <b>2013</b> , 88,		52
828	Why Tc of (CaFeAs)10Pt3.58As8 is twice as high as (CaFe0.95Pt0.05As)10Pt3As8. <b>2013</b> , 88,		32
827	Distinguishing s∃ and s++ electron pairing symmetries by neutron spin resonance in superconducting NaFe0.935Co0.045As. <b>2013</b> , 88,		42
826	Hidden T-linear scattering rate in Ba0.6K0.4Fe2As2 revealed by optical spectroscopy. <i>Physical Review Letters</i> , <b>2013</b> , 111, 117001	7.4	58
825	Transport and thermodynamic properties of (Ca1â⊠Lax)10(Pt3As8)(Fe2As2)5 superconductors. <b>2013</b> , 87,		21

## (2014-2013)

824	Metal-insulator transition in antiferromagnetic Ba1â⊠KxMn2As2 (0â⊠âŪ.4) single crystals studied by 55Mn and 75As NMR. <b>2013</b> , 88,		12
823	Enhancement of the London penetration depth in pnictides at the onset of spin-density-wave order under superconducting dome. <i>Physical Review Letters</i> , <b>2013</b> , 110, 177003	7.4	38
822	Heat capacity jump at Tc and pressure derivatives of superconducting transition temperature in the Ba1â¼KxFe2As2 (0.2â¼â¼.0) series. <b>2013</b> , 87,		36
821	Superconductivity and strong intrinsic defects in LaPd1â⊠Bi2. <b>2013</b> , 88,		25
820	Influence of spin fluctuations on the thermal conductivity in superconducting Ba(Fe1â⊠Cox)2As2. <b>2013</b> , 88,		9
819	High-field critical current enhancement by irradiation induced correlated and random defects in (Ba0.6K0.4)Fe2As2. <b>2013</b> , 103, 202601		36
818	Can nitrogen-based cobalt pnictides exist?. <b>2013</b> , 114, 093701		
817	Strongly enhanced current densities in Sr0.6K0.4Fe2As2 + Sn superconducting tapes. <b>2014</b> , 4, 4465		39
816	Superconductivity in K- and Na-doped BaFe2As2: What can we learn from heat capacity and pressure dependence of Tc. <b>2015</b> , 29, 1430019		3
815	An Anti CuO2-type Metal Hydride Square Net Structure in Ln2M2As2Hx (Ln=La or Sm, M=Ti, V, Cr, or Mn). <b>2015</b> , 127, 2975-2978		1
814	Theoretical study of the new zintl phases compounds K2ACdSb2 (A=(Sr, Ba)). <b>2015</b> , 464, 9-16		
813	Anisotropy in the upper critical field of FeSe and FeSe0.33Te0.67single crystals. <b>2015</b> , 28, 045013		22
812	Doping effect on the physical properties of LixFe2-xAs. <b>2015</b> , 29, 1550019		1
811	Magnetic neutron scattering studies on the Fe-based superconductor system Fe1+yTe1â⊠Sex. <b>2015</b> , 358, 92-107		5
810	Comparison of the local structures of Ca0.82La0.18FeAs2 and Ba0.64K0.36Fe2As2 pnictide superconductors using atomic pair distribution function analysis. <b>2015</b> , 84, 24-27		5
809	Synthesis of high-quality FeSe0.5Te0.5 polycrystal using an easy one-step technique. <b>2015</b> , 644, 523-527	7	20
808	Calculation of the specific heat of optimally K-doped BaFeâAsâ[12015, 27, 335504		
807	Achievement of practical level critical current densities in BaâExKxFeâAsâ¶Ag tapes by conventional cold mechanical deformation. <b>2014</b> , 4, 4065		88

806	Exploration of new superconductors and functional materials, and fabrication of superconducting tapes and wires of iron pnictides. <b>2015</b> , 16, 033503	141
805	Orbital characters and electronic correlations in KCo2Se2. <b>2015</b> , 27, 295501	5
804	Dependences on RE of superconducting properties of transition metal co-doped (Ca,RE)FeAs2 with RE= Laâlīd. <b>2015</b> , 518, 14-17	6
803	Investigation of $J_{c}^{0.4}$ -Suppressing Factors in Flat-Rolled $\rho_{c}^{0.6}$ -Shbox $\rho_$	4
802	Fabrication of Diamond Based Sensors for Use in Extreme Environments. <b>2015</b> , 8, 2054-2061	5
801	An overview of the Fe-chalcogenide superconductors. <b>2015</b> , 48, 323001	19
800	Superconductivity in Hf5Sb3â⊠Rux: Are Ru and Sb a Critical Charge-Transfer Pair for Superconductivity?. <b>2015</b> , 27, 4511-4514	11
799	Structural and Magnetic Phase Transitions near Optimal Superconductivity in BaFe2(As(1-x)Px)2.  Physical Review Letters, <b>2015</b> , 114, 157002  7-4	42
798	Effects of High-Pressure Sintering on Critical Current Density in (Ba,K)Fe2As2 PIT Wires. <b>2015</b> , 25, 1-4	12
797	Observation of mode-like features in tunneling spectra of iron-based superconductors. <b>2015</b> , 24, 077402	3
796	Co and Mn doping effect in polycrystalline (Ca,La) and (Ca,Pr)FeAs2superconductors. 2015, 28, 065001	20
795	Influence of substrate type on transport properties of superconducting FeSe0.5Te0.5thin films. <b>2015</b> , 28, 065005	11
794	New quaternary arsenide oxides with square planar coordination of gold(I) - structure, (197)Au MBsbauer spectroscopic, XANES and XPS characterization of Nd10Au3As8O10 and Sm10Au3As8O10. <b>2015</b> , 44, 5854-66	9
793	Coexistence of Bulk Superconductivity and Magnetism in CeO1â\(\mathbb{I}\)FxBiS2. <b>2015</b> , 84, 024709	49
792	Fluctuation of Diamagnetic Susceptibility in Two-band Superconductors. <b>2015</b> , 28, 319-322	2
791	First-Principle Electronic Structure Calculation of BaFe2 $\hat{a}$ Co x As2(x = 0, 1, 2) Superconductor. <b>2015</b> , 28, 2249-2254	
790	Magnetic states of iron-based superconducting compounds: A comparative study with Fe3Al alloy. <b>2015</b> , 66, 646-650	2
789	NMR evidence for field-induced ferromagnetism in (Li0.8Fe0.2)OHFeSe superconductor. <b>2015</b> , 91,	10

788	Electronic structure and superconductivity of FeSe-related superconductors. 2015, 27, 183201	56
787	Raman Spectroscopy of Ba(Fe1â⊠ Mn x )2As2. <b>2015</b> , 45, 238-243	
786	Antiferromagnetic and nematic phase transitions in BaFe2(As1âषPx)2 studied by ac microcalorimetry and SQUID magnetometry. <b>2015</b> , 91,	6
785	Crystal structure and phase diagrams of iron-based superconductors. <b>2015</b> , 58, 77-89	13
784	Modulation effect of interlayer spacing on the superconductivity of electron-doped FeSe-based intercalates. <b>2015</b> , 54, 3346-51	36
783	Atomic-Scale Derivatives of Solid-State Materials. <b>2015</b> , 27, 3549-3559	10
782	Crossover from hole- to electron-dominant regions in iron-chalcogenide superconductors induced by Te/Se substitution. <b>2015</b> , 54, 043102	4
781	Control over connectivity and magnetism of tetrahedral FeSe2 chains through coordination Fe-amine complexes. <b>2015</b> , 51, 5355-8	22
780	Doping effect on electronic band structure and magnetic properties of MFeAs(M = Li, Na). <b>2015</b> , 04, 1550005	1
779	Electronic structure of (Ca0.85La0.15)FeAs2. <b>2015</b> , 106, 052602	13
778	Iron-based superconductors: Current status of materials and pairing mechanism. 2015, 514, 399-422	263
777	Characteristical Managetic Proposition of Flow Food Large FoTo City In Country 2015 20 2002 2007	
	Structural and Magnetic Properties of Flux-Free Large FeTe Single Crystal. <b>2015</b> , 28, 2893-2897	18
776	Superconductivity and disorder effect in TlNi2Se(2-x)S(x) compounds. <b>2015</b> , 27, 395701	18
77 <sup>6</sup>		
	Superconductivity and disorder effect in TlNi2Se(2-x)S(x) compounds. <b>2015</b> , 27, 395701  Signatures of filamentary superconductivity in antiferromagnetic BaFe 2 As 2 single crystals. <b>2015</b> ,	1
775	Superconductivity and disorder effect in TlNi2Se(2-x)S(x) compounds. <b>2015</b> , 27, 395701  Signatures of filamentary superconductivity in antiferromagnetic BaFe 2 As 2 single crystals. <b>2015</b> , 111, 37005	1
775	Superconductivity and disorder effect in TlNi2Se(2-x)S(x) compounds. 2015, 27, 395701  Signatures of filamentary superconductivity in antiferromagnetic BaFe 2 As 2 single crystals. 2015, 111, 37005  Synthesis, crystal structure and magnetism of Eu3Sc2O5Fe2As2. 2015, 70, 671-676  Magnetic and magnetotransport studies of iron-chalcogenide superconductor Fe(Se0.4Te0.6)0.82:	2

770	Superconductivity of magnetic Sm-substituted LaCo2B2. <b>2015</b> , 117, 17E116	1
769	Magnetic and electronic properties of CaMn2Bi2: A possible hybridization gap semiconductor. <b>2015</b> , 91,	17
768	Doping evolution of antiferromagnetism and transport properties in nonsuperconducting BaFe2âØxNixCrxAs2. <b>2015</b> , 91,	11
767	Growth of High-Quality Superconducting FeSe 0.5 Te 0.5 Thin Films Suitable for Angle-Resolved Photoemission Spectroscopy Measurements via Pulsed Laser Deposition. <b>2015</b> , 32, 087401	3
766	New Superconductivity Dome in LaFeAsO 1âlk F x Accompanied by Structural Transition. <b>2015</b> , 32, 107401	27
765	Superconductivity-induced re-entrance of the orthorhombic distortion in Ba1-xKxFe2As2. <b>2015</b> , 6, 7911	114
764	Magnetic properties of AlFe2B2 and CeMn2Si2 synthesized by melt spinning of stoichiometric compositions. <b>2015</b> , 54, 053003	20
763	Improvement of superconductivity in Fe1+yTe0.6Se0.4 induced by annealing with CaF2 and SmF3. <b>2015</b> , 517, 16-19	7
762	Magnetic ordering and electronic structure of the ternary iron arsenide BaFe2As2. <b>2015</b> , 29, 1550182	
761	The crossover from metal to semi-conductor in Cu-doped LiFeAs system. <b>2015</b> , 29, 1542023	5
761 760	The crossover from metal to semi-conductor in Cu-doped LiFeAs system. <b>2015</b> , 29, 1542023  Synchrotron X-ray diffraction study of 112-type Ca1âlla FeAs2. <b>2015</b> , 518, 10-13	2
760	Synchrotron X-ray diffraction study of 112-type Ca1âlla FeAs2. <b>2015</b> , 518, 10-13  Enhancement of Tc in BiS2-based superconductors NdO0.7F0.3BiS2 by substitution of Pb for Bi.	2
760 759	Synchrotron X-ray diffraction study of 112-type Ca1âlla FeAs2. <b>2015</b> , 518, 10-13  Enhancement of Tc in BiS2-based superconductors NdO0.7F0.3BiS2 by substitution of Pb for Bi. <b>2015</b> , 223, 40-44	7
760 759 758	Synchrotron X-ray diffraction study of 112-type Ca1âlla FeAs2. <b>2015</b> , 518, 10-13  Enhancement of Tc in BiS2-based superconductors NdO0.7F0.3BiS2 by substitution of Pb for Bi. <b>2015</b> , 223, 40-44  Coexistence of superconductivity and antiferromagnetism in (Li0.8Fe0.2)OHFeSe. <b>2015</b> , 14, 325-9	2 7 264
760 759 758 757	Synchrotron X-ray diffraction study of 112-type Ca1âlla FeAs2. 2015, 518, 10-13  Enhancement of Tc in BiS2-based superconductors NdO0.7F0.3BiS2 by substitution of Pb for Bi. 2015, 223, 40-44  Coexistence of superconductivity and antiferromagnetism in (Li0.8Fe0.2)OHFeSe. 2015, 14, 325-9  Synthesis, electron transport properties of transition metal nitrides and applications. 2015, 70, 50-154	2 7 264 89
760 759 758 757 756	Synchrotron X-ray diffraction study of 112-type Ca1âlla FeAs2. <b>2015</b> , 518, 10-13  Enhancement of Tc in BiS2-based superconductors NdO0.7F0.3BiS2 by substitution of Pb for Bi. <b>2015</b> , 223, 40-44  Coexistence of superconductivity and antiferromagnetism in (Li0.8Fe0.2)OHFeSe. <b>2015</b> , 14, 325-9  Synthesis, electron transport properties of transition metal nitrides and applications. <b>2015</b> , 70, 50-154  Characterization of Doped Na(Fe1âll T x )As Single Crystals with T = Pd, Ni, Cr, and Mn. <b>2015</b> , 28, 1123-1127  Distorted phosphorus and copper square-planar layers in LaCu1+xP2 and LaCu4P3: synthesis,	2 7 264 89 3

75 <sup>2</sup>	Robust antiferromagnetism preventing superconductivity in pressurized (Ba 0.61 K 0.39)Mn2Bi2. <b>2014</b> , 4, 7342	4
75 <sup>1</sup>	Estimation of Superconducting Transition Temperature T C for Superconductors of the Doped MgB2 System from the Crystal Lattice Parameters Using Support Vector Regression. <b>2015</b> , 28, 75-81	35
75°	New diluted magnetic semiconductor (BaK)(ZnMn)2As2: Electronic structure and magnetic properties. <b>2015</b> , 98, 93-98	6
749	Different doping effect on physical properties of non-magnetic Pt and Ga in CaFe 4 As 3. <b>2015</b> , 623, 342-347	O
748	Local Electronic and Crystal Structure of Magnetic RCo2As2 (R = La, Ce, Pr, Eu). <b>2015</b> , 28, 995-997	3
747	Review of superconductivity in BiS 2 -based layered materials. <b>2015</b> , 84, 34-48	80
746	Effects of Iodine Annealing on Fe1+yTe0.6Se0.4. <b>2016</b> , 85, 104714	3
745	Ultrafast structural dynamics of the orthorhombic distortion in the Fe-pnictide parent compound BaFe2As2. <b>2016</b> , 3, 023611	7
744	Effect of spacer layer on flux-pinning properties of iron-based superconductors. <b>2016</b> , 2,	
743	Theoretical Study of Upper Critical Magnetic Field (HC2) in Multiband Iron Based Superconductors. <b>2016</b> , 2016, 1-10	1
742	Anisotropic Ginzburgâllandau scaling ofHc2and transport properties of 112-type Ca0.8La0.2Fe0.98Co0.02As2single crystal. <b>2016</b> , 29, 055005	18
741	A new ferromagnetic superconductor: CsEuFe 4 As 4. <b>2016</b> , 61, 1213-1220	42
740	The synthesis and characterization of 1 1 1 1 type diluted ferromagnetic semiconductor (La(1-x)Ca(x))(Zn(1-x) Mn(x))AsO. <b>2016</b> , 28, 026003	5
739	Recent Advances in Layered Metal Chalcogenides as Superconductors and Thermoelectric Materials: Fe-Based and Bi-Based Chalcogenides. <b>2016</b> , 16, 633-51	11
738	First-principles investigation of superconductivity in the body-centred tetragonal. <b>2016</b> , 96, 2059-2073	5
737	Electronic Structure and Magnetism of the Multiband New Superconductor CaRbFe4As4. <b>2016</b> , 85, 124714	8
736	Distinct doping dependence of critical temperature and critical current density in Ba1-xKxFe2As2 superconductor. <b>2016</b> , 6, 26671	23
735	Dynamics of phonons in Sr3Ir4Sn13: an experimental study by ultrafast spectroscopy measurements. <b>2016</b> , 18, 073045	5

734	Research Update: Structural and transport properties of (Ca,La)FeAs2 single crystal. <b>2016</b> , 4, 020702	4
733	Pressure Induced Enhancement of Superconductivity in LaRu2P2. <b>2016</b> , 6, 24479	7
732	Pressure-induced shift of Tc and structural transition in âll 22 âltype pnictide superconductor Ca0.34Na0.66Fe2As2. <b>2016</b> , 6, 075104	2
731	Two distinct superconducting phases in LiFeAs. <b>2016</b> , 6, 27926	11
730	Coupled multiple-mode theory for s pairing mechanism in iron based superconductors. <b>2016</b> , 6, 37508	1
729	Crystal structure instability of FeSe grains: Formation of non-superconducting phase at the grain surface. <b>2016</b> , 55, 053101	7
728	Spin anisotropy due to spin-orbit coupling in optimally hole-doped Ba0.67K0.33Fe2As2. <b>2016</b> , 94,	15
727	Optical properties of AFe2As2 (A=Ca, Sr, and Ba) single crystals. <b>2016</b> , 94,	12
726	Two superconducting domes separated by a possible Lifshitz transition in LaFeAs1â⊠PxO. <b>2016</b> , 119, 083903	4
725	Scrutinizing the double superconducting gaps and strong coupling pairing in (Li(1-x)Fe(x))OHFeSe. <b>2016</b> , 7, 10565	60
724	Effects of introducing isotropic artificial defects on the superconducting properties of differently doped Ba-122 based single crystals. <b>2016</b> , 6, 27783	15
723	Transport properties and anisotropy of superconducting (Li1â⊠Fex)OHFeSe single crystals. <b>2016</b> , 29, 055003	10
722	Coexistence of Superconductivity and Spin Density Wave (SDW) in Ferropnictide Ba1â¼ K x Fe2As2. <b>2016</b> , 29, 1433-1438	2
721	The influence of the structural transition on magnetic fluctuations in NaFeAs. <b>2016</b> , 28, 27LT01	2
720	Evaluation of global and local critical current densities in 122-type iron-based superconducting tapes. <b>2016</b> , 530, 76-78	3
719	Two-Band Calculations on the Superconducting Property of SrPt(_{2}mathrm{As}_{2}). <b>2016</b> , 183, 379-386	
718	Superconductivity at 7.8 K in the ternary LaRu 2 As 2 compound. <b>2016</b> , 61, 921-924	10
717	Phonons and Electronâ <b>P</b> honon Coupling of Newly Discovered ThCr 2 Si 2 -Type Superconductor BaPd 2 As 2 : A Comparison Study with Sr(Ca)Pd 2 As 2. <b>2016</b> , 29, 1219-1225	5

716	Magnetic Field Dependence of Specific Heat in KFe2As2 Single Crystals. 2016, 29, 1279-1286	6
715	BaAl4 derivative phases in the sections {La,Ce}Ni2Si2-{La,Ce}Zn2Si2: phase relations, crystal structures and physical properties. <b>2016</b> , 45, 5262-73	1
714	Electron correlation effects beyond the random phase approximation. <b>2016</b> , 30, 1642006	
713	High Pressure Studies on the Transport Properties and Upper Critical Field (H c2) of Hole-Doped Pr0.8Sr0.2FeAsO Iron Pnictides. <b>2016</b> , 29, 1761-1765	
712	Design of ternary alkaline-earth metal Sn(II) oxides with potential good p-type conductivity. <b>2016</b> , 4, 4592-4599	23
711	On the determination of hardness and elastic modulus in BaFe2As2 lamellar-like material. <b>2016</b> , 31, 1413-142	.2 <sub>7</sub>
710	Excess of manganese in an iron-based superconductor: a first-principles study of its electronic, magnetic and superconducting properties. <b>2016</b> , 3, 056001	4
709	Crystal Growth and Characterization of Iron-Based Superconductor. <b>2016</b> , 143-191	
708	Spin waves and magnetic exchange interactions in the spin-ladder compound RbFe2Se3. <b>2016</b> , 94,	21
707	Study of vortex dynamics in single crystalline Ba0.54K0.46Fe2As2 superconductor using dc and ac magnetization. <b>2016</b> , 686, 938-945	2
706	High-pressure synchrotron M\( \text{S}\) shauer and X-ray diffraction studies: Exploring the structure-related valence fluctuation in EuNi2P2. <b>2016</b> , 501, 101-105	3
705	Controlling Magnetic Ordering in Ca1â\(\text{EuxCo2As2}\) by Chemical Compression. <b>2016</b> , 28, 7459-7469	7
704	Ammonia and iron cointercalated iron sulfide (NH3)Fe0.25Fe2S2: hydrothermal synthesis, crystal structure, weak ferromagnetism and crossover from a negative to positive magnetoresistance. <b>2016</b> , 6, 81886-81893	11
703	Upper critical field and quantum oscillations in tetragonal superconducting FeS. 2016, 94,	10
702	Nodal superconductivity in FeS: Evidence from quasiparticle heat transport. <b>2016</b> , 94,	16
701	From complex magnetism ordering to simple ferromagnetism in two-dimensional LaCrSb3 by hole doping. <b>2016</b> , 94,	2
700	High-Resolution Inelastic X-Ray Scattering I: Context, Spectrometers, Samples, and Superconductors. <b>2016</b> , 1643-1719	10
699	Enhancement of critical current densities in (Ba,K)Fe2As2wires and tapes using HIP technique. <b>2016</b> , 29, 115002	37

698	Model study of coexistence of Jahn-Teller distortion, antiferromagnetism and superconductivity in iron pnictide superconductors. <b>2016</b> , 248, 53-59	2
697	Superconductivity in Ternary Pnictide SrPd2Sb2 Polymorphs. <b>2016</b> , 85, 043701	6
696	Anisotropic thermodynamic and transport properties of single-crystalline CaKFe4As4. <b>2016</b> , 94,	92
695	Anisotropic transport and optical spectroscopy study on antiferromagnetic triangular lattice EuCd2As2: An interplay between magnetism and charge transport properties. <b>2016</b> , 94,	18
694	Understanding Doping, Vacancy, Lattice Stability, and Superconductivity in K Fe Se. <b>2016</b> , 3, 1600098	24
693	Two-Dimensional Superconductivity Emerged at Monatomic Bi(2-) Square Net in Layered Y2O2Bi via Oxygen Incorporation. <b>2016</b> , 138, 11085-8	22
692	Electron-phonon superconductivity in the ternary phosphides BaM2P2 (M=Ni,Rh,and Ir). <b>2016</b> , 94,	9
691	Ultrafast dynamics of quasiparticles and coherent acoustic phonons in slightly underdoped (BaK)Fe2As2. <b>2016</b> , 6, 25962	2
690	Vortex phase transition and anisotropy behavior of optimized (Li1â\(\mathbb{R}\)FeSe single crystals. <b>2016</b> , 29, 105015	13
689	Fluctuation conductivity and possible pseudogap state in FeAs-based superconductor EuFeAsO0.85F0.15. <b>2016</b> , 3, 076001	14
688	Magnetic structures of the Eu and Cr moments in EuCr2As2: Neutron diffraction study. <b>2016</b> , 94,	10
687	Electronic Structures of the Superconducting Single-Layer FeSe/SrTiO(_3) Films. 2016, 81-93	
686	Electron-deficient copper pnictides: A2Mg3Cu9Pn7 (A = Sr, Eu; Pn = P, As) and Eu5Mg2.39Cu16.61As12. <b>2016</b> , 3, 1264-1271	8
685	Vortices in high-performance high-temperature superconductors. <b>2016</b> , 79, 116501	100
684	Tailoring the critical current properties in Cu-sheathed Sr1â⊠KxFe2As2superconducting tapes. <b>2016</b> , 29, 095006	7
683	Phase Diagram and High T(_c) Superconductivity in Single-Layer FeSe Films. <b>2016</b> , 95-113	
682	Irreversibility Line Measurement and Vortex Dynamics in High Magnetic Fields in Ni- and Co-Doped Iron Pnictide Bulk Superconductors. <b>2016</b> , 29, 2735-2742	2
681	Pnictide-height dependent ferromagnetism in CuFeAs and CuFeSb. <b>2016</b> , 686, 38-42	3

680	Structure, magnetization, specific heat, and microwave properties of KxFe\${}_{2mbox{}{text{}}y}\$Se2. <b>2016</b> , 29, 085015	2
679	Evidence for defect-induced superconductivity up to 49 K in (Ca1â⊠Rx)Fe2As2. <b>2016</b> , 93,	20
678	Nonmonotonic pressure evolution of the upper critical field in superconducting FeSe. 2016, 93,	35
677	Fermi surface reconstruction in FeSe under high pressure. <b>2016</b> , 93,	34
676	Magnetotransport study of the pressure-induced antiferromagnetic phase in FeSe. 2016, 93,	20
675	Role of hydrogen in the electronic properties of CaFeAsH-based superconductors. 2016, 93,	4
674	Effect of impurity substitution on band structure and mass renormalization of the correlated FeTe0.5Se0.5 superconductor. <b>2016</b> , 93,	5
673	Comparative study of thermodynamic properties near the structural phase transitions in Sr3Rh4Sn13 and Sr3Ir4Sn13. <b>2016</b> , 93,	12
672	Ab initio theory of iron-based superconductors. <b>2016</b> , 94,	24
671	Spin Ferroquadrupolar Order in the Nematic Phase of FeSe. <i>Physical Review Letters</i> , <b>2016</b> , 116, 247203 7.4	26
670	Spin Ferroquadrupolar Order in the Nematic Phase of FeSe. <i>Physical Review Letters</i> , <b>2016</b> , 116, 247203 7.4  Superconductivity in Layered Systems of Dirac Electrons. <b>2016</b> , 97-122	26
		26
670	Superconductivity in Layered Systems of Dirac Electrons. <b>2016</b> , 97-122  Dynamical screening in correlated electron systems-from lattice models to realistic materials. <b>2016</b> ,	
6 <sub>7</sub> 0	Superconductivity in Layered Systems of Dirac Electrons. <b>2016</b> , 97-122  Dynamical screening in correlated electron systems-from lattice models to realistic materials. <b>2016</b> , 28, 383001  Experimental and Theoretical Studies on the Crystal Structure of Ternary Copper Arsenides	43
670 669 668	Superconductivity in Layered Systems of Dirac Electrons. <b>2016</b> , 97-122  Dynamical screening in correlated electron systems-from lattice models to realistic materials. <b>2016</b> , 28, 383001  Experimental and Theoretical Studies on the Crystal Structure of Ternary Copper Arsenides A2Cu3As3 (A = Sr, Eu). <b>2016</b> , 2016, 3774-3780  Polymorphism in Zintl Phases ACd4Pn3: Modulated Structures of NaCd4Pn3 with Pn = P, As. <b>2016</b> ,	43
670 669 668	Superconductivity in Layered Systems of Dirac Electrons. 2016, 97-122  Dynamical screening in correlated electron systems-from lattice models to realistic materials. 2016, 28, 383001  Experimental and Theoretical Studies on the Crystal Structure of Ternary Copper Arsenides A2Cu3As3 (A = Sr, Eu). 2016, 2016, 3774-3780  Polymorphism in Zintl Phases ACd4Pn3: Modulated Structures of NaCd4Pn3 with Pn = P, As. 2016, 55, 7764-76  The effects of post-growth annealing on the structural and magnetic properties of BaFe2As2. 2016,	43 4
670 669 668 667	Superconductivity in Layered Systems of Dirac Electrons. 2016, 97-122  Dynamical screening in correlated electron systems-from lattice models to realistic materials. 2016, 28, 383001  Experimental and Theoretical Studies on the Crystal Structure of Ternary Copper Arsenides A2Cu3As3 (A = Sr, Eu). 2016, 2016, 3774-3780  Polymorphism in Zintl Phases ACd4Pn3: Modulated Structures of NaCd4Pn3 with Pn = P, As. 2016, 55, 7764-76  The effects of post-growth annealing on the structural and magnetic properties of BaFe2As2. 2016, 28, 115702	43 4 4

662	Absence of nematic order in the pressure-induced intermediate phase of the iron-based superconductor Ba0.85K0.15Fe2As2. <b>2016</b> , 93,	9
661	Effects of single- and multi-substituted Zn ions in doped 122-type iron-based superconductors. <b>2016</b> , 93,	1
660	Superconductivity and ferromagnetism in hole-doped RbEuFe4As4. 2016, 93,	68
659	Doping evolution of the superconducting gap structure in the underdoped iron arsenide Ba1â¤KxFe2As2 revealed by thermal conductivity. <b>2016</b> , 93,	13
658	Effect of external magnetic field on the coexistence of superconductivity and JT distortion in iron pnictides. <b>2016</b> , 248, 110-114	6
657	Superconductivity and multiple pressure-induced phases in BaPt2As2. <b>2016</b> , 94,	6
656	Superconductivity in layered ZrP2â⊠Sexwith PbFCl-type structure. <b>2016</b> , 29, 055004	10
655	Pinning force scaling analysis of Fe-based high-Tc superconductors. <b>2016</b> , 30, 1630017	18
654	Hubbard interactions in iron-based pnictides and chalcogenides: Slater parametrization, screening channels, and frequency dependence. <b>2016</b> , 94,	20
653	Suppression of superconductivity and structural phase transitions under pressure in tetragonal FeS. <b>2016</b> , 6, 31077	10
652	Spin excitations in hole-overdoped iron-based superconductors. <b>2016</b> , 6, 33303	11
651	High-temperature superconductivity in iron pnictides and chalcogenides. <b>2016</b> , 1,	246
650	Experimental and theoretical identification of the Fe(vii) oxidation state in FeO. 2016, 18, 31125-31131	11
649	Emergence of superconductivity in (NH3)yMxMoSe2 (M: Li, Na and K). <b>2016</b> , 6, 29292	9
648	Evolution of superconductivity and magnetism in BiS2-based layered compounds. 2016, 2,	5
647	Optical study of charge dynamics in CaCo 2 As 2. <b>2016</b> , 25, 057201	
646	Interrogating the superconductor Ca(PtAs)(FePtAs) Layer-by-layer. <b>2016</b> , 6, 35365	6
645	Intrinsic and extrinsic pinning in NdFeAs(O,F): vortex trapping and lock-in by the layered structure. <b>2016</b> , 6, 36047	30

644	Angle-resolved spectroscopy study of Ni-based superconductor SrNi2As2. <b>2016</b> , 94,	4
643	Anomalous magneto-elastic and charge doping effects in thallium-doped BaFe2As2. <b>2016</b> , 6, 21660	4
642	Raman scattering studies on the collapsed phase of CaCo 2 As 2. <b>2016</b> , 25, 067803	
641	Neutron diffraction study on heavy-fermion compound CeCrGe3. <b>2016</b> , 94,	2
640	Superconductivity in KCa2Fe4As4F2 with Separate Double Fe2As2 Layers. <b>2016</b> , 138, 7856-9	67
639	Superconductivity in Sm-doped CaFe 2 As 2 single crystals. <b>2016</b> , 25, 067403	
638	Electronic structures and magnetism of YM2Ge2 ( $M = Mna\Omegau$ ): Ge-hight dependent magnetic ordering in YFe2Ge2. <b>2016</b> , 121, 48-53	4
637	Critical current densities and flux creep rates in near optimally doped BaFe2â\RuxAs2 (xâ\(\bar{0}\).7) single crystals. <b>2016</b> , 231-232, 26-30	4
636	Effects of rolling deformation processes on the properties of Ag-sheathed Sr 1 âlk K x Fe 2 As 2 superconducting tapes. <b>2016</b> , 525-526, 94-99	10
635	Quench Behaviors of Monofilament Iron-Based Sr0.6K0.4Fe2As2 Tape With Ag Sheath at Different Temperatures. <b>2016</b> , 26, 1-6	4
634	Electronic structures and magnetism of LaFe2Ge2 and LaFe2Si2: First-principles studies. <b>2016</b> , 525-526, 72-77	2
633	Thermal expansion behaviour and phase stability of AFe2As2 (A = Ca, Sr and Eu) using powder diffraction technique. <b>2016</b> , 86, 1369-1381	
632	YPd2Al and YPd2Zn with LiCu2Sn Type Structure. <b>2016</b> , 642, 627-630	2
631	The synthesis and magnetic structure of the iron selenide Ba0.8Fe2Se2. <b>2016</b> , 667, 012003	
630	Superconductivity at 3.85 K in BaPd 2 As 2 with the ThCr 2 Si 2 -type structure. 2016, 113, 17002	18
629	Critical spin fluctuations and the origin of nematic order in Ba(Fe1â⊠Cox)2As2. <b>2016</b> , 12, 560-563	47
628	Solid state synthesis and characterization of bulk FeTe0.5Se0.5superconductors. <b>2016</b> , 667, 012006	2
627	Flux pinning and relaxation in FeSe0.5Te0.5single crystals. <b>2016</b> , 29, 035006	15

626	Influence of the electronic structure on the transport properties of some iron pnictides. <b>2016</b> , 17, 164-187	14
625	Improvement in granularity of NdFeAsO0.8F0.2 superconductor through Agx doping ( $x = 0.0 a \ 0.3$ ). <b>2016</b> , 520, 1-7	1
624	Progress in nonmagnetic impurity doping studies on Fe-based superconductors. <b>2016</b> , 29, 053001	5
623	The New Superconductor tP-SrPd2Bi2: Structural Polymorphism and Superconductivity in Intermetallics. <b>2016</b> , 55, 3203-5	9
622	Nodeless superconducting gaps in Ca10(Pt4-IAs8)((Fe1-x Pt x )2As2)5 probed by quasiparticle heat transport. <b>2016</b> , 59, 1	О
621	Hydrogen-modified superconductors: A review. <b>2016</b> , 44, 20-34	13
620	Coexistence of clean- and dirty-limit superconductivity in LiFeAs. <b>2016</b> , 93,	10
619	Fabrication of Nb-sheathed FeSe0.5Te0.5 tape by an ex-situ powder-in-tube method. <b>2016</b> , 664, 218-222	7
618	Effect of Cooling Rate on Structure, Composition, and Superconducting Properties of FeTe0.6Se0.4 Prepared by Self-Flux Technique. <b>2016</b> , 29, 1187-1192	2
617	A first principles study on newly proposed (Ca/Sr/Ba)Fe2Bi2 compounds with their parent compounds. <b>2016</b> , 96, 511-523	2
616	Charge nematicity and electronic Raman scattering in iron-based superconductors. <b>2016</b> , 17, 113-139	69
615	Nanoscale Inhomogeneous Superconductivity in Fe(Te1-xSex) Probed by Nanostructure Transport. <b>2016</b> , 10, 429-35	5
614	Thin film growth of CaFe2As2by molecular beam epitaxy. <b>2016</b> , 29, 015013	7
613	Structural transition and superconductivity in hydrothermally synthesized FeX (X = S, Se). <b>2016</b> , 52, 194-7	47
612	Effect of metal (Zn/In/Pb) additions on the microstructures and superconducting properties of Sr1 â[kKxFe2As2 tapes. <b>2016</b> , 112, 128-131	18
611	The phase diagrams of iron-based superconductors: Theory and experiments. <b>2016</b> , 17, 5-35	35
610	Dimensionality of the oxidic layers in pnictide oxides and transition metal p-element ordering in tetrelides and pnictides. <b>2017</b> , 254, 1600084	О
609	High-temperature superconductivity in iron-based compounds. <b>2017</b> , 254, 1770206	

Growth, magnetic and transport properties of Li-doped SrFe2As2 single crystals. **2017**, 254, 1600118

607	A calorimetric investigation of RbFe2As2 single crystals. <b>2017</b> , 254, 1600208	9
606	Evolution of superconducting gap anisotropy in hole-doped 122 iron pnictides. <b>2017</b> , 254, 1600350	1
605	Iron arsenide superconductors (CaFeAs)10MnAs8 with metallic interlayers (M = Pt, Pd; n = 3, 4). <b>2017</b> , 254, 1600417	6
604	Observation of the weak electronic correlations in KFeCoAs (3d): an isoelectronic to the parent compounds of 122 series of iron pnictides BaFeAs. <b>2017</b> , 29, 085503	4
603	First-Order Phase Transition in BaNiGe and the Influence of the Valence Electron Count on Distortion of the ThCrSi Structure Type. <b>2017</b> , 56, 1173-1185	5
602	Superconductivity in the ternary iridiumâlirsenide Balr2As2. 2017, 30, 035007	9
601	Ab initio study of doping effects in the 42214 compounds: A new family of layered iron-based superconductors. <b>2017</b> , 95,	1
600	Rearrangement of van der Waals stacking and formation of a singlet state at $T = 90  \text{K}$ in a cluster magnet. <b>2017</b> , 4, 481-490	17
599	Synthesis, Crystal Structure and Superconductivity in RbLn2Fe4As4O2 (Ln = Sm, Tb, Dy, and Ho). <b>2017</b> , 29, 1805-1812	27
598	First-principles investigations on structure stability, elastic properties, anisotropy and Debye temperature of tetragonal LiFeAs and NaFeAs under pressure. <b>2017</b> , 104, 243-251	26
597	Structural and Superconductivity Properties of BaFe2â⊠ Pt x As2. <b>2017</b> , 30, 1145-1151	6
596	Charge Density Wave in the New Polymorphs of RERuGe (RE = Pr, Sm, Dy). <b>2017</b> , 139, 4130-4143	19
595	G-type magnetic order in ferropnictide CuxFe1âŊAs induced by hole doping on As sites. <b>2017</b> , 95,	1
594	Superconductivity at 35 K by self doping in RbGdFeAsO. <b>2017</b> , 29, 11LT01	17
593	Theoretical Study of Electronic and Magnetic Properties of Newly Derived Ironâ <b>P</b> nictide Compound. <b>2017</b> , 30, 2043-2051	1
592	Eisenbasierte Vielfalt. 2017, 48, 70-77	3
591	Enhanced transport critical current density in Sn-added SmFeAsO1âNFxtapes prepared by the PIT method. <b>2017</b> , 30, 065004	6

590	Selenium doping NaCl-type superconductor: SnAs 1â⊠ Se x (x=0âŪ.13). <b>2017</b> , 252, 106-110	3
589	Transport critical current density of high-strength Sr1â\(\text{KxFe2As2/Ag/Monel composite conductors.}\) 2017, 30, 075010	11
588	Observation of reversible critical current performance under large compressive strain in Sr0.6K0.4Fe2As2tapes. <b>2017</b> , 30, 07LT01	8
587	Physical properties of the body-centred tetragonal. <b>2017</b> , 97, 1866-1883	3
586	ThCr2Si2-type Ru-based superconductors LaRu2M2 (MI≢IP and As): An ab-initio investigation. <b>2017</b> , 695, 2827-2834	15
585	Effect of Co doping and hydrostatic pressure on SrFe2 As2. <b>2017</b> , 254, 1600154	1
584	The synthesis and magnetic properties of BaFe2Se3 single crystals. <b>2017</b> , 7, 30433-30438	4
583	A multiband Eliashberg-approach to iron-based superconductors. <b>2017</b> , 254, 1600828	7
582	Observation of a bi-critical point between antiferromagnetic and superconducting phases in pressurized single crystal Ca0.73La0.27FeAs2. <b>2017</b> , 62, 857-862	7
581	Novel 122-type Ir-based superconductors BaIr 2 Mi 2 (Mille IP and As): A density functional study. <b>2017</b> , 711, 327-334	14
580	Evidence of anisotropic phase correlations above Tc in single crystalline Ba0.54K0.46Fe2As2. <b>2017</b> , 512, 54-57	
579	Discovery of a novel 112-type iron-pnictide and La-doping induced superconductivity in Eu 1 $\hat{a}$ La x FeAs 2 (x = 0 $\hat{a}$ D.15). <b>2017</b> , 62, 218-221	14
578	Electronic structure and magnetism of RbGd2Fe4As4O2. <b>2017</b> , 708, 392-396	3
577	High-temperature superconductivity in one-unit-cell FeSe films. 2017, 29, 153001	40
576	New ternary superconducting compound LaRu 2 As 2 : Physical properties from density functional theory calculations. <b>2017</b> , 26, 037103	29
575	Hole doping and pressure effects on the II-II-V-based diluted magnetic semiconductor (Ba1â¼Kx)(Zn1â¼Mny)2As2. <b>2017</b> , 95,	19
574	NMR investigation of spin fluctuations in the itinerant-electron magnetic compound Sr1â\(\text{QCaxCo2P2}\). <b>2017</b> , 95,	1
573	Complex magnetic phase diagram with multistep spin-flop transitions in La0.25Pr0.75Co2P2. <b>2017</b> , 95,	3

572	Superconducting Properties of 100-m Class Sr0.6K0.4Fe2As2 Tape and Pancake Coils. <b>2017</b> , 27, 1-5	35
57 <sup>1</sup>	Thermally activated flux flow in superconducting epitaxial FeSe0.6Te0.4 thin film. <b>2017</b> , 7, 16-20	17
570	Optimization of Deposition Conditions to Grow High-Quality FeâBeâTe Thin Films. 2017, 27, 1-5	5
569	Crystal structure and superconductivity at about 30 K in ACa2Fe4As4F2 (A = Rb, Cs). <b>2017</b> , 60, 83-89	38
568	Synthesis, crystal structure and physical properties of a new oxypnictide Ba2Ti2Cr2As4O containing [Ti2As2O]2âland [Cr2As2]2âlayers. <b>2017</b> , 694, 1149-1153	4
567	Key Factors for InsulatorâBuperconductor Transition in FeSe Thin Films by Electric Field. <b>2017</b> , 27, 1-5	10
566	Fishtail Effect and the Upper Critical Field in a Superconducting Ca 1 0 (Pt 4 As 8 )(Fe 2 âlk Pt x As 2 ) 5. <b>2017</b> , 30, 2963-2969	O
565	Magnetism and thermodynamics of the anisotropic frustrated spin-1 Heisenberg antiferromagnet on a body-centered cubic lattice. <b>2017</b> , 251, 79-87	5
564	Compressed tetragonal phase in XFe2As2 (X=Na, K, Rb, Cs) and in the alloy Na0.5K0.5Fe2As2. <b>2017</b> , 95,	6
563	High-Temperature Superconductors. <b>2017</b> , 1-1	6
562	Magnetic fluctuations and superconducting properties of CaKFe4As4 studied by As75 NMR. <b>2017</b> , 96,	34
562 561		12
	96,  The Interface Structure of FeSe Thin Film on CaF Substrate and its Influence on the	
561	The Interface Structure of FeSe Thin Film on CaF Substrate and its Influence on the Superconducting Performance. <b>2017</b> , 9, 37446-37453	12
561 560	The Interface Structure of FeSe Thin Film on CaF Substrate and its Influence on the Superconducting Performance. 2017, 9, 37446-37453  Pressure-induced half-collapsed-tetragonal phase in CaKFe4As4. 2017, 96,	12 29
561 560 559	The Interface Structure of FeSe Thin Film on CaF Substrate and its Influence on the Superconducting Performance. 2017, 9, 37446-37453  Pressure-induced half-collapsed-tetragonal phase in CaKFe4As4. 2017, 96,  Magnetic properties of single crystal EuPt2As2. 2017, 728, 959-965  Doping dependence of the vortex dynamics in single-crystal superconducting NaFe\${}_{1-x}\$CoxAs.	12 29 1
<ul><li>561</li><li>560</li><li>559</li><li>558</li></ul>	The Interface Structure of FeSe Thin Film on CaF Substrate and its Influence on the Superconducting Performance. 2017, 9, 37446-37453  Pressure-induced half-collapsed-tetragonal phase in CaKFe4As4. 2017, 96,  Magnetic properties of single crystal EuPt2As2. 2017, 728, 959-965  Doping dependence of the vortex dynamics in single-crystal superconducting NaFe\${}_{1-x}\$CoxAs. 2017, 30, 105006  The influence of the in-plane lattice constant on the superconducting transition temperature of	12 29 1

554	Structure determination in thin film Ba1â\(\textbf{\mathbb{R}}\)LaxFe2As2: Relation between the FeAs4 geometry and superconductivity. <b>2017</b> , 96,	4
553	Picoscale materials engineering. <b>2017</b> , 2,	33
552	Fermi surface and effective masses in photoemission response of the (Ba K )FeAs superconductor. <b>2017</b> , 7, 8787	12
551	Electronic structure of ThRu2Si2 studied by angle-resolved photoelectron spectroscopy: Elucidating the contribution of U 5f states in URu2Si2. <b>2017</b> , 96,	6
550	Investigation of the substitution at the anionic positions BaT2As2 (T = Fe, Ni) superconductors. <b>2017</b> , 62, 1026-1031	
549	Pressure-induced transition to the collapsed tetragonal phase in BaCr2As2. <b>2017</b> , 95,	10
548	Mechanism of the high transition temperature for the 1111-type iron-based superconductors RFeAsO (R=rareearth): Synergistic effects of local structures and 4f electrons. <b>2017</b> , 96,	4
547	Evidence of Mott physics in iron pnictides from x-ray spectroscopy. <b>2017</b> , 96,	20
546	Facile Synthesis, Magnetic and Electric Characterization of Mixed Valence LaKAMnTiO (A = Sr and Ba) Perovskites. <b>2017</b> , 56, 10404-10411	8
545	Ising-type Magnetic Anisotropy in CePdAs. <b>2017</b> , 7, 7338	4
544	Arsenic chemistry of iron-based superconductors and strategy for novel superconducting materials. <b>2017</b> , 2, 450-461	4
543	Point defect induced giant enhancement of flux pinning in Co-doped FeSe0.5Te0.5 superconducting single crystals. <b>2017</b> , 7, 115016	4
542	Band structure and Fermi surfaces of the reentrant ferromagnetic superconductor Eu(Fe0.86Ir0.14)2As2. <b>2017</b> , 96,	
541	Collapsed tetragonal phase transition in LaRu2P2. <b>2017</b> , 96,	7
540	Revisiting the Electron-Doped SmFeAsO: Enhanced Superconductivity up to 58.6 K by Th and F Codoping. <b>2017</b> , 34, 077401	5
539	Direct response of the spin-density wave transition and superconductivity to anion height in SrFe2As2. <b>2017</b> , 96,	1
538	Synthesis, Crystal Structure, and Magnetic Properties of RMgSiPn (R = La, Ce; Pn = P, As). <b>2017</b> , 56, 8348-8354	6
537	Crystal growth and phase diagram of 112-type iron pnictide superconductor Ca1â�LayFe1â�NixAs2. <b>2017</b> , 30, 095002	13

536	Possible superconductivity in the electron-doped chromium pnictide LaOCrAs. 2017, 95,	5
535	High transportJcin stainless steel/Ag-Sn double sheathed Ba122 tapes. <b>2017</b> , 30, 095012	16
534	Absence of magnetism in the superconductor Ba2Ti2Fe2As4O: Insights from inelastic neutron scattering measurements and ab initio calculations of phonon spectra. <b>2017</b> , 95,	5
533	Preparation of new superconductors by metal doping of two-dimensional layered materials using ethylenediamine. <b>2017</b> , 96,	11
532	Driving the Europium Valence State in EuCo2As2 by External and Internal Impact. 2017, 30, 75-78	6
531	The Third-Order Elastic Moduli and Debye Temperature of SrFe2As2 and BaFe2As2: a First-Principles Study. <b>2017</b> , 30, 1749-1756	7
530	Unconventional superconductivity. <b>2017</b> , 66, 75-196	89
529	Phase diagram and transport properties of Sb-doped Ca0.88La0.12Fe2As2 single crystals. <b>2017</b> , 12, 1	1
528	Magnetic AC Loss of Monofilament Sr 0 . 6 K 0 . 4 Fe 2 As 2 /Ag Tape. <b>2017</b> , 30, 701-706	2
527	Combined experimental and theoretical studies of pressure effects in La2Sb. <b>2017</b> , 254, 1600168	2
526	Superconductivity and Dirac fermions in 112-phase pnictides. <b>2017</b> , 254, 1600163	15
525	Direct measurement of the temperature dependence of the in-plane magnetic penetration depth in optimally doped BaFe 2 (As1 $\hat{a}$ NP x ) 2 single crystals. <b>2017</b> , 533, 59-62	
524	Structural instability and superconductivity in the solid solution SrNi2(P1â\(\mathbb{B}\)Gex)2. <b>2017</b> , 254, 1600351	3
523	The Pt Dopant Effect on Physical Properties of Ba0.2La0.8Fe2As2. <b>2017</b> , 30, 3285-3288	5
522	Fabrication of (Ba,K)Fe2As2tapes byex situPIT process using Ag-Sn alloy single sheath. <b>2017</b> , 30, 015012	17
521	Low-energy microscopic models for iron-based superconductors: a review. <b>2017</b> , 80, 014503	86
520	Iron pnictide thin films: Synthesis and physics. <b>2017</b> , 254, 1600341	10
519	Simultaneously scanning two connected tips in a scanning tunneling microscope. <b>2017</b> , 121, 214501	

518	Effect of proton irradiation on the fluctuation-induced magnetoconductivity of FeSe1â⊠Texthin films. <b>2017</b> , 19, 093004	8
517	Spin excitation anisotropy in the optimally isovalent-doped superconductor BaFe2(As0.7P0.3)2. <b>2017</b> , 96,	11
516	Doping evolution of the anisotropic upper critical fields in the iron-based superconductor Ba1â⊠KxFe2As2. <b>2017</b> , 96,	2
515	Deposition and properties of Fe(Se,Te) thin films on vicinal CaF2substrates. <b>2017</b> , 30, 115008	7
514	Monoclinic 122-Type BaIrâ©eâ©with a Channel Framework: A Structural Connection between Clathrate and Layered Compounds. <b>2017</b> , 10,	3
513	Comparative Review on Thin Film Growth of Iron-Based Superconductors. <b>2017</b> , 2, 25	13
512	Crystal Growth Techniques for Layered Superconductors. <b>2017</b> , 2, 32	2
511	(Li1â⊠Fex)OHFeSe Superconductors: Crystal Growth, Structure, and Electromagnetic Properties. <b>2017</b> , 7, 167	4
510	Critical Slowing Down of Quadrupole and Hexadecapole Orderings in Iron Pnictide Superconductor. <b>2017</b> , 86, 064706	7
509	Carrier-Doping Dependence of Critical Current Density in Ba1-xKxFe2As2Single Crystals and Superconducting Wires. <b>2017</b> , 871, 012060	4
508	Superconductivity in 122-Type Pnictides without Iron. <b>2017</b> , 2, 28	8
507	Magnetic properties of exchange-enhanced Pauli paramagnetic metalsAeCo2P2(Ae= Sr, Ba). <b>2017</b> , 868, 012015	1
506	FeTe0.6Se0.4bulk single crystals with high critical current densities under magnetic fields. <b>2017</b> , 871, 012064	O
505	Critical Current Density in the Heterogeneous High-T c Superconductor Ca1â⊠La x Fe2As2. <b>2018</b> , 72, 515-521	
504	Correlation, temperature and disorder: Recent developments in the one-step description of angle-resolved photoemission. <b>2018</b> , 740, 1-34	21
503	Impact of concomitant Y and Mn substitution on superconductivity in La1âŪYyFe1â☑MnxAsO0.89F0.11. <b>2018</b> , 97,	6
502	Recent progress in thin-film growth of Fe-based superconductors: superior superconductivity achieved by thin films. <b>2018</b> , 31, 093001	32
501	Observation of direct evolution from antiferromagnetism to superconductivity in Cu1âlLixFeAs (0âlâl.0). <b>2018</b> , 97,	1

500	Synthesis, Structure, and Properties of the Layered Oxyselenide BaCuOCuSe. 2018, 57, 5108-5113	3
499	SrFe1â¼MoxO2+🛭 parasitic ferromagnetism in an infinite-layer iron oxide with defect structures induced by interlayer oxygen. <b>2018</b> , 5, 046106	
498	Structural and electrical studies of olivine LiNi1 â[k(Co0.5Mn0.5)xPO4 (0 â[k â[l]) at high temperature. <b>2018</b> , 24, 3733-3744	6
497	Newly synthesized MgAl2Ge2: A first-principles comparison with its silicide and carbide counterparts. <b>2018</b> , 117, 139-147	18
496	Formation of AsâAs Interlayer Bonding in the cT Phase of EuFe2As2 and CeFeAsO Under Pressure from First Principle. <b>2018</b> , 31, 3111-3117	1
495	Fermi Surface with Dirac Fermions in CaFeAsF Determined via Quantum Oscillation Measurements. <b>2018</b> , 8,	16
494	The cooling rate effect on structure and flux pinning force of FeTeSe single crystal deposited by self-flux method. <b>2018</b> , 29, 6477-6483	6
493	Superconductivity in a New 1144-Type Family of (La,Na)AFeAs (A = Rb or Cs). <b>2018</b> , 9, 868-873	13
492	Pt-Bi Antibonding Interaction: The Key Factor for Superconductivity in Monoclinic BaPtBi. <b>2018</b> , 57, 1698-170	14
491	Collapsed tetragonal phase as a strongly covalent and fully nonmagnetic state: Persistent magnetism with interlayer AsâAs bond formation in Rh-doped Ca0.8Sr0.2Fe2As2. <b>2018</b> , 97,	5
490	Unconventional superconductivity in iron pnictides: Magnon mediated pairing. <b>2018</b> , 545, 18-25	3
489	An Unusual Triple-Decker Variant of the Tetragonal BaAl-Structure Type: Synthesis, Structural Characterization, and Chemical Bonding of SrCdGe and EuCdGe. <b>2018</b> , 57, 833-842	6
488	Protonation induced high- T c phases in iron-based superconductors evidenced by NMR and magnetization measurements. <b>2018</b> , 63, 11-16	34
487	Advanced first-principles theory of superconductivity including both lattice vibrations and spin fluctuations: The case of FeB4. <b>2018</b> , 97,	17
486	Development of superconducting joints between iron-based superconductor tapes. <b>2018</b> , 31, 06LT02	8
485	Improvements of fabrication processes and enhancement of critical current densities in (Ba,K)Fe2As2HIP wires and tapes. <b>2018</b> , 31, 055016	41
484	Modeling pseudo-elastic behavior in small-scale ThCr2Si2-type crystals. <b>2018</b> , 150, 86-95	4
483	Cr doping effects on structure and superconductivity of Ba2Ti2Fe2As4O. <b>2018</b> , 745, 460-466	3

482	Robust s∃ pairing in CaK(Fe1â⊠Nix)4As4 (x=0 and 0.05) from the response to electron irradiation. <b>2018</b> , 97,	13
481	Antiphase Fermi-surface modulations accompanying displacement excitation in a parent compound of iron-based superconductors. <b>2018</b> , 97,	6
480	Anisotropic two-gap superconductivity and the absence of a Pauli paramagnetic limit in single-crystalline LaO0.5F0.5BiS2. <b>2018</b> , 97,	10
479	Influences of Tape Thickness on the Properties of Ag-Sheathed Sr1-xKxFe2 As2 Superconducting Tapes. <b>2018</b> , 28, 1-5	8
478	Upper critical fields in Ba2Ti2Fe2As4O single crystals: Evidence for dominant Pauli paramagnetic effect. <b>2018</b> , 97,	1
477	Solids, liquids, and gases under high pressure. <b>2018</b> , 90,	216
476	Synthesis and characterization of iron based superconductor Nd-1111. <b>2018</b> , 549, 116-118	5
475	Theoretical Study of Superconducting Gap Parameters, Density of States, and Condensation Energy of Two-Band Iron-Based Superconductor BaFe2(As1â⊠ P x )2. <b>2018</b> , 31, 37-45	1
474	Electronic, Transport, and Magnetic Properties of La-Doped Ba 1 $\hat{a}$ Ik Fe 1 . 9 Pt 0 . 1 As 2 (x = 0, 0.4, 0.6, 0.8) Compounds. <b>2018</b> , 31, 47-53	3
473	Recent advances in iron-based superconductors toward applications. <b>2018</b> , 21, 278-302	200
473 472	Recent advances in iron-based superconductors toward applications. <b>2018</b> , 21, 278-302  First principles predictions of electronic and elastic properties of BaPb 2 As 2 in the ThCr 2 Si 2 -type structure. <b>2018</b> , 544, 18-21	200
	First principles predictions of electronic and elastic properties of BaPb 2 As 2 in the ThCr 2 Si 2	
472	First principles predictions of electronic and elastic properties of BaPb 2 As 2 in the ThCr 2 Si 2 -type structure. <b>2018</b> , 544, 18-21  Possible interface superconductivity in rare-earth-doped CaFe(_{2})As(_{2}) and undoped	1
47 <sup>2</sup>	First principles predictions of electronic and elastic properties of BaPb 2 As 2 in the ThCr 2 Si 2 -type structure. <b>2018</b> , 544, 18-21  Possible interface superconductivity in rare-earth-doped CaFe(_{2})As(_{2}) and undoped CaFe(_{2})As(_{2}). <b>2018</b> , 5, 103-109	2
47 <sup>2</sup> 47 <sup>1</sup> 47 <sup>0</sup>	First principles predictions of electronic and elastic properties of BaPb 2 As 2 in the ThCr 2 Si 2 -type structure. 2018, 544, 18-21  Possible interface superconductivity in rare-earth-doped CaFe(_{2})As(_{2}) and undoped CaFe(_{2})As(_{2}). 2018, 5, 103-109  Pressure induced superconductivity in very lightly doped LaFeAsO0.975F0.025. 2018, 536, 827-829  Effect of biaxial cold pressure densification (BCPD) on Ba0.6K0.4Fe2As2 round wire using	1 2 1
47 <sup>2</sup> 47 <sup>1</sup> 47 <sup>0</sup> 469	First principles predictions of electronic and elastic properties of BaPb 2 As 2 in the ThCr 2 Si 2 -type structure. 2018, 544, 18-21  Possible interface superconductivity in rare-earth-doped CaFe(_{2})As(_{2}) and undoped CaFe(_{2})As(_{2}). 2018, 5, 103-109  Pressure induced superconductivity in very lightly doped LaFeAsO0.975F0.025. 2018, 536, 827-829  Effect of biaxial cold pressure densification (BCPD) on Ba0.6K0.4Fe2As2 round wire using optimized precursor. 2018, 44, 4457-4461  Electronic Properties and Fermi Surface for New Layered High-Temperature Superconductors	1 2 1
472 471 470 469 468	First principles predictions of electronic and elastic properties of BaPb 2 As 2 in the ThCr 2 Si 2 -type structure. 2018, 544, 18-21  Possible interface superconductivity in rare-earth-doped CaFe(_{2})As(_{2}) and undoped CaFe(_{2})As(_{2}). 2018, 5, 103-109  Pressure induced superconductivity in very lightly doped LaFeAsO0.975F0.025. 2018, 536, 827-829  Effect of biaxial cold pressure densification (BCPD) on Ba0.6K0.4Fe2As2 round wire using optimized precursor. 2018, 44, 4457-4461  Electronic Properties and Fermi Surface for New Layered High-Temperature Superconductors CaAFe4As4 (A = K, Rb, and Cs): FLAPW-GGA Calculations. 2018, 31, 1683-1692	1 2 1

464	Disappearance of the Itinerant Electronic Ferromagnetism in Layered Compound Sr2VO3CoAs due to Self-Electron-Doping Effect. <b>2018</b> , 87, 094711	1
463	Fabrication and characterization of CaKFe4As4 round wires sintered at high pressure. <b>2018</b> , 11, 123101	18
462	Effect of non-magnetic rare earth substitution for Zr on mixed anion Zr(P, Se)2 superconductors. <b>2018</b> , 1054, 012002	4
461	Physical properties of ThCr2Si2-type Rh-based compounds ARh2Ge2(A = Ca, Sr, Y and Ba): DFT based first-principles investigation. <b>2018</b> , 32, 1850357	3
460	Progress of novel diluted ferromagnetic semiconductors with decoupled spin and charge doping: Counterparts of Fe-based superconductors. <b>2018</b> , 27, 097502	10
459	Magnetism and superconductivity in Eu(Fe1â⊠Nix)As2 (x = 0, 0.04). <b>2018</b> , 61, 1	6
458	A single-crystal neutron diffraction study on magnetic structure of CsCo 2 Se 2. <b>2018</b> , 27, 117401	
457	Superconductivity in LaPd2Bi2 with CaBe2Ge2-type structure. <b>2018</b> , 61, 1	4
456	A Triplet Resonance in Superconducting Fe 1.03 Se 0.4 Te 0.6. <b>2018</b> , 35, 127401	О
455	Superconductivity in a 122-type Fe-based compound (La,Na,K)FeAs. <b>2018</b> , 8, 16827	O
454	Correlation-driven Lifshitz transition in electron-doped iron selenides (Li,Fe)OHFeSe. 2018, 98,	2
453	Multigap Superconductivity in RbCa2Fe4As4F2 Investigated Using BR Measurements. <b>2018</b> , 87, 124705	10
452	Microscopic origin of Cooper pairing in the iron-based superconductor Ba1â⊠KxFe2As2. <b>2018</b> , 3,	10
451	Temperature-dependent local structure and superconductivity of BaPd2As2 and SrPd2As2. <b>2018</b> , 98,	1
450	Eu11Zn4Sn2As12: A Ferromagnetic Zintl Semiconductor with a Layered Structure Featuring Extended Zn4As6 Sheets and Ethane-like Sn2As6 Units. <b>2018</b> , 30, 7067-7076	7
449	Pressure effects on superconductivity and structural parameters of ThFeAsN. <b>2018</b> , 123, 67004	3
448	Single-crystal growth of the iron-based superconductor La0.34Na0.66Fe2As2. <b>2018</b> , 31, 125008	2
447	Odd-frequency pairing in the edge states of superconducting pnictides in the coexistence phase with antiferromagnetism. <b>2018</b> , 98,	2

446	A brief review on BR studies of unconventional Fe- and Cr-based superconductors. 2018, 61, 1	17
445	Sign-reversal superconducting gaps revealed by phase-referenced quasiparticle interference of impurity-induced bound states in (Li1a\( \text{IF}\) Ex)OHFe1a\( \text{JZ}\) TnySe. <b>2018</b> , 98,	10
444	Local structure study of the iron-based systems of BaFe2As2 and LiFeAs by X-ray PDF and XAFS analyses. <b>2018</b> , 555, 45-53	2
443	Neutron diffraction study on magnetic structures and transitions in Sr2Cr3As2O2. <b>2018</b> , 98,	4
442	Universal scaling behavior of the upper critical field in strained FeSe0.7Te0.3 thin films. <b>2018</b> , 20, 093012	3
441	Current-voltage characteristics and vortex dynamics of superconducting Ba0.54K0.46Fe2As2 single crystal. <b>2018</b> , 550, 244-249	
440	Interplay of lattice, electronic, and spin degrees of freedom in detwinned BaFe2As2: A Raman scattering study. <b>2018</b> , 98,	8
439	Superconductivity in Anti-ThCrSi-type ErOBi Induced by Incorporation of Excess Oxygen with CaO Oxidant. <b>2018</b> , 57, 10587-10590	9
438	Pressure-temperature phase diagrams of CaK(Fe1â⊠Nix)4As4 superconductors. <b>2018</b> , 97,	8
437	High transport current superconductivity in powder-in-tube Ba0.6K0.4Fe2As2tapes at 27 T. <b>2018</b> , 31, 015017	40
436	Rapid Sonochemical Synthesis of an Intercalated Superconductor. <b>2018</b> , 3, 5652-5659	1
435	Electronic properties of LaTE2Ge2 (TE = Fe, Co, Ni, Cu and Ru). <b>2018</b> , 280, 13-17	2
434	Magnetic interactions in a proposed diluted magnetic semiconductor (Ba $1 \pm 1 $	4
433	Doping evolution of spin fluctuations and their peculiar suppression at low temperatures in Ca(Fe1âIdCox)2As2. <b>2018</b> , 97,	4
432	Electron spin resonance in the superconducting state of Ba0.6K0.4Fe2As2. <b>2018</b> ,	
431	Temperature dependence of the superconducting energy gaps in CaLa(PtAs)(FeAs) single crystal. <b>2018</b> , 8, 8648	6
430	Vibrational anomalies in AFe2As2 (A=Ca, Sr, and Ba) single crystals. <b>2018</b> , 98,	2
429	Physical properties and potential applications of two-dimensional metallic transition metal dichalcogenides. <b>2018</b> , 376, 1-19	31

428	Fe-Based Superconductors of (LnNa)FeAs (Ln = Ce, Pr). <b>2018</b> , 57, 9223-9229	3
427	Layered Superconductors. <b>2018</b> , 3, 4	
426	The melilite-type compound (Sr1-x,Ax)2MnGe2S6O (A = K, La) being a room temperature ferromagnetic semiconductor. <b>2018</b> , 63, 887-891	3
425	Indication of subdominant d-wave interaction in superconducting CaKFe4As4. 2018, 98,	11
424	Imaging Anomalous Nematic Order and Strain in Optimally Doped BaFe_{2}(As,P)_{2}. <i>Physical Review Letters</i> , <b>2018</b> , 121, 027001	10
423	Doping effects of Cr on the physical properties of BaFe1.9â⊠Ni0.1CrxAs2. <b>2018</b> , 98,	3
422	Structural phase transition, antiferromagnetism and two superconducting domes in LaFeAsO1-xFx (0 2018, 61, 1	5
421	Crystal and Magnetic Structures of the Chain Antiferromagnet CaFeAl. <b>2018</b> , 57, 5820-5829	2
420	Synthesis and structural characterization of Bi2Sr2Ca2(Cu1-XFeX)nO10+[ $(x = 0.01, n=3)$ ). <b>2018</b> ,	
419	Strong Flux Pinning Caused by Phase Distribution Characteristics in (Ba,K)Fe2As2 Films. <b>2018</b> , 28, 1-5	1
418	Peculiar phase diagram with isolated superconducting regions in ThFeAsN O. 2018, 30, 255602	8
417	Phase transition in CaFeAsH: bridging 1111 and 122 iron-based superconductors. <b>2018</b> , 47, 12964-12971	1
416	Dependence of the absolute value of the penetration depth in (Ba1â\(\text{\text{K}}\text{K}\text{x}\)Fe2As2 on doping. <b>2018</b> , 98,	2
415	Tight-binding study of the frequency and temperature dependent spin susceptibility of orbitally ordered iron-based superconductors. <b>2018</b> ,	
414	Effects of vanadium doping on BaFe 2 As 2. <b>2018</b> , 122, 67006	1
413	Superconducting SrSnP with Strong SnâP Antibonding Interaction: Is the Sn Atom Single or Mixed Valent?. <b>2018</b> , 30, 6005-6013	8
412	Investigation of transport properties of FeTe compound. 2018,	
411	Study of the Rare Earth Effects on the Magnetic Fluctuations in RbLn2Fe4As4O2 (Ln (=) Tb, Dy, and Ho) by MBsbauer Spectroscopy. <b>2019</b> , 32, 361-365	

410	Effects of Deposition Temperature on the Structural and Physical Properties of Ba(Fe1.8Co0.2)2As2 Thin Film. <b>2019</b> , 32, 869-875	1
409	Effects of core density and impurities on the critical current density of CaKFe4As4 superconducting tapes. <b>2019</b> , 32, 105014	7
408	Persistent antiferromagnetic order in heavily overdoped Ca La FeAs. <b>2019</b> , 31, 485705	2
407	Quaternary antiferromagnetic Ba2BiFeS5 with isolated FeS4 tetrahedra. <b>2019</b> , 28, 087401	1
406	Direct Microwave Synthesis of 11-Type Fe(Te,Se) Polycrystalline Superconductors with Enhanced Critical Current Density. <b>2019</b> , 36, 017401	1
405	Enhancement of Magnetic and Transport Properties of Superconducting Fe1âMMnxSe0.5Te0.5 Single Crystals. <b>2019</b> , 71, 3285-3292	4
404	Nanoscale interlayer defects in iron arsenides. <b>2019</b> , 277, 422-426	1
403	Advances in new generation diluted magnetic semiconductors with independent spin and charge doping. <b>2019</b> , 40, 081505	4
402	Effects of Swift-Particle Irradiations on Critical Current Density in CaKFe4As4. <b>2019</b> , 1293, 012013	5
401	Fabrication of (Ba,Na)Fe2As2 round wires using HIP process. <b>2019</b> , 1293, 012043	3
400	Effect of non-magnetic rare earth substitution for Zr on mixed anion Zr(P, Se)2 superconductors II. <b>2019</b> , 1293, 012003	Ο
399	Synthesis and Structure of a Nonstoichiometric ZrPtSb Compound. <b>2019</b> , 58, 12017-12024	1
398	Raman scattering study of lattice and magnetic excitations in CrAs. <b>2019</b> , 100,	1
397	Temperature-dependent transport properties of a FeTe compound. <b>2019</b> , 42, 1	2
396	Observation of two collapsed phases in CaRbFe4As4. <b>2019</b> , 100,	2
395	Spiral magnetic ordering of the Eu moments in EuNi2As2. <b>2019</b> , 99,	5
394	In-plane magnetic penetration depth in FeSe1-xSx (x = 0, 0.04, 0.09) and FeTe1-xSex (x = 0.40) single crystals. <b>2019</b> , 92, 195-204	1
393	Material Development and Physical Properties of BiS2-Based Layered Compounds. <b>2019</b> , 88, 041001	46

392	Facile synthesis of size-tunable tin arsenide nanocrystals. <b>2019</b> , 55, 1560-1563	16
391	Anomalous Dome-like Superconductivity in RE(CuNi)AsO (RE La, Pr, Nd). <b>2019</b> , 14, 171-179	3
390	Partial order induced superconductivity in Fe2+ iron. <b>2019</b> , 126, 47001	
389	Enhancement of the critical current density in Cu/Ag composite sheathed (Ba, K)Fe2As2 tapes by pre-annealing process. <b>2019</b> , 6, 096003	5
388	Effect of Co Doping on the Superconducting Properties of Polycrystalline Fe1.01-xCoxTe0.52Se0.48. <b>2019</b> , 32, 3715-3727	1
387	Large critical current density in Cu/Ag composite sheathed (Ba,K)Fe2As2 tapes fabricated under ambient pressure. <b>2019</b> , 32, 065008	1
386	Enhancement of superconducting properties in polycrystalline Fe(Se, Te) via a dual coordination effect. <b>2019</b> , 169, 19-22	4
385	Theoretical investigation of the superconductivity mechanism of Balr2As2. <b>2019</b> , 563, 42-47	O
384	Electrical resistivity under pressure and thermal expansion of LaPt 2 Si 2 single crystal. <b>2019</b> , 125, 143902	3
383	CaFe2Ge2 with square-planar iron layers âlClosing a gap in the row of CaT2Ge2 (T = MnâlIn). <b>2019</b> , 276, 368-375	O
382	Measurements of the superconducting anisotropy in FeSe with a resonance frequency technique. <b>2019</b> , 9, 045220	4
381	Structure-property relationship in layered BaMn2Sb2 and Ba2Mn3Sb2O2. <b>2019</b> , 99,	2
380	Single-Crystal Growth and Extremely High Hc2 of 12442-Type Fe-Based Superconductor KCa2Fe4As4F2. <b>2019</b> , 123, 13925-13929	21
379	Critical Currents of 100-m Class Ag-Sheathed Sr0.6K0.4Fe2As2 Tape Under Various Temperatures, Magnetic Fields, and Angles. <b>2019</b> , 29, 1-5	3
378	The effect of pressure and doping on the critical current density in nickel doped BaFe2As2. <b>2019</b> , 32, 064001	2
377	Effects of different directional rolling on the fabrication of 7-filament Ba1-xKxFe2As2 tapes. <b>2019</b> , 561, 30-34	5
376	Fe-based superconducting thin filmsåßreparation and tuning of superconducting properties. <b>2019</b> , 32, 093001	32
375	Hydrostatic pressure effect on superconductivity and vortex pinning mechanism of Sr(Fe0.88Co0.12)2As2 single crystal. <b>2019</b> , 563, 22-27	2

374	The formation of defects and their influence on inter- and intra-granular current in sintered polycrystalline 122 phase Fe-based superconductors. <b>2019</b> , 32, 084003	10
373	Platelet-shape LiFePO4/Fe2P/C composite material as a high-rate positive electrode for Li-ion batteries. <b>2019</b> , 335, 113-120	4
372	Electronic, transport, and magnetic properties of (Ca, Ba)0.9La0.1Fe1.9Pt0.1As2 compounds. <b>2019</b> , 33, 1950008	1
371	The physical properties of ThCr2Si2- type nickel-based superconductors BaNi2T2 (T = P, As): An ab-initio study. <b>2019</b> , 59, 58-69	5
370	Coexistence of SC and AFM in two-orbital model for s∃-wave iron based superconductors. <b>2019</b> , 295, 16-21	2
369	Large and significantly anisotropic critical current density induced by planar defects in CaKFe4As4 single crystals. <b>2019</b> , 99,	28
368	. <b>2019</b> , 55, 1-30	75
367	Band-selective clean-limit and dirty-limit superconductivity with nodeless gaps in the bilayer iron-based superconductor CsCa2Fe4As4F2. <b>2019</b> , 99,	13
366	The physical properties of ThCr2Si2-type Ru-based compounds SrRu2X2 (X = P, Ge, As): An ab-inito investigation. <b>2019</b> , 562, 48-55	1
365	Accurate determination of the Fermi surface of tetragonal FeS via quantum oscillation measurements and quasiparticle self-consistent GW calculations. <b>2019</b> , 99,	2
364	Spin reorientation of the Fe moments in Eu0.5Ca0.5Fe2As2: Evidence for strong interplay of Eu and Fe magnetism. <b>2019</b> , 99,	2
363	Structural, electronic, and dynamical properties of the tetragonal and collapsed tetragonal phases of KFe2As2. <b>2019</b> , 99,	6
362	Nuclear resonant small-angle scattering for investigation of microstructures in electronic States. <b>2019</b> ,	
361	Local magnetism, magnetic order and spin freezing in the 'nonmetallic metal' FeCrAs. <b>2019</b> , 31, 285803	6
360	Physical properties of ThCr2Si2-type Ni-based compounds SrNi2M2 (M= As and Ge): DFT based Ab-inito calculations. <b>2019</b> , 560, 19-25	1
359	Ferromagnetism in fluoride-antimonide SrF(Zn1-2xMnxCux)Sb with a quasi two dimensional structure. <b>2019</b> , 483, 95-99	4
358	ThCr2Si2 structure type: The âperovskiteâlof intermetallics. <b>2019</b> , 272, 198-209	29
357	Enhanced superconductivity induced by several-unit-cells diffusion in an FeTe/FeSe bilayer heterostructure. <b>2019</b> , 99,	9

356	Theoretical investigation of the coexistence of superconductivity and spin density wave (SDW) in two-band model for the iron-based superconductor BaFe2(As1âNPx)2. <b>2019</b> , 92, 1		3
355	Lifshitz transition in new doped 112 superconductors. <b>2019</b> , 107, 126-136		9
354	Superconductivity in Uncollapsed Tetragonal LaFeAs. <b>2019</b> , 10, 1018-1023		8
353	High critical current density in Cu/Ag composited sheathed Ba0.6K0.4Fe2As2 tapes prepared via hot isostatic pressing. <b>2019</b> , 32, 044007		9
352	19F NMR Study of the Bilayer Iron-Based Superconductor KCa2Fe4As4F2 *. <b>2019</b> , 36, 127401		2
351	Fe-family of superconductors: Influence of Ni dopant on the superconductivity in BaFe2As2 crystal and the relaxation volume. <b>2019</b> , 4, 3069-3076		1
350	Synthesis and physical properties of CeRu2As2 and CeIr2As2. <b>2019</b> , 100,		2
349	Iron-Based Superconductors. <b>2019</b> , 1-20		
348	Effect of Nonlocal Correlations on the Electronic Structure of LiFeAs. <i>Physical Review Letters</i> , <b>2019</b> , 123, 256401	7.4	15
347	Possible enhancement of superconductivity by Sb doping in rare earth doped 112 compounds: an ab-initio study. <b>2019</b> , 1-12		1
346	Thermodynamic Properties of Stoichiometric Non-Superconducting Phase YBaCuO. <b>2019</b> , 12,		1
345	Superconducting and tetragonal-to-orthorhombic transitions in single crystals of FeSe1â⊠Tex (0â⊡k âŪ.61). <b>2019</b> , 100,		15
344	Optical and photoemission investigation of structural and magnetic transitions in the iron-based superconductor Sr0.67Na0.33Fe2As2. <b>2019</b> , 100,		2
343	Phase Transitions and Critical Properties of the Heisenberg Antiferromagnetic Model on a Body-Centered Cubic Lattice with Second Nearest Neighbor Interaction. <b>2019</b> , 129, 903-910		9
342	Computational study on unconventional superconductivity and mechanical properties of novel antiferrromagnetic (Ca,Sr,Ba)Fe2Bi2 compounds. <b>2019</b> , 33, 1950341		2
341	Synthesis of Iron-Based Superconductor Ba0.6K0.4Fe2As2 by Mechanical Alloying. <b>2019</b> , 46, 248-250		2
340	New layered chromium chalcogenides CsLiCrSe, RbLiCrS and CsLiCrS: structures and properties. <b>2019</b> , 48, 17572-17578		4
339	Electronic Structure and Linhard Function of Iron-Based Superconductor La0.5â⊠Na0.5 + xFe2As2. <b>2019</b> , 32, 855-861		O

338	Effects of heat treatment temperature on the superconducting properties of Ba1â⊠ K x Fe2As2 tapes. <b>2019</b> , 32, 025007	5
337	First-principles study of the magnetic and electronic properties of ACr2As2 (A = Sr, Ba). <b>2019</b> , 476, 254-257	2
336	Recent breakthrough development in iron-based superconducting wires for practical applications. <b>2019</b> , 32, 023002	35
335	Effect of pressure on the self-hole-doped superconductor RbGdFeAsO. <b>2019</b> , 31, 044001	1
334	Structural and physical properties of Na-substituted K0.8Fe2-ySe2 single crystal. <b>2019</b> , 777, 1074-1079	
333	Angular Dependence of the Critical Current Density in Two-Band Ginzburg-Landau Theory. <b>2019</b> , 32, 1921-1926	1
332	Direct study of structural phase transformation in single crystalline bulk and thin film BaFeAs. <b>2019</b> , 119, 1-7	2
331	Multigap nodeless superconductivity in CsCa2Fe4As4F2 probed by heat transport. <b>2019</b> , 99,	14
330	Fluctuation conductivity in the presence of magnetic field and nematicity in the ferro-pnictide superconductor BaFe2(As0.68P0.32)2. <b>2019</b> , 288, 74-78	1
329	DFT study of electronic structure properties of SrAFe4As4 (A = Rb and Cs) superconductors. <b>2019</b> , 156, 206-214	2
328	Electronic, Structural, and Magnetic Properties of Hole-Doped Iron-Based Superconductors Using First Principle Study. <b>2020</b> , 33, 921-930	O
327	Isovalent Substitution Effects of Arsenic on Structural and Electrical Properties of Iron-Based Superconductor NdFeAsO0.8F0.2. <b>2020</b> , 33, 387-396	1
326	New materials physics. <b>2020</b> , 83, 016501	19
325	Crystal Growth of Materials with the ThCr2Si2 Structure Type. <b>2020</b> , 55, 1900116	5
324	Distorted FeSe4 unit in ammonium ion intercalated FeSe superconductor. <b>2020</b> , 111, 107605	
323	Intra-layer atomic ordering and semi-conductivity in CsAMS2 (A = Li, Ag; M = Co, Fe). <b>2020</b> , 283, 121134	
322	Phase diagram of the antiferromagnetic Heisenberg model on a bcc lattice with competing first and second neighbor interactions. <b>2020</b> , 545, 123548	12
321	Fabrications and evaluations of critical current density of (Ba,Na)Fe2As2 HIP round wires. <b>2020</b> , 568, 1353580	5

## (2020-2020)

320	Synthesis of electron- and hole-doped bulk BaFe2As2 superconductors by mechanical alloying. <b>2020</b> , 46, 8625-8630	4
319	Optimization of superconducting properties of the stoichiometric CaKFe4As4. <b>2020</b> , 33, 025003	10
318	Magnetic Orders and Electronic Structures of Compressive- and Tensile-Strained KCa2Fe4As4F2 Films. <b>2020</b> , 33, 1377-1383	1
317	Crystal Growth and Investigation of High-Pressure Physical Properties of Fe2As. <b>2020</b> , 10, 790	
316	Effects of Point Defects Introduced by Co-doping and Proton Irradiation in CaKFe4As4. <b>2020</b> , 1590, 012014	3
315	Thermodynamic anisotropy in the samarium-based pnictide single-crystal superconductor. <b>2020</b> , 126, 1	
314	Anisotropic optical properties of detwinned BaFe2As2. <b>2020</b> , 102,	2
313	Effect of oxygen contamination on densification of Fe(Se,Te). <b>2020</b> , 1559, 012051	1
312	Effect of annealing on structure and superconducting properties in Fe(Se,Te). 2020, 1559, 012053	
311	Mgsbauer study of Ba2Ti2Fe2As4O. <b>2020</b> , 848, 155706	1
310	Mssbauer study of Ba2Ti2Fe2As4O. <b>2020</b> , 848, 155706  A New Quasi-One-Dimensional Ternary Molybdenum Pnictide Rb2Mo3As3 with Superconducting Transition at 10.5K. <b>2020</b> , 37, 097401	3
	A New Quasi-One-Dimensional Ternary Molybdenum Pnictide Rb2Mo3As3 with Superconducting	
310	A New Quasi-One-Dimensional Ternary Molybdenum Pnictide Rb2Mo3As3 with Superconducting Transition at 10.5K. <b>2020</b> , 37, 097401  Isotropic s-wave superconductivity in the noncentrosymmetric charge density wave	3
310	A New Quasi-One-Dimensional Ternary Molybdenum Pnictide Rb2Mo3As3 with Superconducting Transition at 10.5K. 2020, 37, 097401  Isotropic s-wave superconductivity in the noncentrosymmetric charge density wave superconductor SrPt2As2. 2020, 102,  The effects of charge-doping and structural-parameter variations on magnetic behavior of	3
310 309 308	A New Quasi-One-Dimensional Ternary Molybdenum Pnictide Rb2Mo3As3 with Superconducting Transition at 10.5K. 2020, 37, 097401  Isotropic s-wave superconductivity in the noncentrosymmetric charge density wave superconductor SrPt2As2. 2020, 102,  The effects of charge-doping and structural-parameter variations on magnetic behavior of BaFe2As2 compound. 2020, 10, 219-224	3
310 309 308 307	A New Quasi-One-Dimensional Ternary Molybdenum Pnictide Rb2Mo3As3 with Superconducting Transition at 10.5K. 2020, 37, 097401  Isotropic s-wave superconductivity in the noncentrosymmetric charge density wave superconductor SrPt2As2. 2020, 102,  The effects of charge-doping and structural-parameter variations on magnetic behavior of BaFe2As2 compound. 2020, 10, 219-224  Electronic and Magnetic Anisotropies in FeSe Family of Iron-Based Superconductors. 2020, 8,  Hydrostatic and Uniaxial Pressure Tuning of Iron-Based Superconductors: Insights into	2
310 309 308 307 306	A New Quasi-One-Dimensional Ternary Molybdenum Pnictide Rb2Mo3As3 with Superconducting Transition at 10.5K. 2020, 37, 097401  Isotropic s-wave superconductivity in the noncentrosymmetric charge density wave superconductor SrPt2As2. 2020, 102,  The effects of charge-doping and structural-parameter variations on magnetic behavior of BaFe2As2 compound. 2020, 10, 219-224  Electronic and Magnetic Anisotropies in FeSe Family of Iron-Based Superconductors. 2020, 8,  Hydrostatic and Uniaxial Pressure Tuning of Iron-Based Superconductors: Insights into Superconductivity, Magnetism, Nematicity, and Collapsed Tetragonal Transitions. 2020, 532, 2000248  Time-Resolved Study of Pseudogap and Superconducting Quasiparticle Dynamics in	3 2 1

302	Electronic and Magnetic Properties of Cation Ordered SrMnCrAsO. 2020, 59, 7553-7560	1
301	AFeSe2 (A=Tl, K, Rb, or Cs): Iron-based superconducting analog of the cuprates. <b>2020</b> , 101,	1
300	Mechanochemically assisted low temperature synthesis route of the 1144 Ca-K Iron Based Superconductor. <b>2020</b> , 33, 074003	6
299	NMR and NQR studies on transition-metal arsenide superconductors LaRu2As2, KCa2Fe4As4F2, and A 2Cr3As3. <b>2020</b> , 29, 067402	5
298	Fluctuations and pairing in Fe-based superconductors: light scattering experiments. <b>2020</b> , 32, 413001	2
297	High-temperature Majorana fermions in magnet-superconductor hybrid systems. <b>2020</b> , 101,	4
296	Influence of pressure on the transport, magnetic, and structural properties of superconducting CrNbSe single crystal <b>2020</b> , 10, 13112-13125	1
295	Magnetic states and electronic properties of Sr4V2O6Fe2As2 studied by DFT calculations. <b>2020</b> , 179, 109676	
294	Low temperature specific heat of 12442-type KCa2Fe4As4F2 single crystals. <b>2020</b> , 63, 1	9
293	Enhancement of critical current density in helium ion irradiated Ba(Fe, Co)2As2 thin films. <b>2020</b> , 33, 075012	1
292	Single crystal growth and effects of Ni doping on the novel 12442-type iron-based superconductor RbCa2Fe4As4F2. <b>2020</b> , 22, 073007	5
291	Band energies in two-band model for Fe based superconductors in the coexistence state. <b>2020</b> , 798, 012001	
<b>2</b> 90	Evolution of superconductivity and antiferromagnetic order in Ba(Fe0.92â⊠Co0.08Vx)2As2. <b>2020</b> , 101,	O
289	Preface to the special issue âflocus on 10 Years of Iron-Based Superconductorsâ[ <b>2020</b> , 33, 090301	1
288	Electron correlation induced orbital selective Lifshitz transition in new hybrid 12442 iron based superconductors. <b>2020</b> , 183, 109802	4
287	Antiferromagnetic Kondo lattice compound Ce2O2Bi with anti-ThCr2Si2-type structure. <b>2020</b> , 836, 155229	1
286	Magnetic fluctuation and suppression in high-temperature superconductor Ba(Fe1-xCox)2As2. <b>2020</b> , 575, 1353703	
285	The effect of the sintering process on Agâādded FeSe0.94 superconducting wire. <b>2020</b> , 33, 095006	1

## (2020-2020)

284	Superconductivity-induced transverse plasma mode and phonon anomaly in the c-axis response of the bilayer compound RbCa2Fe4As4F2. <b>2020</b> , 101,	2
283	Structural and physical properties of the new layered transition metal material Na4Cu3TaAs4. <b>2020</b> , 63, 816-822	
282	Heavily Hydride-ion-doped 1111-type Iron-based Superconductors: Synthesis, Physical Properties and Electronic Structure. <b>2020</b> , 89, 051006	6
281	Synthesis routes to eliminate oxide impurity segregation and their influence on intergrain connectivity in K-doped BaFe2As2 polycrystalline bulks. <b>2020</b> , 33, 084010	5
280	Muon spin rotation and infrared spectroscopy study of Ba1â⊠NaxFe2As2. <b>2020</b> , 101,	1
279	Physical Properties of [A 6Cl][Fe24Se26](A = K, Rb) with Self-Similar Structure. <b>2020</b> , 37, 017401	
278	Escape rate in Josephson junctions between single-band and two-band superconductors. <b>2020</b> , 574, 1353647	1
277	Ferromagnetic cluster-glass phase in Ca(Co1âᢂrx)2âŊAs2 crystals. <b>2020</b> , 102,	2
276	Superconductivity of KFe2As2 Under Pressure: Ab Initio Study of Tetragonal and Collapsed Tetragonal Phases. <b>2020</b> , 33, 2347-2354	1
275	Doping dependence and high-pressure studies on Eu x Ca1 âß Fe2As2 (0 â⅓ â⅓). <b>2020</b> , 33, 095010	O
274	Upper Critical Field of a Two-Band SrFe2 âlkNixAs2 Superconductor. <b>2020</b> , 111, 403-407	2
273	Iron-based superconductors: tales from the nuclei. <b>2020</b> , 43, 1-43	1
272	Anisotropy of the transport properties of NdFeAs(O,F) thin films grown on vicinal substrates. <b>2020</b> , 33, 044016	1
271	Magnetic and superconducting anisotropy in Ni-doped RbEuFe4As4 single crystals. <b>2020</b> , 101,	3
270	Single crystal growth and physical property characterization of ternary phosphide chalcogenide ZrP1.49Se0.51. <b>2020</b> , 141, 109423	1
269	Phase transitions and superconductivity of iron-based superconductors from first-principles. <b>2020</b> , 384, 126345	2
268	Synthesis, Crystal and Electronic Structure of Layered AMSb Compounds (A = Rb, Cs; M = Zn, Cd). <b>2020</b> , 646, 1079-1085	4
267	Centrosymmetric LaRh2Ga2. <b>2020</b> , 235, 41-46	1

266	Strong Pauli paramagnetic effect in the upper critical field of KCa2Fe4As4F2. <b>2020</b> , 63,	12
265	First-principles study of electron-phonon coupling and magnetoresistance of LaBi under pressure. <b>2020</b> , 101,	1
264	Iron based chalcogenide and pnictide superconductors: From discovery to chemical ways forward. <b>2020</b> , 59, 100282	O
263	High-critical-current-ratio superconducting joint between Ba0.6K0.4Fe2As2 tapes fabricated by angle-polishing method. <b>2020</b> , 33, 084011	2
262	Enhancement of critical current density in (Ba,Na)Fe2As2 round wires using high-pressure sintering. <b>2020</b> , 33, 065001	8
261	Ab-initio study of the electronic structure and magnetic properties of ACr2Pn2 (A =Ba, Sr, Ca, Sc, K; Pn=As, P). <b>2021</b> , 150, 109850	O
260	High pressure phase of Ba2FeS3: An antiferromagnet with one-dimensional spin chains. <b>2021</b> , 859, 157839	6
259	1144 Fe based superconductors: natural example of orbital selective self-doping and chemical pressure induced Lifshitz transition. <b>2021</b> , 186, 109991	4
258	Physical properties and phase diagram of NaFe1â⊠ V x As. <b>2021</b> , 30, 017401	
257	Realization of epitaxial thin films of the superconductor K-doped BaFe2As2. <b>2021</b> , 5,	1
256	The effect of the Ag addition on FeSe superconducting wire by the ex-situ PIT method. <b>2021</b> , 32, 2887-2894	
255	Eisengruppe: Elemente der achten Nebengruppe. <b>2021</b> , 663-702	
254	Distinct evolution of charge occupations on Fe 3d orbitals in hole-doped iron arsenic superconductors. <b>2021</b> , 133, 17004	0
253	Iron-Based Practical Superconductors. <b>2021</b> , 313-353	
252	Internal and External Pressure Effects on Superconductivity in FeTexSe1-x (x = 0.46, 0.54) Single Crystals. <b>2021</b> , 34, 725-731	0
251	Pressure tuning of the iron-based superconductor (Ca0.73La0.27)FeAs2. <b>2021</b> , 103,	O
250	High-Temperature Cuprate Superconductors and Later Discoveries. <b>2021</b> , 73-121	
249	NMR of Magnetic Materials: Determination of Magnetic Structures by â�n-Siteâ[NMR Measurements. <b>2021</b> ,	

248	LaO as a candidate substrate for realizing superconductivity in an FeSe epitaxial film. 2021, 103,	1
247	Quantum Mechanical Calculations of High-T<sub>c</sub> Fe-Superconductors. <b>2021</b> , 11, 84-98	Ο
246	A Theoretical Investigation on the Physical Properties of SrPd2Sb2 Superconductor. <b>2021</b> , 34, 1133-1139	6
245	Effect of heat treatments on superconducting properties and connectivity in K-doped BaFeAs. <b>2021</b> , 11, 3143	1
244	Elucidating the origin of planar defects that enhance critical current density in CaKFe4As4 single crystals. <b>2021</b> , 34, 034003	5
243	Chemistry in Superconductors. <b>2021</b> , 121, 2966-2991	7
242	Electrochemical Synthesis and Crystal Structure of the Organic Ion Intercalated Superconductor (TMA)FeSe with = 43 K. <b>2021</b> , 143, 3043-3048	9
241	Breakdown of Hund's rule for CuFeAs. <b>2021</b> , 103,	
240	Large negative magnetoresistance in the antiferromagnet BaMn2Bi2. <b>2021</b> , 103,	0
239	Visualization of the grain structure in high-performance Ba1â⊠ K x Fe2As2 superconducting tapes. <b>2021</b> , 34, 045017	2
238	Inhomogeneous superconductivity in LuxZr1â\(\mathbb{B}\)12 dodecaborides with dynamic charge stripes. <b>2021</b> , 103,	2
237	Interfacial Superconductivity Achieved in Parent AEFeAs (AE = Ca, Sr, Ba) by a Simple and Realistic Annealing Route. <b>2021</b> , 21, 2191-2198	1
236	Frustration effect on escape rate in Josephson junctions between single-band and three-band superconductors in the macroscopic quantum tunneling regime. <b>2021</b> , 47, 282-286	О
235	Drastic improvement of Curie temperature by chemical pressure in N-type diluted magnetic semiconductor Ba(Zn,Co)[Formula: see text]As[Formula: see text]. <b>2021</b> , 11, 7652	3
234	Superconductivity in Co-Layered LaCoSi. <b>2021</b> , 60, 6157-6161	3
233	Angle-resolved photoemission studies of quantum materials. <b>2021</b> , 93,	45
232	High-pressure synthesis, crystal structure, and properties of iron-based spin-chain compound Ba9Fe3Se15. <b>2021</b> , 5,	1
231	Development of the iron-based superconducting coils for high magnetic field application. <b>2021</b> , 584, 1353855	1

230	Two-orbital model for interference of pseudo-gaps in the superconducting state of iron-based superconductors. <b>2021</b> , 330, 114273	O
229	WITHDRAWN: Complete phase diagram of FeSe1âß (0 âß âြ) single crystals via hydrothermal method. <b>2021</b> , 110175	
228	The Physical Properties of ThCr2Si2- Type Co-based Compound SrCo2Si2: An ab-initio Study. <b>2021</b> , 50-59	
227	High-performance Ba1â⊠KxFe2As2 superconducting tapes with grain texture engineered via a scalable fabrication. <b>2021</b> , 64, 2530-2540	8
226	Inverse magnetic hysteresis of the Josephson supercurrent: Study of the magnetic properties of thin niobium/permalloy (Fe20Ni80) interfaces. <b>2021</b> , 103,	2
225	Reentrant metal-insulator transition and competing magnetic interactions on a triangular lattice with second nearest-neighbor hopping. <b>2021</b> , 103,	
224	Sensitivity of As K-edge absorption to rare earth (RE) doping in Ca1â⊠RExFeAs2: A first principles study. <b>2021</b> , 153, 109993	8
223	Enhancing Transport Performance in 7-filamentary Ba0.6K0.4Fe2As2 Wires and Tapes via Hot Isostatic Pressing. <b>2021</b> , 585, 1353870	4
222	Charge-doping-induced variation of the superconducting BaFe2As2 electronic structure and the emerging physical effects: a DFT+DMFT study. <b>2021</b> , 56, 14157-14169	O
221	Intertwined charge, spin, and pairing orders in doped iron ladders. <b>2021</b> , 103,	O
220	Numerical and Experimental Analysis of Quench Behaviors in Iron-Based Sr/Ba122 Superconducting Tape at Liquid Helium Temperature. <b>2021</b> , 34, 2011-2016	
219	Disappearance and Survival of Superconductivity in FeSe under High Pressure. <b>2021</b> , 90, 073706	1
218	Ternary ACd4P3 (A = Na, K) Nanostructures via a Hydride Solution-Phase Route.	О
217	Correlation of Tunable CoSi Tetrahedron with the Superconducting Properties of LaCoSi. <b>2021</b> , 60, 10880-1	088 <u>4</u>
216	Block-layer model for intergrowth structures. <b>2021</b> , 14, 3629-3635	1
215	Pressure-induced structural and electronic transitions in InTel. <b>2021</b> , 104,	Ο
214	HHG-laser-based time- and angle-resolved photoemission spectroscopy of quantum materials. <b>2021</b> , 251, 147105	1
213	Characterization of Spatial Distribution of Local Critical Current Density in a Co-Doped BaFe2As2 Film Based on Magnetic Microscopy. <b>2021</b> , 31, 1-4	O

212 Intrinsic defects and local charge ordering of single-crystal FeTe. **2021**, 79, 552-556

211	Evolution of Superconducting Properties in FeSeTe Films Before and After Structure Avalanche. <b>2021</b> , 13, 42138-42145	O
<b>21</b> 0	Fabrication of small superconducting coils using (Ba,A)Fe2As2 (A: Na, K) round wires with large critical current densities. <b>2021</b> , 34, 105008	3
209	Structural modulation and physical properties of cobalt-doped layered La2 M 5As3O2 (M = Cu, Ni) compounds*. <b>2021</b> , 30, 076106	
208	Electronic Structure and Superconductivity of Compressed Metal Tetrahydrides. <b>2021</b> , 27, 14858-14870	3
207	Suppression of antiferromagnetic order and strong ferromagnetic spin fluctuations in Ca(Co1â�Nix)2â�As2 single crystals. <b>2021</b> , 104,	
206	Critical Current Density and Vortex Dynamics in Pristine and Irradiated KCaFeAsF. 2021, 14,	1
205	First-principles calculations of structural, electronic, magnetic, thermoelectric, and thermodynamic properties of BaMn2P2 in the Anti and ferromagnetic phase. <b>2021</b> , 302, 122388	3
204	Critical behavior of ferromagnetic transition in La0.85Co1.68As2 crystal. 2022, 541, 168517	
203	Observation of two-dimensional superconductivity in an ultrathin ironâ⊞rsenic superconductor. <b>2021</b> , 8, 025024	O
202	Angle-Resolved Photoemission Spectroscopy Studies on the Electronic Structure and Superconductivity Mechanism for High Temperature Superconductors. <b>2021</b> , 0-0	1
201	Introduction to Fe-Based Superconductors. <b>2021</b> , 1-25	
200	High-Resolution Inelastic X-Ray Scattering I: Context, Spectrometers, Samples, and Superconductors. <b>2015</b> , 1-68	5
199	Itinerant Electron Scenario. <b>2015</b> , 255-329	9
198	Point-Contact Spectroscopy of Multigap Superconductors. <b>2010</b> , 187-210	1
197	Current status of iron-based superconductors. <b>2012</b> , 703-711	1
196	Optical properties of Ba0.6K0.4Fe2As2 thin film prepared by pulsed laser deposition and subsequent post-annealing process. <b>2017</b> , 17, 976-979	2
195	Anomalous transverse resistance in 122-type iron-based superconductors. <b>2019</b> , 9, 664	2

194	Transport critical currents in the iron pnictide superconducting wires prepared by theex situPIT method. <b>2010</b> , 23, 055009	51
193	Short-range ferromagnetic order due to Ir substitutions in single-crystallineBa(CoIr)As(0 âlk âld.25). <b>2020</b> ,	O
192	Ion irradiation of iron chalcogenide superconducting films. <b>2020</b> , 33, 094008	1
191	Strong flux pinning and anomalous anisotropy of Sr0.6K0.4Fe2As2 superconducting tapes. <b>2020</b> , 33, 125001	3
190	Pressure dependent elastic, electronic, superconducting, and optical properties of ternary barium phosphides (BaM 2P2; M = Ni, Rh): DFT based insights. <b>2020</b> , 95, 105809	9
189	Eliashberg theory for spin fluctuation mediated superconductivity: Application to bulk and monolayer FeSe. <b>2020</b> , 102,	12
188	Effects of disorder on the intrinsically hole-doped iron-based superconductor KCa2Fe4As4F2 by cobalt substitution. <b>2017</b> , 96,	17
187	Optimization of the crystal growth of the superconductor CaKFe4As4 from solution in the FeAsâtaFe2As2âtFe2As2 system. <b>2017</b> , 1,	49
186	Filling the holes in the CaFe4As3 structure: Synthesis and magnetism of CaCo5As3. 2017, 1,	1
185	Prediction of a new class of half-metallic ferromagnets from first principles. <b>2017</b> , 1,	7
184	Superconductivity at 33âB7 K in ALn2Fe4As4O2 (A=Kand Cs;Ln=lanthanides). <b>2017</b> , 1,	23
183	Superconductivity in the ternary compound SrPt10P4 with complex new structure. <b>2017</b> , 1,	4
182	Ultrahigh critical current densities, the vortex phase diagram, and the effect of granularity of the stoichiometric high-Tc superconductor CaKFe4As4. <b>2018</b> , 2,	39
181	Ambipolar suppression of superconductivity by ionic gating in optimally doped BaFe2(As,P)2 ultrathin films. <b>2019</b> , 3,	9
180	Electronic structures of quasi-one-dimensional cuprate superconductors Ba2CuO3+[12019, 3,	9
179	Anisotropic physical properties and large critical current density in KCa2Fe4As4F2 single crystal. <b>2020</b> , 4,	7
178	Pairing symmetry and topological surface state in iron-chalcogenide superconductors. <b>2020</b> , 2,	6
177	Structure-mining: screening structure models by automated fitting to the atomic pair distribution function over large numbers of models. <b>2020</b> , 76, 395-409	9

176	Effect ofLn-Site Disorder onTcof Oxypnictide SuperconductorLnFeAsO1-xFx(Ln=Nd, Ceâldd, and LaâlDy). <b>2009</b> , 78, 073701	6
175	The magnetic phase diagram of Ca 1â⊠ Sr x Co 2 As 2 single crystals. <b>2013,</b> 104, 67005	9
174	Fabrication and Properties of PIT Processed Iron-Based Ba-122 Superconducting Tapes Using Double Sheath of Stainless Steel and Ag-Sn Alloy. <b>2019</b> , 83, 346-351	2
173	Simple Chemical Synthesis of Ternary Intermetallic RENi2Si2 (RE = Y, La) Nanoparticles in Molten LiClâtaH2 System. <b>2020</b> , 61, 1037-1040	9
172	New high-temperature superconductors based on rare earth and transition metal oxyarsenides and related phases: synthesis, properties and simulation. <b>2008</b> , 178, 1273	23
171	FeAs systems: a new class of high-temperature superconductors. <b>2008</b> , 178, 1307	24
170	Chemically degraded grain boundaries in fine-grain Ba0.6K0.4Fe2As2 polycrystalline bulks. <b>2020</b> , 13, 113002	4
169	On the s <sup>±</sup> -Wave Superconductivity in the Iron-Based Superconductors:  A Perspective Based on a Detailed Study of  Ba <sub>0.6</sub> K <sub>0.4</sub> Fe <sub>2</sub> As <sub>2</sub> 222<	2 gt;
168	Single crystal growth and physical property study of 1111-type Fe-based superconducting system CaFeAsF. <b>2018</b> , 67, 177401	2
167	Frontiers of Research on Iron-Based Superconductors toward Their Application. <b>2012</b> , 51, 010005	47
166	Evolution of Tetragonal Phase in the FeSe Wire Fabricated by a Novel Chemical-Transformation Powder-in-Tube Process. <b>2012</b> , 51, 010101	14
165	Existence of a vortex-glass phase transition in an optimally doped BaFe1.8Co0.2As2single crystal. <b>2013</b> , 15, 16-19	2
164	Anisotropic superconductivity of high quality FeSe1-xSingle crystal. <b>2014</b> , 16, 26-30	2
163	Upper critical field and superconducting anisotropy of BaFe2-xRuxAs2(x=0.48 and 0.75) single crystals. <b>2014</b> , 16, 31-35	1
162	Investigation of Structural, Electronics, Optical, Mechanical and Thermodynamic Properties of YRu2P2 Compound for Superconducting Application. <b>2021</b> , 34, 3089	2
161	Robust superconductivity against water corrosion in Ba1â¼ K x Fe2As2 bulks. <b>2021</b> , 34, 125008	
160	Competitive and cooperative electronic states in Ba(Fe1 $\hat{a}$ MTx)2As2 with T = Co, Ni, Cr. <b>2021</b> , 6,	2
159	The structural evolution and superconductivity under pressure for superconductor AFe 2 As 2 (A = Ba, Sr).	

158	Search for New High-Tc Superconductors at Elevated Temperatures. 1	
157	Self-regulated growth of candidate topological superconducting parkerite by molecular beam epitaxy. <b>2021</b> , 9, 101110	O
156	NMR Study of Iron-Based Superconductor under High Pressure. <b>2009</b> , 19, 129-137	
155	High-Pressure Synthesis of New Fe-based Superconductors. <b>2009</b> , 19, 106-112	
154	Nanoscale Structures and Pseudogap in Under-doped High-Tc Superconductors. <b>2010</b> , 211-229	
153	Electronic structures cobalt group pnictides: BaT2P2 and BaT2As2 (T=Co, Rh, Ir). <b>2011</b> , 60, 067101	
152	Superconductivity and spin fluctuations. <b>2011</b> , 6, 429-439	4
151	Influence of Structure on Superconductivity in Iron-Based Superconductors by Doping or under Pressure. <b>2012</b> , 01, 1-6	
150	Iron-Based Superconductors. <b>2012</b> , 1-52	
149	Quantum Oscillations in Iron Pnictide Superconductors. <b>2012</b> , 125-159	1
148	Angle-Resolved Photoemission Spectroscopy of Iron Pnictides. <b>2012</b> , 89-124	
148	Angle-Resolved Photoemission Spectroscopy of Iron Pnictides. <b>2012</b> , 89-124  Material Specific Model Hamiltonians and Analysis on the Pairing Mechanism. <b>2012</b> , 357-430	
·		
147	Material Specific Model Hamiltonians and Analysis on the Pairing Mechanism. <b>2012</b> , 357-430	
147	Material Specific Model Hamiltonians and Analysis on the Pairing Mechanism. <b>2012</b> , 357-430  Magnetism in Parent Compounds of Iron-Based Superconductors. <b>2012</b> , 473-512	
147 146 145	Material Specific Model Hamiltonians and Analysis on the Pairing Mechanism. 2012, 357-430  Magnetism in Parent Compounds of Iron-Based Superconductors. 2012, 473-512  Optical Investigation on Iron-Based Superconductors. 2012, 161-241	1
147 146 145	Material Specific Model Hamiltonians and Analysis on the Pairing Mechanism. 2012, 357-430  Magnetism in Parent Compounds of Iron-Based Superconductors. 2012, 473-512  Optical Investigation on Iron-Based Superconductors. 2012, 161-241  Antiferromagnetic Spin Fluctuations in the Fe-Based Superconductors. 2012, 243-274  Synthesis and Physical Properties of the New Potassium Iron Selenide Superconductor	1

140	Magnetic and transport properties or single crystals of Fe-based superconductors of 122 ramily.  2014, 184, 897-902	Ο
139	Magnetic Order and Dynamics: Neutron Scattering. <b>2015</b> , 151-186	
138	Optical and Transport Properties. <b>2015</b> , 187-219	
137	Introduction: Discovery and Current Status. <b>2015</b> , 3-19	
136	First-Principles Studies in Fe-Based Superconductors. <b>2015</b> , 223-253	
135	Magnetic neutron scattering studies on the Fe-based superconductor system Fe1+yTe1-xSex. <b>2015</b> , 64, 097503	1
134	Coexistence of Spin Density Wave (SDW) and Superconductivity in Ba<sub>1-x</sub>K<sub>x</sub>Fe<sub>2</sub>As<sub>2</sub>. <b>2015</b> , 05, 319-331	
133	Investigation on the flux pinning force and flux pinning mechanism in Ba1-xKxFe2As2 single crystal with Tc = $38.5$ K. <b>2015</b> , 64, 117401	
132	Introduction. <b>2016</b> , 1-20	
131	Mulliken Occupation as the Indicator of Transition to Superconducting State in SrFe2As2and BaFe2As2. <b>2016</b> , 130, 655-658	
130	Te Katk⊞s⊞n⊞n FeSe-11 Bile¶klerine Etkisi, ¶etimi ve Karakterizasyonu. <b>2016</b> , 31, 175-180	
129	Iron-Based Superconductors. <b>2017</b> , 9-27	
128	Superconductivities of pressurized iron pnictide superconductors. 2017, 66, 037402	3
127	Introduction. <b>2017</b> , 1-12	
126	Iron Based Supercondutors: Introduction to the Volume. <b>2017</b> , 1-6	
125	Hybridization Effect in BaFe2(As1â⊠Px)2Observed by Hard X-ray Photoemission Spectroscopy. <b>2017</b> , 86, 053702	1
124	Infrared spectroscopy study of ironbased superconductor Li0.8Fe0.2 ODFeSe. <b>2018</b> , 67, 207102	
123	Angle-resolved photoemission studies on iron based high temperature superconductors. <b>2018</b> , 67, 207413	2

122	Self-doped iron-based superconductors with intergrowth structures. <b>2018</b> , 67, 207406	2
121	Uniaxial Stress Technique. <b>2018</b> , 13-48	
120	Recent progress of 122-type iron-based superconducting wires and tapes. <b>2018</b> , 67, 207402	
119	Antiferromagnetic order and spin dynamics in iron-based superconductors. <b>2018</b> , 67, 207407	1
118	Research progress about 111-typed iron based superconductor. <b>2018</b> , 67, 207414	
117	Imaging the magnetic states in an actinide ferromagnet UMn2Ge2. <b>2018</b> , 2,	1
116	Eisengruppe: Elemente der achten Nebengruppe. <b>2019</b> , 1-40	
115	High-Resolution Inelastic X-Ray Scattering I: Context, Spectrometers, Samples, and Superconductors. <b>2019</b> , 1-82	O
114	BaRu2As2 Malzemesinin Fiziksel ⊠elliklerinin Yoūnluk Fonksiyonel Teorisi Kullan⊟larak Bcelenmesi.	
113	Co Doping and High Pressure Studies of the Iron Arsenide La0.4Na0.6Fe2As2. <b>2020</b> , 89, 055001	О
112	Physical properties and magnetic structure of a layered antiferromagnet PrPd0.82Bi2. <b>2020</b> , 29, 067502	
111	Effects of Splayed Columnar Defects on Critical Current Density in CaKFe4As4. <b>2020</b> , 1590, 012015	O
110	High-Resolution Inelastic X-Ray Scattering I: Context, Spectrometers, Samples, and Superconductors. <b>2020</b> , 2131-2212	
109	First-order transition in trigonal structure CaMn2P2. <b>2020</b> , 132, 46001	O
108	Synthesis and Magnetic Properties in Quaternary Ca1-xPrxCo2As2 Single Crystals. 2020,	1
107	Pd-P antibonding interactions in APd2P2 (A=Ca and Sr) superconductors. <b>2020</b> , 4,	1
106	Multipole Fluctuation of Iron Pnictide Superconductor Ba(Fe1â⊠Cox)2As2. <b>2020</b> ,	
105	Superconducting properties of 1144-type iron-based superconductors by mechanochemically assisted synthesis. 1	1

104	Pressure Dependence of Superconducting Properties, Pinning Mechanism, and Crystal Structure of the FeMnSeTe Superconductor. <b>2021</b> , 6, 30419-30431	
103	Critical Current and Pinning Features of a CaKFeAs Polycrystalline Sample. <b>2021</b> , 14,	O
102	Surface morphology and electronic structure in stoichiometric superconductor CaKFe4As4 probed by scanning tunneling microscopy/spectroscopy. <b>2021</b> , 64, 1	О
101	First Principles of the Classical Mechanics and the Foundations of Statistical Mechanics on the Example of a Disordered Spin System. <b>2020</b> , 55, 265-274	2
100	Zintl chemistry: Current status and future perspectives. <b>2021</b> , 133841	2
99	Rotational symmetry breaking at the incommensurate charge-density-wave transition in Ba(Ni,Co)2(As,P)2: Possible nematic phase induced by charge/orbital fluctuations. <b>2021</b> , 104,	1
98	Transverse distribution of critical current density in Ag-sheathed Ba1âlk K x Fe2As2 tapes. <b>2022</b> , 35, 015004	О
97	High-performance Ba1â $\mbox{M}$ K x Fe2As2 superconducting joints for persistent current operation. <b>2022</b> , 35, 03LT01	O
96	Mechanical properties and densification mechanism of powder-in-tube BaxK1-xFe2As2 superconductors.	1
95	Electronic structure and structural stability of (Ba0.75Ae0.25)Fe2As2 (Ae = Li, Na, Rb). <b>2022</b> , 593, 1354013	
94	Evidence of strong correlation and magnetotransport scaling in YbFe2As2. 2022, 630, 413696	
93	Probing the current-phase relation in Josephson point-contact junctions between [Formula: see text]In[Formula: see text] and [Formula: see text]K[Formula: see text](FeAs)[Formula: see text] superconductors <b>2021</b> , 11, 23986	O
92	Theoretical studies of high-Tc Fe-superconductors based on BaFe2As2 in presence of dopants Rh and Pd. <b>2022</b> , 54, 95-100	
91	Evolution of Bonding and Magnetism Changes in Valence Electron Count in CuFeCoGe 2022,	
90	In Situ Visualization of Local Distortions in the High- Molecule-Intercalated Li(CHN)FeSe Superconductor <b>2022</b> ,	О
89	Mixed-state Hall scaling behavior and vortex phase diagram in FeSe0.7Te0.3 thin films. <b>2022</b> , 105,	O
88	Effects of precursor powder particle size on the powder-in-tube Ba1â⊠KxFe2As2 superconducting tapes. <b>2022</b> , 35, 055008	1
87	High-Pressure Studies of Correlated Electron Systems. 2100623	О

86	Local Atomic Configuration Control of Superconductivity in the Undoped Pnictide Parent Compound BaFe2As2.	O
85	Electrical Resistivity and Magnetization Study on LaFe2As2, La0.8Ba0.2Fe2As2, and La1-xBaxPt0.1Fe1.9As2 ( $x = 0, 0.05, 0.2, 0.4, and 0.6$ ) Superconducting Compounds. <b>2022</b> , 51, 2624-2644	
84	Enhanced Nernst effect above Tc in the quasi-two-dimensional iron pnictide superconductor CsCa2Fe4As4. <b>2022</b> , 105,	О
83	Influences of Pb Substitution on Microstructure, Electrical Transport, and Mechanical Properties of Single-Crystal FeTe0.5Se0.5 Superconductors. 1	O
82	Investigation of the flux dynamics in KCa2Fe4As4F2 single crystal by ac susceptibility measurements. <b>2022</b> , 35, 055013	О
81	Enhanced critical current density in K-doped Ba122 polycrystalline bulk superconductors via fast densification <b>2022</b> , 25, 103992	O
80	Transport and magnetic properties in polycrystalline Ba(Mn1â\(\mathbb{Q}\)Crx). <b>2022</b> , 413880	
79	Progress of ultra-high-field superconducting magnets in China. <b>2022</b> , 35, 023001	1
78	Weakness of Correlation Effect Manifestation in BaNi2As2: An ARPES and LDA + DMFT Study. <b>2021</b> , 125, 28075-28087	O
77	Bulk and Single Crystal Growth Progress of Iron-Based Superconductors (FBS): 1111 and 1144. <b>2022</b> , 12, 20	1
76	First-principles study of the electronic structure of CaKRu4P4. <b>2021</b> , 104,	
75	Dynamic crossover across the peak effect in Ba1-xKxFe2As2 superconductor for H $ $ c-axis and H $ $ ab-plane.	
74	Tailoring the critical temperature of Ca/K-1144 superconductors: the effect of aliovalent substitution on tetragonality.	2
73	Physical properties and electronic structure of single-crystal KCo2As2. <b>2022</b> , 6,	О
<del>7</del> 2	Antiferromagnetic structure and magnetic properties of Dy2O2Te: An isostructural analog of the rare-earth superconductors R2. <b>2022</b> , 105,	
71	The Magnetic Suppression and Electronic Structure Evolution of K1-xFe2Se2 with Different K Vacancy Concentration. 1	
70	Progress in the development of the 122-type IBS wires. <b>2022</b> , 100010	1
69	Electronic structure, magnetic, and thermoelectric properties of BaMn2As2 compound: a first-principles study.	O

68 Multiband superconductivity in SrFe2â\(\mathbb{U}\)NixAs2. **2022**, 4, 1

67	Temperature-dependent structure of an intermetallic ErPd2Si2 single crystal: a combined synchrotron and in-house X-ray diffraction study. 1-7	O
66	Theoretical Model Study of Low Energy Spin Excitations in Iron-Chalcogenide AxFe2-xSe2 : One band approach.	0
65	Competing long-range and short-range interactions in ferromagnetic semiconductors: Evidence from first principle calculations. <b>2022</b> , 169518	O
64	Magnetic phase diagram of the solid solution LaMn2(Ge1â⊠Six)2 (0 â⊡k â⊡) unraveled by powder neutron diffraction. <b>2022</b> , 12,	О
63	AsâBe Pentagonal Linkers to Induce Chirality and Polarity in Mixed-Valent FeâBe Tetrahedral Chains Resulting in Hidden Magnetic Ordering.	1
62	First-principles prediction of outstanding mechanical and thermodynamic properties of YX2Si2 (XI=IPd and Rh) superconductors. <b>2022</b> , 31, 103785	1
61	A first principle study of electronic structure and magnetic properties of TlFe2Se2. <b>2022</b> ,	
60	A brief review of the physical properties of charge density wave superconductor LaPt2Si2. <b>2022</b> , 35, 084006	
59	Multiple magnetic orders in LaFeAs1-xPxO uncover universality of iron-pnictide superconductors. <b>2022</b> , 5,	O
58	Anomalous high-field magnetotransport in CaFeAsF due to the quantum Hall effect. 2022, 7,	О
57	A Mini Review on Thin Film Superconductors. <b>2022</b> , 10, 1184	O
56	Density-functional theory study of magnetic and electronic properties of KFe2Se2 under pressure. <b>2022</b> , 561, 111604	О
55	Conventional type-II superconductivity in locally noncentrosymmetric LaRh2As2 single crystals. <b>2022</b> , 106,	O
54	K-doped Ba122 epitaxial thin film on MgO substrate by buffer engineering.	О
53	Structural and magnetic properties of CaCo2-As2 (x = $0\hat{a}\bar{b}$ .3) in ThCr2Si2-type structure. <b>2022</b> , 414214	
52	Three-dimensional microstructure and critical current properties of ultrafine grain Ba(Fe,Co)2As2 bulk superconductors. <b>2022</b> , 923, 166358	
51	Growth and characterization of superconducting Ca\$_{1-x}\$Na\$_x\$Fe\$_2\$As\$_2\$ single crystals by NaAs-flux method.	

50	Spin-flip-driven reversal of the angle-dependent magnetic torque in layered antiferromagnetic Ca0.9Sr0.1Co2As2. <b>2022</b> , 12,	1
49	First-principles study on the magnetic and electronic properties of the high-pressure orthorhombic phase of MnSe. <b>2022</b> , 106,	
48	Effect of S-doping on the magnetic and electrical properties of FeSe superconductor. 2022, 1354126	О
47	Study of superconducting gap in presence of antiferromagnetism in iron pnictide superconductors. <b>2022</b> , 126, 103525	
46	Transport properties of an antiferromagnet Ba2FeS3 with one-dimensional spin chains under pressure. <b>2022</b> , 325, 132870	
45	First-principles study of K, Ni and P doped superconductor AFe2As2 (A=Ba, Sr). <b>2022</b> , 355, 114931	O
44	Introduction. <b>2022</b> , 1-19	0
43	Electronic Phase Separation in Magnetic Materials. <b>2022</b> , 123, 674-708	O
42	The Effect of Powder-Impregnated Post-Rolling Sintering Process on SmFeAsO1-xFx Tapes Fabricated by Powder-in-Tube Method.	0
41	Hybridization of CaFe1â $\mbox{M}$ CoxAsF (x = 0, 0.06, 0.11, 0.144) studied by x-ray absorption spectroscopy and ultraviolet photoemission spectroscopy. <b>2022</b> , 48, 692-695	O
40	Significant enhancement of transport Jc in Cu/Ag-sheathed (Ba,K)Fe2As2 superconducting tapes by pre-composite technique.	0
39	First-principles calculations to investigate structural, electronics, optical and mechanical properties of LaRu2P2 compound for superconducting application. 1-9	0
38	Pressure driven magnetic order in Sr\$\$_{1-x}\$\$Ca\$\$_x\$\$Co\$\$_2\$\$P\$\$_2\$\$. <b>2022</b> , 12,	0
37	Pressure-temperature phase diagram of CaK(Fe1â\mathbb{M}mx)4As4(. <b>2022</b> , 106,	0
36	Impact of atomic defects in the electronic states of FeSe1â⊠Sx superconducting crystals.	0
35	Reentrant superconductivity due to inter-band off-diagonal hopping in a two-band superconductivity model. <b>2022</b> , 95,	O
34	Strong band renormalization and emergent ferromagnetism induced by electron-antiferromagnetic-magnon coupling. <b>2022</b> , 13,	0
33	A bi-layer barrier design for 122-type iron-based superconducting wires and tapes. <b>2022</b> , 103598	O

32	In-plane electronic anisotropy revealed by interlayer resistivity measurements on the iron-based superconductor parent compound CaFeAsF. <b>2022</b> , 106,	O
31	Pinning potential in highly performant CaKFe4As4 superconductor from DC magnetic relaxation and AC multi-frequency susceptibility studies. <b>2022</b> , 12,	O
30	High upper critical field (120 T) with small anisotropy of highly hydrogen-substituted SmFeAsO epitaxial film. <b>2022</b> , 6,	0
29	Fermi Surface Geometry of Heavily Hole Doped CaKFe4As4 Revealed by Angle-Resolved Photoemission Spectroscopy. <b>2022</b> , 91,	0
28	Interface effects on current transport properties in multi-layered (Ba, K)Fe2As2 superconducting wires.	0
27	Superconductivity enhanced by pair fluctuations between wide and narrow bands. 2022, 106,	O
26	Heat capacity double transitions in time-reversal symmetry broken superconductors. 2022, 106,	Ο
25	Critical current degradation behavior of 7-filamentary Ba1â⊠ K x Fe2As2 tapes under uniaxial strain. <b>2023</b> , 36, 015004	Ο
24	Pressure Evolution of Ultrafast Photocarrier Dynamics and Electronâ <b>P</b> honon Coupling in FeTe0.5Se0.5. <b>2022</b> , 15, 8467	0
23	Modulations in Superconductors: Probes of Underlying Physics. 2209457	Ο
22	Evolution of magnetic properties in iron-based superconductor Eu-doped CaFe2As2. 2,	0
21	Eisengruppe: Elemente der achten Nebengruppe. <b>2023</b> , 1-43	O
20	Fabrication of multi-filament(Ba,A)Fe2As2 (A: Na, K) HIP round wires and a small superconducting coil. <b>2023</b> , 36, 015009	0
19	Flipping of antiferromagnetic to superconducting states in pressurized quasi-one-dimensional manganese-based compounds. <b>2022</b> , 106,	2
18	Synthesis and Characterization of [Fe3(As3)3As4]3â∏a Binary Fe/As Zintl Cluster With an Fe3 Core.	0
17	Theoretical Investigation of the Superconducting and Thermodynamic Properties of Two-Band Model High-Temperature Iron-Based Superconductor Ba1â\(\mathbb{B}\)NaxFe2As2. <b>2023</b> , 67, 722	Ο
16	Magnetic Vortex Phase Diagram for a Non-Optimized CaKFe4As4 Superconductor Presenting a Wide Vortex Liquid Region and an Ultra-High Upper Critical Field. <b>2023</b> , 13, 884	0

14	Unconventional density waves and superconductivities in Fe-based superconductors and other strongly correlated electron systems. 1-89	O
13	Evolution of anisotropic magnetic properties through helix-to-fan transition in helical antiferromagnetic EuCo2As2. <b>2023</b> , 6,	O
12	Tetragonal SnOFeSe: A possible parent compound of the FeSe-based superconductor. 2023, 107,	O
11	Structural and electronic structure evolution of K x Fe2â $$ Se2 from semiconducting phase to superconducting phase. <b>2023</b> , 36, 045011	O
10	Flux Pinning Properties of 7-Filament Cu/Ag-Sheathed Ba1-xKxFe2As2 Tapes at 4.2 K. <b>2023</b> , 33, 1-5	O
9	Comparative study of the structural, mechanical, electronic, optical and thermodynamic properties of superconducting disilicide YT2Si2 (T=Co, Ni, Ru, Rh, Pd, Ir) by DFT simulation. <b>2023</b> , 178, 111342	O
8	Possible Raman signature of broken symmetry states near the quantum critical point in P doped BaFe2As2: Experiment and theory. <b>2023</b> , 606, 1354211	O
7	Electronic properties and surface states of RbNi2Se2. <b>2023</b> , 654, 414697	O
6	Macroscopically ordered phase separation: A new strategy for improving the superconducting performance in Fe(Se, Te). <b>2023</b> , 17, 100354	O
5	Constitutive behaviour study of Ba x K1âlk Fe2As2 iron-based superconducting powder. <b>2023</b> , 36, 045016	O
4	Spin-flip-driven anomalous Hall effect and anisotropic magnetoresistance in a layered Ising antiferromagnet. <b>2023</b> , 13,	0
3	Symmetry of Identical Particles, Modern Achievements in the Pauli Exclusion Principle, in Superconductivity and in Some Other Phenomena. <b>2023</b> , 15, 701	O
2	A Study of the Temperature-Dependent Surface and Upper Critical Magnetic Fields in KFeSe and LaSrCuO Superconductors. <b>2023</b> , 13, 526	О
1	Ferromagnetic quantum critical phenomena in single-crystalline SrCo2(Ge1âᢂPx)2. <b>2023</b> , 107,	O